Studies on the role of inflammation and stem cells in cardiac ischaemic injury

Ahmed, Ishtiaq M.

Studies on the role of inflammation and stem cells in cardiac ischaemic injury

Ishtiaq M Ahmed

BSc (Hons), MBChB, MRCS

Thesis submitted for the degree of Doctor of Philosophy

University of Durham

School of Biological and Biomedical Sciences

2008

Originality statement

I hereby declare that this submission is my own work and to the best of my knowledge it contains no materials previously published or written by another person. No part of the material offered has previously been submitted for a degree in this or any other University. Any contribution made to this research by others is explicitly acknowledged in this thesis and quotations and paraphrases suitably indicated.

Abstract

The regenerative capacity of human myocardium is unable to compensate adequately for the significant loss of heart muscle that occurs in acute myocardial infarction (MI). However, recent studies indicate that the adult heart may contain populations of cells that have stem cell characteristics and which could have regenerative potential. In order to better examine the biology of such cells, this study developed a mouse model of MI that combined low mortality, reproducible infarct size and the opportunity for reperfusion studies. One potential barrier to the expression of regenerative capacity at the time of acute MI is inflammation, which, as well as contributing to myocardial injury, may prevent the activation and function of putative stem cells. The C5/C5a axis in the complement cascade is a key mediator of the inflammatory events involved in MI and therefore represents an attractive target. An antibody to the C5a receptor was used *in vivo* in the murine model of MI. Although the neutrophil infiltration at the time of MI was significantly reduced ($p<0.05$), the size of MI was unchanged in comparison to control, suggesting that other regenerative strategies must be explored. Therefore in pursuit of a mechanism by which the heart may regenerate, cells were isolated and assayed *in vitro* for their stem cell capacity. Cells expressing platelet derived growth factor receptor alpha (PDGFRA) were candidates for such stem cells, both as these are present in the proepicardium and epicardium in the embryo, and that *Pdgfra*$^{-/-}$ mice demonstrate cardiac abnormalities. A combined approach was employed, using genetically modified mice expressing Green Fluorescence Protein (GFP) under the transcriptional control of the *Pdgfra* locus, expression of surface antigens as well as the ability of candidate stem cells to demonstrate self renewal and proliferation in a colony forming unit fibroblast assay (CFU-F). A Sca-1^{+}/PECAM^{-}/PDGFRA^{GFP+} fraction isolated from the adult heart was found to be enriched for colony forming activity. Two populations were found which formed colonies, the PDGFRA^{GFPHIGH} population which had 'stem cell' like properties in terms of proliferation, prolonged self renewal and multipotent *in vitro* differentiation, and the PDGFRA^{GFPMEDIUM} population which had 'progenitor cell' like properties in that although it had proliferative ability, the potential of this population to continue to self renew and differentiate into multiple lineages was limited. The number of candidate stem

cells and progenitor cells in the heart increased post infarct as evidenced by an increase in number of PDGFRA^{GFPHIGH} and PDGFRA^{GFPMEDIUM} cells, together with a greater colony forming ability of the PDGFRA^{GFPHIGH} cells. These effects were magnified in a proregenerative transgenic model, *Pdgfra*$^{GFP/+}$*;mIGF*, in which there was over expression of insulin-like growth factor 1 (IGF-1), supporting the argument that Sca-1^{+}/PECAM^{-} /PDGFRA^{GFP+} cells may have a role to play in the regenerative capacity of the adult heart.

Acknowledgements

My sincere thanks to my laboratory supervisor Professor Richard Harvey who shared with me his expertise and research insight throughout the project and also to Professor Robert Graham for giving me the opportunity to carry out this research at the Victor Chang Cardiac Research Institute. I feel very fortunate to have had this opportunity to delve into the fascinating world of regenerative biology and work in such a rich academic environment.

I am indebted to my thesis supervisors Dr Nicholas Hole and Mr Andrew Owens for their initial inspiration to undertake this PhD and whose thoughtful advice served to give me a sense of direction during my studies. I am very grateful for their enthusiasm, encouragement, guidance and patience throughout my period of study. Not only have they been great mentors but have been a cornerstone in my professional development.

Very special thanks to all of my laboratory colleagues who have formed the 'stem cell' group. They have all played a critical and unique roll and it really has been an inspiration to work with them all. Particularly I would like to mention Dr Vashe Chandrakanthan, who has always shown great kindness and patience in teaching me the fundamentals of flow cytometry and cell culture as well as performing the differentiation assays and helping with management of colonies. Dr Owen Prall has been of tireless help and support throughout the PhD, particularly in regards to the *Pdgfra*$^{GFP/+}$ mice and I wish to thank him for always being available and willing to discuss all aspects of the science. Similarly, Dr Munira Xaymardan has been a constant source of inspiration and am very grateful to her for teaching me the techniques of immunohistochemistry. Dr Christine Biben, Dr James Chong and Dr Chris Blair have always been willing again to discuss all aspects of my work and I am very grateful for their advice and time. Thanks also go to Ms Kate Kollar, Ms Somayaeh Nasr-Esfahhani and Ms Karina Evans for help in managing the mice strains and their postoperative care.

I am indebted to Dr Xiao-Jun Du and his team for allowing me to observe the workings of his laboratory at the Baker Heart Institute, and for his invaluable advice on operating on small animals and their care.

The work using C5a receptor antibody would not have been possible without Dr Peter Whitfield, Dr Hyun Lee and Professor Charles Mackay. I would like to thank them for providing the antibody and the *hC5aR*$^{+/+}$ mice and their advice during this time.

Many thanks to the IT department, John Spaile, Milton Lai, Robert Owe-Young and George Constantiescue for resuscitating my computer and their advice on all such related issues.

My thanks to the Victor Chang Cardiac Research Institute and the Australian Stem Cell Centre for their funding of this project.

I am very grateful to all my family, particularly my mother and father, my deepest thanks for your loving support and encouragement over the years and for always encouraging me to do my best in all matters of life.

Finally to my wife Amreen, thank you so much for your energy and love, constant support and encouragement during this chapter of our lives.

List of Abbreviations

7AAD	7 Amino-Actinomycin
ACE	angiotensin converting enzyme
ASD	atrial septal defect
BSA	bovine serum albumin
BrDU	bromodeoxyuridine
CK	creatine kinase
CK-MB	creatine kinase-MB subfraction
CSC	cardiac stem cell
CS	cardiosphere
DMEM	dulbecco's modified Eagle's medium
EDTA	ethelynediaminetetraceticacid
EGFP	enhanced green fluorescent protein
EMT	epithelial to mesenchymal transformation
FACS	fluorescence activated cell sorting
FCS	foetal calf serum
GFP	green fluorescent protein
ICAM	intercellular adhesion molecule
IGF	insulin-like growth factor
mIGF	muscle specific insulin-like growth factor
IHD	ischaemic heart disease
IL	interleukin
LAD	left anterior descending (artery)
MAC	membrane attack complex
MACS	magnet activated cell sorting
MDR	multi drug resistance (protein)
MEM	minimum essential medium
MHC	myosin heavy chain
MI	myocardial Infarction
MPO	myeloperoxidase

mTOR	mammalian target of rapamycin
OCT	optimal cutting temperature compound
PBS	phosphate buffered saline
PAF	platelet activating factor
PDGFR	platelet derived growth factor
PDGFRA	platelet derived growth factor receptor alpha
PDGFRB	platelet derived growth factor receptor beta
PDK	phosphoinositide dependent kinase
PECAM	platelet endothelial cell adhesion molecule
PFA	paraformaldehyde
PI3K	phosphatidylinositol-3-kinase
PTA	patent truncus arteriosus
SC	stem cell
SCA	stem cell antigen
SGK1	serum and glucocorticoid regulated kinase
SP	side population
TTC	triphenyl tetrazolium chloride
UCP	uncoupling protein
VEGFR	vascular endothelial growth factor
VSD	ventricular septal defect
WHO	world health organisation
Wt1	wilm's tumour protein

Table of contents

List of Figures

List of tables

Chapter 1

Introduction

1.1 Coronary heart disease

There has been a steady rise in the prevalence of cardiovascular disease over the last century. The World Health Organisation (WHO) estimate that cardiovascular disease is currently the leading cause of death worldwide, claiming 14.7 million lives in 1990 and 17 million in 1999 (Bonow et al., 2002). Ischaemic heart disease (IHD) is actually on its own the single leading cause of death worldwide. (Bonow et al., 2002). Of particular concern is that the burden of cardiovascular disease in developing countries is projected to match that in the developed world due to accelerated economic development, and lifestyle changes which promote atherosclerosis leading to a rise in ischaemic heart disease (Bayes de Luna, 1999). The keystone in therapy for ischaemic heart disease primarily involves revascularisation. This involves thrombolytic drug therapies, percutaneous intervention and surgery. However, the progressive nature of coronary artery disease dictates that a large percentage of individuals with ischaemic heart disease go on to develop ischaemic heart failure as they exhaust the medical and surgical options available (Hellermann et al., 2002).

The prognosis of heart failure is poor, with median survival after onset of 1.7 years in men and 3.2 years in women (Braunwald and Bristow, 2000). Heart failure is a condition that primarily affects the elderly and with the progressive aging of the population, the prevalence of heart failure is certain to increase over the next decade, contributing an enormous burden on health services and cost to society, currently accounting for 2% of all health care spending (McMurray and Pfeffer, 2005). Therapy for heart failure aims to relieve symptoms, avoid hospital admissions and to prolong life. The mainstay of drugs used to achieve this have included diuretics, angiotensin converting enzyme (ACE) inhibitors and β blockers (McMurray and Pfeffer, 2005). Other interventions can include implantable cardioverter defibrillators (ICD) to reduce the risk of sudden death from ventricular arrhythmia (Bristow et al., 2004; Moss et al., 2002) and resynchronisation therapy to enhance pump function of the heart (Cleland et al., 2005). In terms of surgery, the gold standard for end stage heart disease is transplantation, however due to donor shortages and morbidity associated with lifelong immunosuppressive therapy, other

surgical options including mechanical ventricular assist devices are being developed, as a means to 'bridge' people until donor organs become available and also as a destination therapy. These have been shown to have significant benefits in terms of mortality compared to optimal medical therapy (Rose et al., 2001). As technology improves, mechanical assist devices are showing improvements in complications of sepsis, device failure and thrombo-embolic events.

Although these therapies ameliorate symptoms and improve survival, none are able to directly reverse the disease process itself. Therefore these treatment options all suffer from the same fundamental limitation that none can repair the damage that has already been done.

If new myocardium could be grown in diseased hearts then the possibility that this disease process could be reversed may be realised and the dogma that the heart does not have regenerative ability could be challenged.

1.2 Is the heart a terminally differentiated organ?

There has been a commonly held view that the heart is a post mitotic organ without regenerative capacity especially since the usual pathophysiology after ischaemic injury is the loss of myocytes and replacement by connective tissue scar (Anversa and Kajstura, 1998; Nadal-Ginard et al., 2003). It was postulated that myocytes could not enter into the proliferative phase of the cell cycle, but could only undergo cellular hypertrophy. The concept that myocytes cannot divide originated from both the difficulty of identifying mitotic figures in the cells and the absence of any substantive DNA synthesis in myocyte nuclei (Anversa and Kajstura, 1998).

However, there has been a steady accumulation of evidence to challenge this view, beginning with studies in the 1960s when an increase in myocyte number in hypertrophic human left ventricles was observed (Linzbach, 1960). A few years later it was reported that some ventricular myocytes could pass through all phases of the cell cycle

(Rumyantsev, 1964). These observations have been confirmed in recent years by Anversa and colleagues (Kajstura et al., 1998).

There is additional evidence from instances of ischaemic heart disease. Kajstura et al examined myocyte proliferation in end stage cardiac failure in human hearts. They found a small number of mitotic figures in control hearts, but a 10 fold increase in patients with end stage ischaemic heart disease, suggesting that cell division may occur at a low rate in normal myocardium, but play a role in response to cardiac damage (Kajstura et al., 1998). This was supported by further work by the same group (Beltrami et al., 2001). This study examined hearts of patients who had died after myocardial infarction (MI). Myocytes that had entered the cell cycle in preparation for cell division were measured using the nuclear labelling antigen Ki67, a marker which is associated with cell division. Ki67 was detected in 4% of myocyte nuclei in regions adjacent to the infarct area and in 1% of those regions remote from the infarct. Events characteristic of cell division such as mitotic spindles, karyokinesis and cytokinesis were also observed. These results suggested that the adult myocytes were capable of re-entering the cell cycle, but only in those areas where oxygenation was maintained such as the peri-infarct zone.

The question of the origin of the mitotic cells could begin to be addressed by transplantation studies. Quani et al examined cases where a male patient had received a heart from a female donor (Quaini et al., 2002). The presence or absence of the Y chromosome was used to detect cells of recipient or donor origin. In the transplanted hearts, cells of the myocardium ($9 \pm 4\%$), arterioles ($10 \pm 3\%$) and capillaries ($7 \pm 1\%$) contained the Y chromosome. Of the myocytes which contained the Y chromosome $17.2 \pm 4.2\%$ were replicating (measured by Ki67 labelling). They also examined control hearts and transplanted hearts for cells expressing c-kit, MDR1 and Sca-1. These are surface proteins characteristic of but not exclusive to stem cells (Demeule et al., 2001; Jiang et al., 2000a; Thiebaut et al., 1987; Torrente et al., 2001; Wu et al., 2000). Cells expressing these markers were found to be small and round with a large nucleus and a thin rim of cytoplasm. These cells were also negative for markers of haematopoietic cells, differentiated myocytes, smooth muscle cells, endothelial cells and fibroblasts. They

found that cells expressing stem cell markers were found in control hearts but their numbers were up to 4 fold higher in the hearts which had been transplanted from the female donors into male recipients. 12 to 16% of these cells also expressed the Y chromosome indicating they had translocated from the host to the donor tissue. The authors speculate that the mechanical factors involved due to the implantation of the normal heart into a recipient where the heart will be subject to a changed haemodynamic load may trigger the translocation of primitive cells into the transplanted heart, and that these cells may be involved in contributing to optimizing cardiac mass and restoring function in the short term.

The evidence for replicating myocytes and cells expressing stem cell markers in transplants does not address whether there is a demand for such cells in normal physiological states. Such evidence could be gained by predicting normal cell turnover. Anversa's group calculated that a rat left ventricle contains 23 x 10^6 myocytes at 4 months of age and 19 x 10^6 myocytes at 29 months (Anversa et al., 1990). Since the average rate of death was calculated as 1.34 x 10^6 myocytes per month, it was estimated that all myocardial cells would have died within 17 months of life (Kajstura et al., 1996). Clearly this is not the case, giving weight to the argument that myocardial cells are replenished and that cardiac cell turnover is possible.

From this data it could be postulated that cell turnover in the heart is not static, but dynamic in nature. The fact that there is evidence for cycling cells in the heart suggests that the heart may actually have the potential to repair and regenerate but that regeneration might be too inefficient to repair the extensive myocardial injury after an ischaemic event. The question which one must ask is what is the source of these cells which may have this potential? One source could be stem or progenitor cells. Hsieh et al explored the degree to which stem or progenitor cells may contribute to renewal of adult mammalian cardiomyocytes (Hsieh et al., 2007). A transgenic approach was used to map cell fate in the adult murine heart. Treatment with 4-OH-tamoxifen induced heart specific expression of Cre recombinase (expressed under the tamoxifen-conditional transcriptional control of the α-myosin heavy chain (α-MHC) promoter), resulted in the

permanent marking of cells with green fluorescent protein (GFP). All of the progeny of these cells continue to express GFP, so allowing examination of the replicative potential of the marked cells. Cells which do not express the α-MHC gene at the time of tamoxifen treatment, such as uncommitted stem cells, would not be genetically labelled with GFP. Thus the hypothesis was that if the numbers of GFP marked myocardial cells diminished over time, this would be evidence for repopulation from a stem cell source. The authors found that during normal aging up to one year the percentage of GFP^+ cardiomyocytes did not change. However 3 months after myocardial infarction, the percentage of GFP^+ cardiomyocytes had decreased significantly not only in the peri-infarct area, but also in regions remote from the infarct. These results provided indirect evidence for the involvement of a non myocyte cell contribution in the response post infarct, and supports the argument that a stem cell population may play a role at least in response to myocardial infarction.

Evidence for a regenerative response in the adult heart can also be drawn from other animal models.

1.3 Regeneration in urodele amphibians and zebrafish

Selected non-mammalian vertebrates, including urodele amphibians and zebrafish show an elevated regenerative ability in comparison to their mammalian counterparts, reviewed in (Brockes and Kumar, 2002). An adult newt can regenerate its jaws, lens, retina, limbs and large sections of the heart in response to molecular signals which signal tissue damage. In the urodele amphibian it has been reported that adult cardiomyocytes re-enter the cell cycle and divide in the zone surrounding a blood clot. Zebrafish are also able to regenerate cardiac muscle after major injury. Poss et al showed that following resection of the apex of the ventricle, cardiomyocyte hyperplasia renews the myocardium and restricts scar formation (Poss et al., 2002). Transgenic reporter strains have in recent years been used to try to establish mechanisms involved in this process. Lepilina et al showed that an initial blastema is formed consisting of progenitor cells. These cells, expressing pre- cardiac markers such as Nkx2-5, can then undergo differentiation and

proliferation. Epicardial tissue surrounding both cardiac chambers then expands, creating a new epithelial cover for the exposed myocardium. A sub population of the epicardial cells localises to the wound. This subpopulation of cells which express the T-box transcription factor tbx18 undergoes epithelial to mesenchymal transition (EMT), penetrates the regenerating tissue and provides new vasculature to the regenerating muscle. The epicardial cells have been found to express fibroblast growth factor receptors particularly fgf2 and fgf4. During regeneration fgf17b was found to be induced in the myocardium. When fgf signalling was blocked, epicardial EMT and coronary neovascularisation was arrested (Lepilina et al., 2006). These findings demonstrated the importance of the epicardial tissues which together with fgf signalling were crucial to achieve cardiac regeneration in the zebrafish heart.

These findings suggest that it is possible that the machinery to facilitate regeneration from progenitor cells may be present but lie dormant in adult mammals. However, cardiac tissue regeneration from precursor cells does occur at least once in their lifetime; during embryogenesis. In view of this it is important to briefly look at mammalian heart development to try to delineate sources of potential progenitors or stem cells during embryogenesis so as to help understand the cellular origin of cells which may have the potential to be able to contribute to repair and regeneration of the heart in the adult.

1.4 Sources of resident cardiogenic precursors

1.4.1 Cardiac progenitor cells during embryogenesis

The heart is composed of many different tissues including myocytes, conduction system cells, smooth muscle, endothelial cells, interstitial cells and connective tissue. During development the differentiation of these multiple lineages is under tight spatial and temporal control resulting in the coordinated formation of the separate components of the heart as reviewed by Laugwitz et al (Laugwitz et al., 2008). In the embryo three main sources of heart cell precursors have been identified, the cardiogenic mesoderm, the cardiac neural crest and the proepicardial organ. Each one of these represents a separate

pool of progenitor cells which give rise to distinct cardiac structures in the embryo (figure 1.1). Myocardial progenitor cells originate in the primitive streak which is a transitory embryonic structure, present as a strip of cells that align to the anterior-posterior axis of the embryo. The cells in the primitive streak involute (a process called gastrulation) resulting in the formation of the three cell regions that are the source for all subsequent cell types. The mesoderm gives rise to the musculoskeletal system, connective tissue, blood and internal organs such as the heart. The ectoderm develops into brain, skin, nails and epithelium of the nose, mouth, anal canal and nervous system and the endoderm forms the inner linings of the digestive tract and respiratory passages, the liver and pancreas. The mesodermal cells at the primitive streak migrate to the anterior part of the embryo at about embryonic day 6.5 and come to lie under the head folds and form the cardiac crescent, which is cardiogenic mesoderm (E7.5). The cardiac crescent fuses in the midline to form the early cardiac tube. It subsequently undergoes looping (E8.5) and then by E10.5 the heart has well defined chambers. By E14.5 septation has occurred separating the chambers, and the heart is connected to the pulmonary trunk and aorta. Cardiac neural crest migrates to the heart at a later stage of development, and gives rise to the vascular smooth muscle of the aortic arch, ductus arteriosus and the great vessels (Jiang et al., 2000b). The mesenchyme portion of the developing heart and the majority of the epicardial cells are derived from the proepicardium which is a cluster of mesothelial cells located in the caudal regions of the developing vertebrate heart. Lineage tracing studies have suggested this proepicardium, a distinct extra cardiac structure, is the source of many non-cardiomyocyte cardiac cell types including endothelium, smooth muscle and fibroblasts (Mikawa and Gourdie, 1996; Poelmann et al., 1993). Progenitors bud off from the proepicardium, traverse the pericardial cavity and re-attach to the surface of the heart forming the epicardium. These epicardially derived cells (EPDC) then invade the cardiomyocyte layer by a process called epithelial to mesenchymal transformation and differentiate into endothelial, smooth muscle and fibroblast cells. The epicardium also supplies growth factors including fibroblast growth factors 9/16/20 which are required for cardiomyocyte growth (Lavine et al., 2005). Disruption of epicardial specific genes has resulted in a phenotype of a thin myocardium (Moore et al., 1999) and there are reports of contribution of proepicardially derived cells to

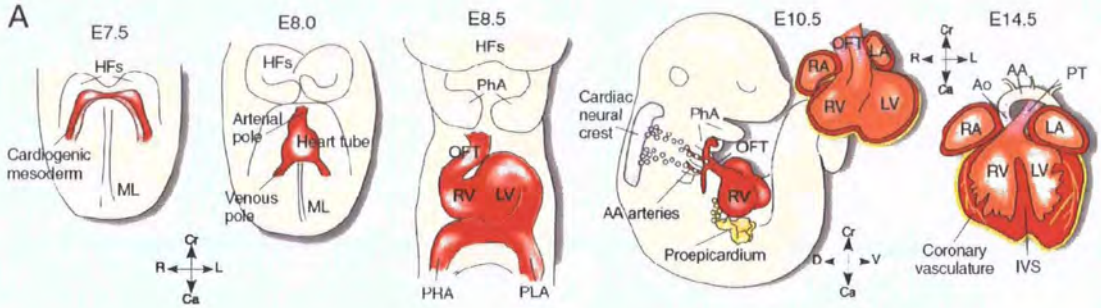

Figure 1.1 Cardiac development

Contribution of the three populations of embryonic heart progenitors, cardiogenic mesoderm, cardiac neural crest and proepicardial organ to the different heart compartments during cardiac morphogenesis. Progenitors of the cardiogenic mesoderm are first recognisable under the head folds (HF) of the embryo at E7.5, then move to the midline (ML) and initially form the heart tube and ultimately the four chambers of the heart. After the looping of the heart tube (E8.5), cardiac neural crest progenitors migrate from the dorsal neural tube to engulf the aortic arch arteries and contribute to vascular smooth muscle cells of the outflow tract (OFT) at E10.5). At the same time the proepicardial organ precursors migrate to the heart and contribute to coronary vasculature, fibroblasts and myocardium. Cranial (Cr)-caudal (Ca), right (R) and Left (L), dorsal (D)-Ventral (V) axes are indicated. AA, aortic arch;IVS interventricular septum; LA, left atrium; LV, left ventricle; Ph pharyngeal arches; PLA primitive left atrium; PRA, primitive right atrium; RA, right atrium; RV right ventricle. Reprinted with permission (Laugwitz et al, 2008).

myocardium (Wessels and Perez-Pomares, 2004) *in vitro* hence suggesting a potential role for these cells in cardiomyogenesis. Interestingly recent data has corroborated the evidence for the contribution of epicardial cells to cardiomyocytes. Cai et al report the identification in mouse of a cardiac myocyte lineage that derives from the proepicardial organ (Cai et al., 2008). Using a Cre knock-in into the endogenous *Tbx18* locus, they crossed *Tbx18:Cre* mice with the lineage reporter $R26R^{lacZ}$. Early analysis of *LacZ* expression in embryos from this cross was consistent with that of endogenous *Tbx18*. At E10.5 there was evidence of *Tbx* derived lineages in the forming ventricles and atria and co-staining with cardiac troponinT (cTnT), cardiac TroponinI (cTnI), and the transcription factors Nkx2-5 and GATA4 showing that these *Tbx* derived cells were probably cardiomyocytes. Adult lineage analysis showed that *Tbx18* derivatives were seen in smooth muscle of the coronary vessels, ventricular and atrial myocytes and atrio-ventricular valves. *Tbx18* lineage traced cells that co-stained with cardiac Troponin T demonstrating their cardiomyocyte status. *Tbx18* lineages did not give rise to coronary endothelial cells, however approximately 30% of cardiac fibroblasts were shown to derive from *Tbx18* lineages. Further work on epicardial progenitors used the fact that Wilms Tumour protein 1 (Wt1) was found to be expressed in proepicardium and epicardium (Zhou et al., 2008). Similar lineage tracing experiments demonstrated that Wt1 derived cells contribute to cardiomyocytes, endothelial and smooth muscle lineages during normal development. The Wt1 derived cardiomyocytes were shown to express Gata4 and Nkx2-5. The above data demonstrate evidence for a potentially important progenitor cell or stem cell which could be involved in cardiac repair or regeneration, which is located in the proepicardial organ and epicardium of the developing heart.

As explained above, three major sources of heart cell precursors have been identified in the embryo, the cardiogenic mesoderm, the cardiac neural crest and the proepicardial organ. The cardiac crescent which is part of the cardiogenic mesoderm is often referred to as the first heart field. It gives rise to the linear heart tube and ultimately the atrial chambers and ventricular region. No specific markers have been identified for this population. The second cardiogenic region, known as the second heart field lies dorsal to the linear heart tube and is derived from the pharyngeal mesoderm medial to the cardiac

crescent (Laugwitz et al., 2008). Cells from this second heart field are added to the developing heart tube and give rise to the outflow tract, the right ventricular region and the majority of the atrial tissue (reviewed by Buckingham et al (Buckingham et al., 2005)). Recent studies have shown the expression of islet-1 transcription factor (Isl1) as a marker of the second myocardial lineage during mammalian cardiogenesis (Cai et al., 2003). *Isl1* knockout mice were found to have an abnormal cardiac phenotype. Mutant hearts were found to be misshapen and failed to undergo looping morphogenesis, with an absent right ventricle and outflow tract resulting in death by E10.5. Lineage tracing confirmed these findings, showing that cells which had previously expressed Isl1 contributed to the majority of the cells in the outflow tract, right ventricle, atria and parts of the left ventricle. It appeared that Isl1 was required for cell proliferation, migration and survival , its transcription being turned off as the precursor cells differentiated. After birth relatively few $Isl1^+$ cells are detectable in the myocardium, the organ distribution matching the contributions of $Isl1^+$ precursors suggesting that these cells are developmental remnants of the foetal progenitor population. Laugwitz et al and Moretti et al studied the contribution of $Isl1^+$ precursors to cardiac cell lineages in the adult heart (Laugwitz et al., 2008; Laugwitz et al., 2005; Moretti et al., 2006). Cre mediated removal of a stop sequence in the cells that express Isl1 resulted in the expression of *LacZ*. In this way all cells that once expressed Isl1 during development were marked. This showed a high proportion of right ventricular myocardium and parts of both atria consisted of cells which expressed *LacZ* and the myocytic protein sarcomeric α-actinin. By analysing *LacZ* expression and acetylcholinesterase expression it was shown that $Isl1^+$ progenitors contribute also to the conduction system, primarily to the sino-atrial node. Additionally *LacZ* expression was found in the proximal aorta and pulmonary outflow tract. Co-expression of *LacZ* with endothelial and smooth muscle specific markers such as CD31 and smooth muscle myosin heavy chain respectively showed that $Isl1^+$ precursors could give rise to vascular lineages also. Therefore it appears that Isl defines a multipotent progenitor in the developing heart which contributes to distinct cell lineages within heart compartments known to originate from the second heart field. The effect of in vivo transplantation of $Isl1^+$ cells has not yet been determined.

Hence it seems that $Isl1^{+}$ cells and epicardially derived cells are integral to cardiomyogenesis and that remnants of these cells which remain in the adult could act as a putative stem or progenitor cell population. In addition , recent work from Prall et al (personal communication Dr O Prall, Victor Chang Cardiac Research Institue, Sydney) has shown the presence of cells expressing platelet derived growth factor receptor alpha (PDGFRA) in the proepicardial organ at E9.0. These cells were found on the epicardial surface of the heart at E9.0 to E10.5, and from E12.5 they appear in the myocardial interstitium. There is evidence of a cardiac developmental role for these cells also.

1.4.2 Platelet Derived Growth Factor- its role in development and the adult

Platelet-derived growth factor (PDGF) is a potent mitogen and chemotactic factor for a variety of mesenchymal cells, such as fibroblasts, vascular smooth muscle cells, glomerular mesangial cells and brain glial cells. Activation of its receptors Platelet derived growth factor receptor alpha (PDGFRA) and Platelet derived growth factor receptor beta (PDGFRB) stimulates fibroblast migration, proliferation and activation (Raines, 2004; Simm et al., 1998; Yu et al., 2001). In the mid 1970's several groups demonstrated that this growth factor in serum was derived from the alpha storage granules in platelets (Kohler and Lipton, 1974; Ross et al., 1974).

The PDGFs are a family of dimeric disulphide-bound growth factors that can activate two structurally related tyrosine kinase receptors, PDGFRA and PDGFRB. These receptors are transmembrane proteins that have an extracellular ligand-binding domain, a transmembrane domain and a cytoplasmic tyrosine kinase domain (Fantl et al., 1993). The alpha and beta receptors have molecular sizes of approximately 170kd and 180kd respectively and are the products of 2 separate but highly homologous genes on chromosomes 7 and 22 respectively (Dalla-Favera et al., 1982). On ligand binding, PDGF receptors homodimerise or heterodimerise into PDGFAA, PDGFAB or PDGFBB initiating signal cascades (Heldin, 1996). Both receptors can activate similar signal transduction pathways including the phosphatidylinositol 3-kinase (PI3K), Ras mitogen-activated protein kinase (Ras-MAPK), and phospholipase$C\gamma$ pathways. The PI3K

pathway is essential for PDGF-induced cell migration, actin reorganization and prevention of cell death (Vanhaesebroeck et al., 1997). Ras is important for the mitogenic effect of PDGF.

The biologically active ligands are homodimers or heterodimers. The homodimers are PDGF-AA, PDGF-BB, PDGF-CC and PDGF-DD and the heterodimer is PDGFR-AB. All PDGF ligands, except PDGF-DD induce PDGFRA dimerisation. PDGF-BB and PDGF-DD activate PDGFRB dimerisation. PDGFRAB heterodimer is activated by all ligands except PDGF-AA. The predominant signaling appears to be PDGF-AA and PDGF-CC through PDGFRA homodimers, PDGFR-AB through PDGFRA homodimers and PDGFRAB heterodimers, and PDGFR-BB and PDGFR-DD through PDGFRB homodimers. PDGFR genes are receptor tyrosine kinases (RTKs) and are likely to have evolutionary origins in common with other RTKs whose expression has often defined stem/progenitor cell populations. Human PDGFRA is located within 0.9Mb of the haematopoietic stem cell marker c-kit (Yoshida et al., 1998). Levels of PDGFR expression on cells varies considerably, but of note PDGFRA and PDGFRB are expressed on vascular smooth muscle cells, vascular endothelial cells, fibroblasts, platelets, macrophages and keratinocytes (Heldin and Westermark, 1999).

1.4.2.1 Developmental role of PDGF-B and PDGFRB

Pdgf-b or *Pdgfrb* negative mice die during late gestation from cardiovascular complications (Leveen et al., 1994; Soriano, 1994). The mutant mice look normal up until E16-19 when there is dilatation of the heart and large blood vessels and dilatation and rupture of capillaries. Other findings include abnormal kidney glomeruli, capillary microaneurysms, arterial smooth muscle cell hyperplasia, cardiac muscle hypertrophy and widespread oedema and haemorrhage. The significance of biological signaling in vivo of PDGF-BB via PDGFRB is discussed below. PDGF-DD signaling via PDGFRB has not been fully clarified (Heldin and Westermark, 1999). In the mouse embryo PDGF-B expression appears restricted to vascular endothelium and megakaryocytes (Heldin and Westermark, 1999; Lindahl et al., 1997). PDGFRB positive mesenchymal cells are found

in cells distinct from but tightly associated with endothelial cells. It is assumed that these cells may constitute vascular smooth muscle or pericyte progenitors (Heldin and Westermark, 1999; Hellstrom et al., 1999; Lindahl et al., 1997). The spatial and temporal expression patterns of PDGF-BB and PDGFRB suggest that PDGF-BB released from endothelial cells normally promote proliferation in adjacent vascular smooth muscle or pericyte progenitors. This hypothesis is confirmed by the *Pdgfr-b* and *Pdgfrb* null phenotypes. The embryonic null phenotypes show a reduced BrdU labeling index (indicating reduced cell turnover) and a reduction in the number of smooth muscle cell and pericyte progenitors.

1.4.2.2 Developmental role of PDGF-A and PDGFRA

Cardiac defects in *Pdgfra* null embryos include aortic arch artery malformations, persistent truncus arteriosus (PTA), atrial and ventricular septal defects (ASD and VSD), myocardial wall thinning and abnormal atrio-ventricular valves and dilatation of the pericardium, leading to death between E8 and E16 (personal communication, Dr O Prall, Victor Chang Cardiac Research Institute). Other defects include spina bifida and cleft face (Soriano, 1997). Deletion of *Pdgfra* specifically in neural crest cells (NCCs) with Wnt1-Cre produces aortic arch artery malformations, PTA and VSD (Tallquist and Soriano, 2003). This may suggest a role for *Pdgfra* in NCC progenitors. Null mutations of *Pdgf-a* or *Pdgf-c* display subsets of the defects seen in *Pdgfra* null embryos(Ding et al., 2004). *Pdgf-a/-c* null animals completely phenocopy the loss of PDGFRA function suggesting that both PDGF-A and PDGF-C signal through PDGFRA during embryogenesis(Ding et al., 2004).

1.4.2.3 Over expression of PDGF in the heart

Ponten et al (Ponten et al., 2003) over expressed PDGF-CC in the heart using the α-myosin heavy chain promotor. Initially these PDGF-CC transgenic mice appeared normal during embryonic development and birth as compared to WT littermates. At 2 weeks mild fibrosis but no hypertrophy was observed and the animals are reported to have

appeared normal. After 1 month heart:body weight ratios in aged matched animals were significantly higher in the females. Starting from 3 months female mice died due to heart failure. Male mice did not die spontaneously before sacrifice at 7 months. PDGF-CC transgenic hearts developed a progressive hypertrophy. There was an increased number of interstial fibroblasts leading to disorganized myocardial architecture in the transgenic hearts. Masson's Trichrome stain showed progressive collagen deposition with age, suggesting these transgenic mice develop a progressive cardiac fibrosis. Transgenic heterozygote mice were normal and fertile. On examination of blood vessels it was shown that blood vessel density in transgenic hearts was generally lower after the age of 3 months. In transgenic hearts the normal capillary network was gradually replaced by dilated capillaries. PDGFRA was also found to be up-regulated in transgenic hearts compared with the WT, and an increased number of proliferating fibroblasts were found suggesting that in these transgenic hearts with activation of PDGF-C, PDGFRA is activated. The up regulation of the PDGFRA mRNA was suggested in this study to reflect an increased number of interstitial fibroblasts.

1.4.2.4 The role of Platelet derived growth factor in myocardial infarction

Infarct healing is regulated by a well orchestrated inflammatory response that ultimately leads to scar formation (Frangogiannis et al., 2002). Myocardial necrosis results in an influx of inflammatory mediators. Activated neutrophils secrete proteolytic enzymes and help to debride the infarct area. After the inflammation, there is a proliferative phase of healing when fibroblasts accumulate in the infarct granulation tissue and deposit extracellular matrix proteins. The granulation tissue is eventually replaced by collagen-rich scar. During the proliferative phase the wound is very vascular to provide oxygen and nutrients to the proliferating cells. This angiogenesis is eventually suppressed and many of the infarct neo-vessels acquire a muscular coat (Ren et al., 2002) while uncoated vessels regress. Resolution of this inflammatory response and maturation of the neovasculature are important to prevent uncontrolled angiogenesis and expansion of granulation tissue. PDGF signaling is important in directing the regulation of fibrous tissue deposition and angiogenesis. Activation of PDGFRA and PDGFRB stimulates

fibroblast migration, proliferation and activation (Raines, 2004; Simm et al., 1998; Yu et al., 2001). Endothelial cells form vascular tubes and direct the recruitment of mural cell precursors by secreting PDGF-BB. PDGFRB is expressed by pericytes and smooth muscle cells, hence recruitment of mural cells by infarct neovessels may be important in mediating suppression of the angiogenic process and resolution of the inflammatory infiltrate during wound maturation (Hirschi et al., 1999).

Zymeck and colleagues examined the effects of using systemic neutralizing antibodies to disrupt PDGFRA signaling (Zymek et al., 2006). They showed that both PDGF receptors have important actions in regulation of the cellular events associated with scar formation. Although PDGFRA inhibition did not affect vascular maturation, it significantly decreased collagen deposition in the infarcted myocardium. This is consistent with the established role of PDGFRA in the development of myocardial fibrosis. PDGF-AA potently stimulated cardiac fibroblast proliferation also (Li et al., 2000).

Resolution of inflammation is critical for effective cardiac repair after myocardial infarction. PDGFRB helps to stabilize the infarct vasculature, promoting resolution of inflammation, and then together with PDGFRA , promotes scar stability and collagen deposition. Defective scar formation may adversely affect cardiac function by having implications on remodeling post infarct.

Hence it is clear there are well described mechanisms of contribution and involvement of specific cells and regions of the heart in development. The existence of these embryonic multipotent cardiac progenitor cells has in parallel prompted a search for the prescence of such cells in the post natal heart.

1.4.3 Cardiac progenitor cells in the adult

As seen earlier, evidence of mitosis in the peri-infarct areas of the heart suggested cell replication, but the origin of this activity was not identified (Beltrami et al., 2001). Two separate groups then went on to describe the existence of resident stem cells as identified

by expression of the stem cell characteristic markers c-kit and Sca-1 (Beltrami et al., 2003; Oh et al., 2003). Beltrami et al concentrated on c-kit$^+$ cells primarily because they had previously demonstrated a potential role for bone marrow derived Lin$^-$c-kit$^+$ cells in myocardial regeneration (Orlic et al., 2001) and the fact that both heart and bone marrow have mesodermal origin and the use of c-kit as a haematopoietic stem cell marker (Morrison et al., 1997). One Lin-ckit$^+$ cell was found for every 1 x 10^4 myocytes. These Lin$^-$c-kit$^+$ cells were found in small clusters in the intersticia between myocytes (figure 1.2). Some of the cells in these clusters expressed transcription factors associated with early cardiac development such as GATA4 (Molkentin et al., 1997) and Nkx2-5 (Biben et al., 2000), providing evidence that they may have a cardiomyogenic fate. Lin$^-$c-kit$^+$ cells were isolated by flow cytometry and found to be negative for myocyte markers (α-sarcomeric actin, cardiac myosin, connexin 43), endothelial cell (von Willebrand factor, CD31) and smooth muscle cell (α-smooth muscle actin) cytoplasmic proteins. These cells were shown to be clonogenic, self renewing and in vitro gave rise to the three different cardiogenic lineages, cardiomyocytes, smooth muscle and endothelial cells. Beltrami et al also examined in vivo potential of the c-kit$^+$ cells by injecting cells which had been labelled with enhanced green fluorescent protein (EGFP) into hearts of syngeneic rodents five hours after surgical induction of MI (Beltrami et al., 2003). On examination of these hearts at ten days post infarct, regenerating bands of EGFP positive myocytes, arterioles and capillaries were observed which were positive for BrDU indicating they had undergone recent cell division.

The authors claimed these results were highly unlikely to be a result of fusion events because (1) The number of new myocytes was orders of magnitude higher than the injected cells, which in addition gave rise to smooth muscle and endothelial cells. (2) As the cells were injected five hours after the infarct was initiated, it would be unlikely that there would be viable myocytes available for the injected cells to fuse to. (3) No myocytes with biochemical tags of the injected cells (BrDU or EGFP) were found in the spared myocardium where there are many more fusion partners. (4) The size of the newly formed myocytes were much smaller than the spared myocytes. (5) If the new myocytes

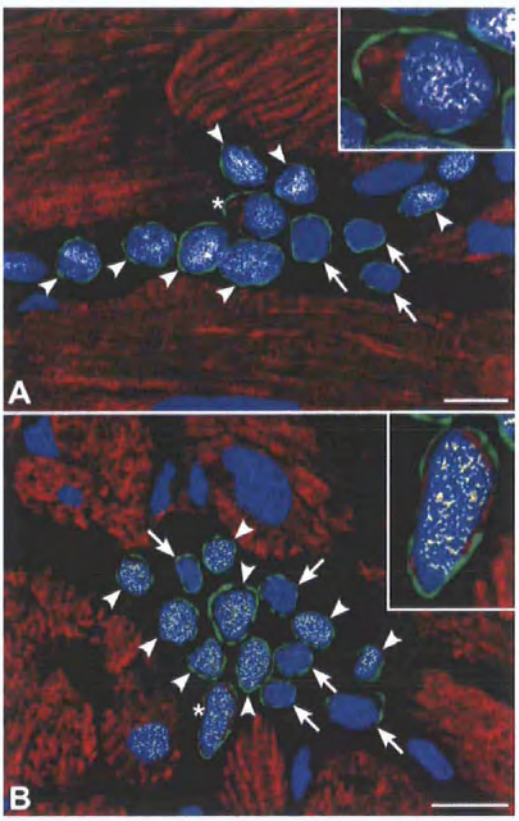

Figure 1.2 Clusters of primitive and early committed cells located in the interstitial space between cardiac muscle fibres.

These cells expressed early cardiac and progenitor cell markers. (A) Clusters of eleven ckit+ cells (green), with three cells expressing c-kit only (arrows), seven cells expressing Nkx2-5 (white dots; arrowheads) in the nuclei (blue, propidium iodide), and one (asterisk and insert) expressing Nkx2-5 and α-sarcomeric actin (red) in the cytoplasm. (B) Cluster of fifteen c-kit+ cells with five expressing c-kit only (arrows), eight cells expressing MEF2C (yellow dots; arrowheads), and one expressing MEF2C and α-sarcomeric actin (asterisk and insert). Bars=10μm.
Reproduced with permission from (Beltrami et al, 2003).

were a result of fusion, they would have double the anticipated DNA content. In this case they did not.

Challenging the premise that the c-kit$^+$ cells described were resident in the heart as claimed by Anversa et al, work from Fazel et al suggested that the c-kit$^+$ cells in the heart originate from the bone marrow (Fazel et al., 2006). They rarely found c-kit$^+$ cells in the heart prior to MI, however post infarct they found that c-kit$^+$ cells could readily be detected with approximately 30% expressing CD45 and over 95% expressing VEGFR2 . The authors state it is not clear whether this represents a preferential proliferation of CD45$^-$ cells or a down regulation of CD45, if these cells really were haematopoietic origin . In order to address whether these c-kit$^+$ cells were from the bone marrow, they engineered GFP bone marrow chimeric mice to track GFP expressing bone marrow cells. Control C57B6 mice were shown not to have any GFP expressing cells in the bone marrow. Post infarct they found that 74% of the c-kit$^+$ cells in the heart expressed GFP and that none of these were cardiomyocytes. Next, to assess the importance of c-kit expressing cells, MI was induced in c-kit mutant mice kit$^{W/kitW\text{-}v}$. These mice have defective haematopoietic stem cell (HSC) mobilisation but otherwise are phenotypically normal. In these mice there was a 2-fold increase in mortality post MI. This phenotype was reproduced in mice treated with Gleevec which is a tyrosine kinase inhibitor and therefore inhibits c-kit function. c-kit dysfunction appeared to increase apoptosis and decrease the number of cells in the heart undergoing mitosis. Fazel et al did not actually show that the multipotent and clonogenic ckit$^+$ cells isolated from the heart by Beltrami et al were from bone marrow, however they raised the possibility that those putative cardiac c-kit$^+$ stem cells isolated by Beltrami et al (Beltrami et al., 2003)may not actually be from the heart. It was demonstrated that the mutant kit$^{W/kitW\text{-}v}$ mice had impaired angiogenesis which could be rescued by transplantation of c-kit$^{+/+}$ bone marrow cells . The authors postulated that because angiopoietin2 levels and VEGF levels are reduced in the kit$^{W/kitWv}$ mice, the normal pro-angiogenic mileu post infarct is not established. Together with this they found a reduction in endothelial cells in the cell cycle in the mutant mice, hence concluding that c-kit cells recruited post infarct from the bone marrow are vital in

establishing a pro-angiogenic milieu which is critical in the formation of granulation repair tissue post infarct.

Oh et al reported a resident population of cardiac progenitor cells which were characterised by the expression of Stem cell antigen (Sca-1) (Oh et al., 2003). Sca-1 was first reported as one of the cell surface markers of haematopoietic stem cells (Okumoto et al., 2003). They isolated a myocyte depleted population from adult murine hearts and found approximately 14-17% of the cells expressed Sca-1. They found that cardiac $Sca1^+$ cells were small interstitial cells, the majority co-expressing PECAM1. These cardiac $Sca1^+$ cells lacked blood cell lineage markers (CD4, CD8, B220, Gr1, Mac-1 and TER119), also they were negative for c-kit, von Willebrand factor, CD45 and CD34. Cardiac $Sca1^+$ cells were found not to express the cardiac transcription factor Nkx2-5, however GATA-4 and MEF-2C were expressed in a proportion of cells. In vitro differentiation studies using 5-azacytidine induced α-sarcomeric actin, cardiac troponin I, α and β myosin heavy chain and Nkx2-5, indicating a potential role for these $Sca1^+$ cells as a myocardial progenitor. Labelled Sca-1^+ cells were also injected intravenously into mice post infarct to assess their ability to home to infarcted tissue and contribute to cardiomyogenesis. A Cre/Lox Donor/Reporter system was used where Sca-1^+ cells from an αMHC-Cre mouse were injected into R26R reporter mice. In this system cardiomyocytic differentiation of donor cells would be reflected by induction of αMHC, a late but stringent criterion of cardiac differentiation, resulting in parallel expression of αMHC-Cre. Fusion was determined by expression of functional *LacZ* in the induced cell and all subsequent progeny. Freshly isolated Sca-1^+ cells from αMHC-Cre mice did not express Cre. Although it was shown that Sca-1^+ cells could home to the infarct area and differentiate into cells expressing α-sarcomeric actin, 50% of the cells appeared to have fused with recipient myocytes. No functional studies were undertaken in this study and clonality or self renewal were not determined.

MDR1 cells (Multi-drug resistance gene 1), otherwise known as side population (SP) cells in the heart were described by Quani et al (Quaini et al., 2002). They were identified by having the ability to efflux Hoechst 33342 dye (Goodell et al., 1996; Martin et al.,

2004). The ability of SP cells to efflux Hoechst 33342 dye is known to be dependent on the expression of Abcg2, a member of the family of ATP-binding cassette (ABC) transporters (Kim et al., 2002). SP cells were first isolated from bone marrow (Goodell et al., 1996)and were shown to be enriched for long term repopulating haematopoietic stem cells (Parmar et al., 2003). Pfister et al demonstrated a cardiac SP which were immunophenotypically different from bone marrow SP cells (Pfister et al., 2005) (Jackson et al., 2001). Pfister et al showed that $CD31^{-}/Sca1^{+}$ cardiac side population cells represented a specific cardiac progenitor cell population capable of self renewal and biochemical and functional cardiomyogenic differentiation into mature contracting cardiomyocytes. Cardiac side population cells were largely negative for CD45 and CD34, the majority do express Sca-1 but were negative for c-kit (however the authors do state a caveat that the low expression of c-kit may have been due to enzymatic cleavage during digestion of the heart). Bone marrow SP cells stain positively for CD45 and CD34 as well as c-kit, Sca-1 and CD31. $Sca1^{+}$ cardiac side population cells which had been freshly isolated showed expression of GATA4 and Nkx2-5 which have both been shown to play a crucial role in cardiomyogenesis(Biben et al., 2000; Brown et al., 2004; Srivastava and Olson, 2000). Contractile proteins associated with later cardiac development including α-sarcomeric actinin and α-myosin heavy chain were not observed in freshly isolated $Sca1^{+}$ cardiac side population cells. The $CD31^{+}/Sca1^{+}$ cardiac side population cells comprised the majority of total cardiac side population cells , only 10% were CD31-/Sca1+. When co-cultured with adult cardiomyocytes, CD31-/Sca1+ cardiac side population cells showed evidence of electromechanical coupling with the adult cardiomyocytes and expression of the gap junction protein connexin 43. 10% showed evidence of sarcomeric organisation together with spontaneous contraction and calcium transients, providing further support for a cardiomyocyte phenotype. In contrast $CD31^{+}/Sca1^{+}$ cardiac side population cells and also bone marrow side population cells did not show these features. As yet clonality and self renewal of these cells has not been determined and in vivo transplantation work is also awaited.

One approach to identifying putative stem cells is to examine their ability to form three-dimensional aggregates containing both self renewing cells and differentiated progeny.

This approach has proved particularly useful in the study of neural stem cells, where 'neurospheres' have been produced (Reynolds and Rietze, 2005). Using this approach in respect of putative cardiac stem cells, several groups have described the production of 'cardiospheres' from mixed populations of cells called 'cardiosphere cells' (CSs) isolated from adult heart (Messina et al., 2004; Smith et al., 2007). Heart specimen biopsies were digested and cardiospheres were cultured. These consisted of spherical multicellular clusters which consisted of many proliferative cells expressing stem cell antigens, and other cells towards the periphery of the sphere undergoing spontaneous cardiac differentiation. Cardiosphere cells were found to be composed of clonally derived cells which had the ability to self renew. Both human and mouse cardiosphere cells were found to express c-kit, Sca-1 and CD34 with few expressing CD31. They were negative for CD45. Some cells in the cardiosphere were found to express markers of cardiac differentiation including cardiac troponin I and myosin heavy chain. When dissociated into single cells and cultured on collagen coated dishes cardiosphere derived cells from mouse heart assumed a cardiomyocyte morphology and began to spontaneously contract. *In vivo* injection of these cells into infarcted myocardium showed no subsequent change in infarct size, however it was reported that bands of regenerating myocardium were present in those hearts which received the cardiospheres. Hence cardiospheres appear to be a mixture of cardiac stem and progenitor cells and although they demonstrated some regenerative potential *in vivo*, it is difficult to ascertain exactly which cell type was responsible for this. The authors postulate that the cardiosphere could in effect act as a stem cell niche providing support for the progenitor cells. An important point shown however was the potential to isolate cells from small fragments of cardiac tissue which could then be expanded *in vitro* without losing their differentiation potential.

Taken collectively this data provides an argument that there may be cell populations in the heart that could be putative stem cells or progenitor cells. It is not certain whether these cells contribute to either normal cardiac homeostasis or response to injury, however in the model used by Hsieh et al the suggestion is that their contribution would primarily be the latter (Hsieh et al., 2007). In summary the heart does appear not to be static , but a very dynamic organ. Although the heart has a poor ability to regenerate in normal

circumstances post infarct, the magnitude of this specific pathological insult may exceed any endogenous repair capacity. Certainly there is evidence from other tissues, such as intestine, which are rich in endogenous tissue specific stem cells, showing a poor response to such a severe insult as infarction and therefore failure to regenerate after such an injury should not be equated with the absence of stem cells (Murry et al., 2006). This outcome of ischemic injury could well be because resident stem and progenitor cells within the infarct die, and other local stem cells may be inhibited by the acute inflammatory processes at the time of a myocardial infarct or may be unable to mobilise to the damaged area (Santini et al., 2007; Segers and Lee, 2008). Although myocardial infarcts do not appear to regenerate effectively spontaneously, it appears that the endogenous repair and regenerative mechanisms may be manipulated and exploited to achieve this objective. Local growth factor activation of cardiac stem cells within the myocardium have been shown to rescue hearts subject to ischaemic injury and help to reconstitute myocardium and function of the heart as described below (Linke et al., 2005; Santini et al., 2007; Urbanek et al., 2005).

1.5 Studies using proregenerative models

From the evidence cited above it is suggestive that primitive cells with regenerative abilities may reside in the heart and under favourable conditions may have the ability to influence repair and regeneration. However it is clear that they fail to respond under normal circumstances to prevent the extent of damage which ensues following an acute ischaemic insult. The reason for this is not clear. Urbanek et al aimed to explore the concept that if properly activated, cardiac stem cells may be able to contribute to cardiac regeneration in these circumstances by using insulin-like growth factor (IGF-1) and hepatocyte growth factor (HGF) to recruit and activate primitive cells in the heart (Urbanek et al., 2005) . IGF-1 is a cytokine which has been reported to be mitogenic, anti-apoptotic and necessary for neural stem cell growth (Arsenijevic et al., 2001). It has also been found to promote myocyte formation and reduce death after infarction (Li et al., 1999). HGF stimulates cell migration by expression of metalloproteinases which breaks down extracellular matrix and enables cell migration (Powell et al., 2001). If cardiac stem

cells express receptors to these growth factors then HGF and IGF-1 may have complementary functions in the translocation and proliferation of putative stem and progenitor cells in the heart. Urbanek et al defined cardiac stem cells (CSCs) in this study as those cells found in the heart which expressed c-kit, MDR1 or Sca-1. They found that CSCs possess the receptor for HGF, and IGF-1. In vitro studies showed that HGF had a chemoattractant effect on CSCs and both HGF and IGF-1 decreased apoptosis of CSCs *in vitro* (Urbanek et al., 2005).

CSCs were shown to be responsive to treatment with HGF and IGF-1 *in vivo*. After induction of myocardial infarction and direct intra-myocardial injection of HGF and IGF-1 into the peri-infarct area CSCs which had been labelled with EGFP were found to translocate to the infarct area and differentiate into cardiomyocytes together with arterioles and capillaries which would help to support the newly forming myocardium. 84% of myocytes and vessels in the regenerating area were positive for BrDU at 16 days post infarct indicating they had undergone recent cell division, and treated hearts showed improved haemodynamics and reduced mortality (Urbanek et al., 2005). Combined with the in vitro studies described above, this in vivo data suggested that at least in mice, HGF and IGF-1 may play a role in regeneration in the heart, potentially employing CSCs. These observations were extended to larger mammals. Linke and colleagues tested the effects of HGF and IGF-1 in dogs after myocardial infarction (Linke et al., 2005). It was found that activation of the CSCs by intramyocardial injection of HGF and IGF-1 resulted in formation of myocytes (expressing α-sarcomeric actin, cardiac myosin heavy chain, troponin I and α-actinin) and coronary vessels within the infarct area. Connexin 43 was also present showing evidence for electrical coupling. The number of CSCs significantly increased in the area adjacent to the infarct and in remote areas, as well as the number of cells which were actually in the cell cycle. Treated hearts showed improved haemodynamic function. These studies employed direct injection of cytokines. In order to regulate expression of these cytokines in a tissue-specific manner, several studies have adopted a transgenic approach.

α-MHC/mIGF-1 transgenic mice, which carry a cardiac restricted expression of muscle specific IGF-1 transgene (mIGF-1) were shown to restore cardiac function in infarcted hearts by blocking scar formation and enabling myocardial reconstruction (Santini et al., 2007). This transgenic mouse had a rat mIGF-1 cDNA driven by the mouse α-myosin heavy chain promoter to restrict expression of mIGF-1 to the mouse myocardium. Restorative capacity of mIGF-1 transgenic hearts was analysed by ligation of the left coronary artery. In wild type mice, infarcts were characterised by progressive formation of fibrous tissue accompanied by functional impairment when measured at 1 month and worsening at 2 months. In contrast, infarcted mIGF-1 transgenic hearts showed a moderate but significant reduction in function after 1 month, with no significant changes after 2 months compared with wild type ligated mice. The mIGF-1 mice also showed a significantly smaller infarct size and reduced scar formation compared with control hearts at 2 months post surgery (figure 1.3). There may be a number of mechanisms for these differences, including the role of inflammation. After myocardial injury there is a cascade of inflammatory events including activation of complement, chemokine upregulation and activation of cytokine cascades (Frangogiannis et al., 2002). Twenty four hours after induction of injury wild type hearts showed a significant increase in the proinflammatory cytokines IL-6 and IL1β, however in the mIGF-1 transgenic hearts levels were unchanged. Also, anti-inflammatory cytokines IL-4 and IL-10 were found to be down regulated in wild type hearts after injury compared to the mIGF-1 transgenic hearts. IL-10 normally suppresses injury and blocks scar formation (Liechty et al., 2000). It is known that many of the cellular growth responses attributable to IGF-1 are mediated by activation of the PI3K/Akt/mTOR phosphorylation cascade, leading to prosurvival signalling in vivo (Matsui et al., 2001). Akt is known to act as a protective agent in cardiomyocyte survival and function (Chao et al., 2003). Phosphoprotein profiling showed that Akt phosphorylation was not activated in mIGF-1 transgenic hearts and phosphorylation levels of downstream mTOR (mammalian target of rapamycin) and p70S6K intermediates were unaffected. However in mIGF-1 transgenic mice there was phophorylation of S6 ribosomal protein at 2, 4 and 6 months compared to wild type hearts. This relative activation of S6 appeared to be independent of Akt signalling which decreased postnatally in wild type and mIGF-1 transgenic hearts.

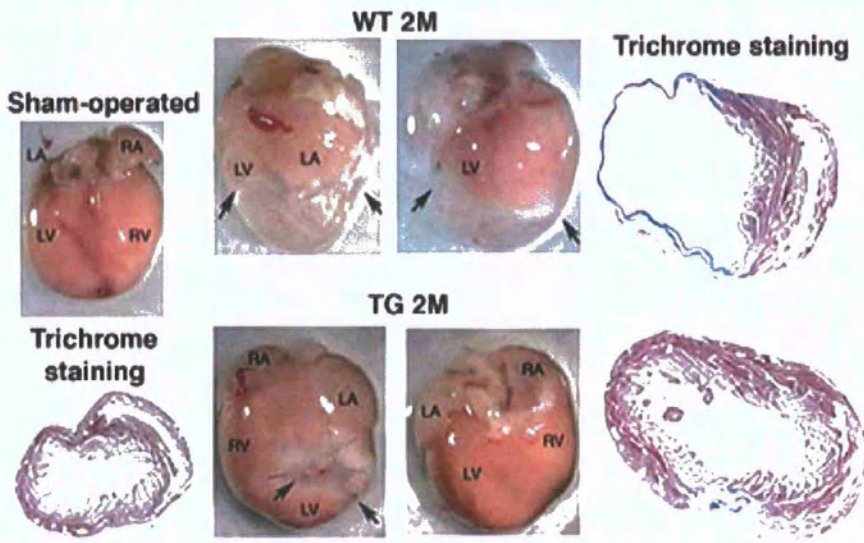

Figure 1.3 Enhanced cardiac repair in mIGF-1 transgenic mice after myocardial infarction.

Wholemount histological analysis of sham operated control (WT) heart (left) and infarcted hearts of WT and transgenic (TG) (right) 2 months after myocardial infarction. Arrows indicate fibrotic tissue. LA (left atrium); LV (left ventricle); RA (right atrium); RV right ventricle. Histological analysis by trichrome staining for collagen is shown for each treatment. Adapted by permission from (Santini et al, 2007).

PI3K (3-Phosphoinositide dependent protein kinase-1) also signals through PDK1 (pyruvate dehydrogenase kinase). This can directly phosphorylate p70S6K independently of Akt (Pullen et al., 1998) and promote survival through other intermediates such as SGK1 (serum and glucocorticoid regulated kinase), a PI3K dependant kinase that is expressed in the heart and promotes survival in cardiomyocytes (Aoyama et al., 2005). Note that increased levels of phosphorylated PDK1 were found in mIGF-1 transgenic hearts and it was shown to complex with SGK1 in mIGF-1 transgenic hearts but not in wild type hearts. Also, no interaction between PDK1 and any of the Akt isoforms was detected in mIGF-1 transgenic hearts , indicating that the cardiac signalling cascade induced by mIGF-1 was independent of Akt and p70S6K and preferentially used the PDK1/SGK1 pathway to increase protein synthesis and growth. This intracellular signalling cascade postulated by Santini et al could be the basis for the improved healing capacity conferred on the transgenic hearts (figure 1.4). Following on from this a TUNEL assay was used to show decreased apoptosis in the area surrounding injury in the mIGF-1 transgenic hearts in comparison to wild type. Increased levels of mitochondrial uncoupling protein UCP1 (uncoupling protein1) in transgenic hearts was also found post cardiac injury indicating some degree of protection from ischaemic injury possibly by limiting damage which may be caused by oxygen free radical release (Hoerter et al., 2004).

BrDU was used to assess cell turnover in the peri-infarct area in the mIGF-1 transgenic hearts. At 1 month post infarct, the number of proliferating cells in the infarct border zone was significantly higher in mIGF-1 transgenic hearts compared to wild type. Although they found incorporation of BrDU in cardiomyocyte nuclei there was also abundant staining in cells which were not muscle. The origin and fate of these cells were not investigated however it was thought they may contribute to the mIGF-1 mediated recovery. There was no evidence of hypertrophy in mIGF-1 transgenic or wild type cardiomyocytes.

Hence it was postulated that the mIGF-1 transgenic mice were able to resolve inflammation more rapidly and also promoted prosurvival signals which enabled a more

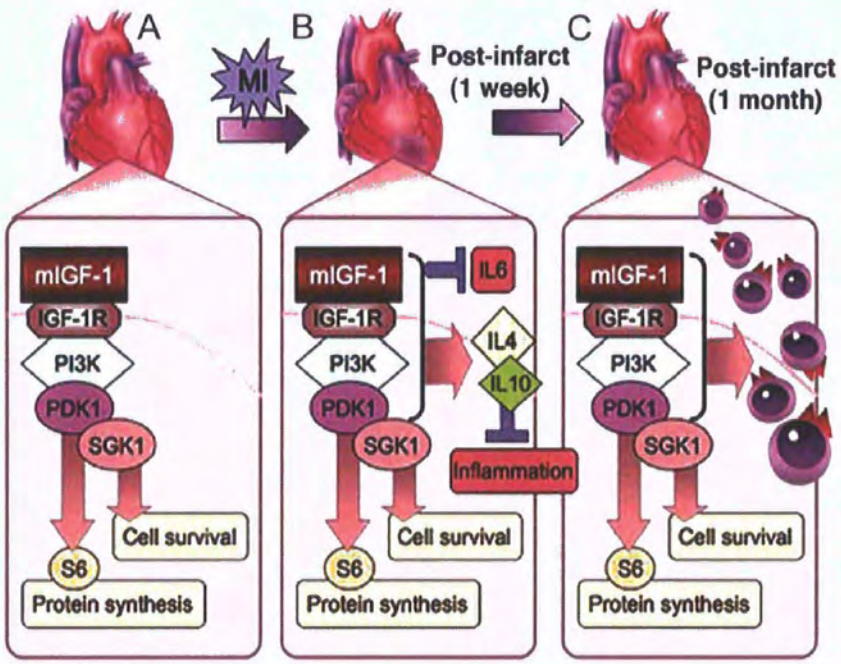

Figure 1.4 Mechanisms of mIGF-1 induced recovery in injured hearts.

(A) Transgenic mIGF-1 induces protein synthesis and cell survival pathways in cardiac tissue through a PDK1/SGK1 phosphorylation cascade, bypassing Akt, mTOR and p70S6K intermmediates. (B) After myocardial infarction (MI) pathways induced by mIGF-1 result in rapid repression of proinflammatory cytokines such as IL6 that promote fibrosis and cardiac decompensation while activating cytokines such as IL4 and IL10 that resolve inflammation. (C) This permissive tissue environment enables efficient cardiac wall replacement, as shown by increased proliferation of cells at 1 month after injury, and functional repair in mIGF-1 transgenic hearts. Adapted with permission from (Santini et al, 2007).

substantial repair to take place in comparison to wild type controls. Although there was no direct evidence that reduction of inflammation facilitated stem or progenitor cell mediated repair, one mechanism for the poor response of the putative stem and progenitor cells in the heart to engage in regeneration may have been due to the inhibitory effect of the intense inflammatory response at the time of infarct. Modulation of the inflammatory response in ischaemic injury has been shown to be a potentially useful target to reduce injury at the time of ischaemia and possibly promote repair.

1.6 The inflammatory response in myocardial ischaemia and its modulation

Inflammation plays a major role in the myocardial necrosis resulting from occlusion of a coronary artery during myocardial infarction. In order to look at strategies of how to reduce damage or promote repair post infarct one must examine the pathophysiology of this process. Ischaemia results in an intense inflammatory reaction as reviewed by Frangogiannis (Frangogiannis et al., 2002). This inflammatory reaction is known to be augmented if the infarcted tissue is then reperfused. Initial attempts to target inflammation were not particularly specific. Corticosteroids were used in animal models of myocardial ischaemia to try to ameliorate the inflammation (Libby et al., 1973). This initial work in dogs was shown to actually decrease the infarct size. Due to these promising results clinical studies were undertaken using methylprednisolone in humans post MI (Roberts et al., 1976). Unfortunately this appeared to inhibit the number of infiltrating leukocytes and delayed collagen deposition which is a vital part of the immediate healing process, resulting in a negative outcome. Hence if the inflammatory response is to be targeted it would be important to attempt to ameliorate the inflammatory response without interfering with myocardial healing.

Neutrophils have been shown to be instrumental in the myocardial injury sustained at the time of an ischaemic insult. Neutrophils become trapped in microvasculature exacerbating ischaemic damage due to capillary plugging (Engler et al., 1986), as well as mediating damage by the release of toxic products including proteolytic enzymes and

reactive oxygen species (Frangogiannis et al., 2002). Once ischaemic damage ensues, neutrophils eventually adhere to endothelium, by initially rolling along the surface and eventually slowing until they change shape and extravasate into extravascular tissue (Adams and Shaw, 1994). This is mediated by a family of adhesion molecules called the selectins, E-selectin, P-Selectin and L-Selectin (McEver et al., 1995). Once the neutrophils are rolling along the endothelium in response to the selectins, another set of adhesion molecules called the β2 Integrins are necessary for adhesion and migration of the leukocytes. β2 integrins are heterodimeric glycoproteins constitutively expressed on the surface of neutrophils. Adherence of neutrophils to endothelium is mediated by interaction with its counter ligand ICAM-1 on endothelium (Jordan et al., 1999). Once neutrophils have adhered to the endothelium, the neutrophils can then migrate into the inflamed tissue. Chemokines at the site of inflammation are vital to facilitate neutrophil chemotaxis. IL-8 and C5a are both increased at sites of inflammation (Ivey et al., 1995). Also, activated neutrophils release Leukotriene B4 (LTB4), a potent chemotactic agent and Platelet Actvating Factor (PAF) is produced from endothelial cells in response to thrombin, promoting neutrophil adhesion to endothelial cells (Montrucchio et al., 1993). Inhibition studies of PAF have shown a reduction in neutrophil infiltration in a rabbit model of infarction (Morgan et al., 1999). In addition, monoclonal antibodies against L-selectin and P-selectin have been shown to reduce myocardial necrosis and reduce neutrophil accumulation in a feline model of ischaemia (Ma et al., 1993; Weyrich et al., 1993).

Nitric oxide (NO) has also been shown to be able to modulate the neutrophil mediated damage post infarct. NO is formed from vascular endothelium and can directly affect the endothelium and neutrophils so as to reduce the extent of injury post infarct. NO is known to inhibit superoxide production, degranulation and adherence to endothelium of neutrophils (Kubes et al., 1991; Sato et al., 1996). At the level of the endothelium nitric oxide attenuates up regulation of P-Selectin, E-Selectin and ICAM-1 (De Caterina et al., 1995; Ohashi et al., 1997). Hence NO has been reported to be able to provide some cardioprotection from neutrophil mediated ischaemic injury.

As well as showing the importance of the role of neutrophils in mediating myocardial injury these studies also suggest a therapeutic role in manipulating this neutrophil response in an ischaemic environment. Superoxide anions are generated from the neutrophil membrane associated NADPH oxidase (Jordan et al., 1999) which can be activated by soluble pro-inflammatory cytokines including C5a. C5a is a complement product which is formed as part of the complement cascade which is activated at the time of myocardial ischaemia.and is a potent chemoattractant for neutrophil recruitment (Guo and Ward, 2005).

1.7 Complement activation

The activation of the complement cascade in myocardial infarction was first demonstrated by Hill and Ward (Hill and Ward, 1971). Traditionally the complement system has been seen as a central part of the innate immune system in host defence against invading pathogens and in clearing cell debris, however complement activation is now known to be involved in the pathogenesis of many inflammatory disorders including the injury sustained in myocardial ischaemia and ischaemia reperfusion.

The complement system refers to a series of proteins circulating in the blood. The proteins circulate in an inactive form but once triggered they become sequentially activated as shown in figure 1.5. Three pathways of complement activation have been recognized, the classical, alternative and lectin-binding pathways. The classical pathway is activated by antigen-antibody complexes. The alternative pathway is directly initiated by surface molecules containing carbohydrates or lipids and the lectin binding pathway is triggered by binding of either mannose-binding lectin protein or ficolin to bacterial/fungal carbohydrate structures (Guo and Ward, 2005). All complement pathways appear to be involved in ischaemic injury (Guo and Ward, 2005) and all eventually have the same functions:

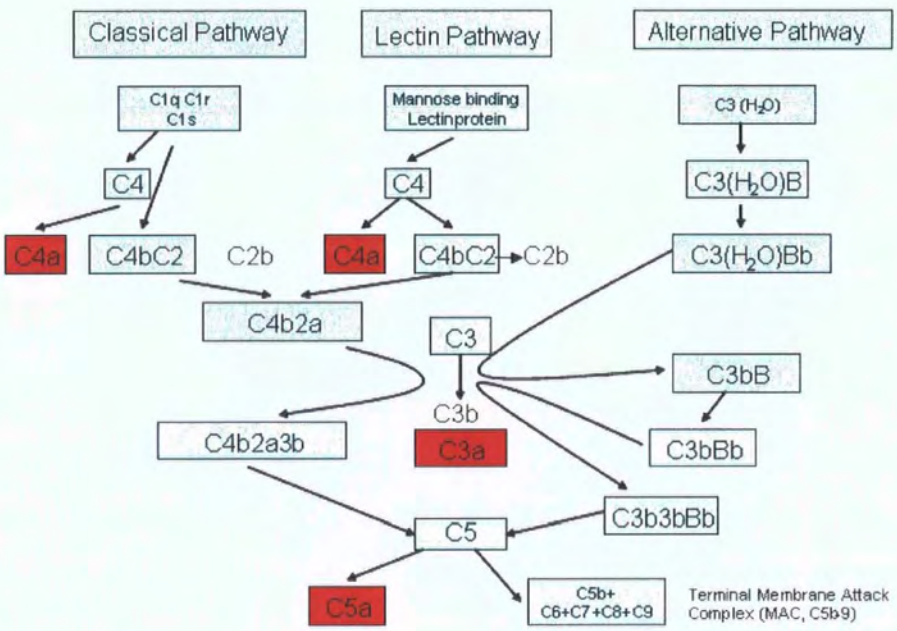

Figure 1.5 The complement pathway.

Illustration of the complement activation products C3a, C4a , C5a and the membrane attack complex (C5b-9). C3a, C4a and C5a are all anaphylotoxins. C5b-9 can cause direct cellular injury and lysis of bacteria. Figure adapted from (Guo and Ward, 2005).

1. Trigger Inflammation
2. Chemoattraction for phagocytes
3. Opsonisation (promote attachment of antigens to phagocytes)
4. Cause lysis of gram negative bacteria
5. Activate B cells
6. Remove harmful immune complexes from the body

The activation of the complement pathway is central to the body's defence against infection. Unfortunately the complement system cannot distinguish self from non-self and therefore activation of this cascade can result in local tissue injury (Wang, 2006)., as occurs during myocardial ischaemia.

All of the complement pathways converge at the complement proteins C3 and C5 (Wang, 2006). The C3 and C5 proteins are cleaved by multisubunit convertases. C5a is a potent anaphylotoxin for neutrophils, monocytes and macrophages, whereas C5b goes on to form the C5b-9 membrane attack complex (MAC) which can cause lysis of cells and bacteria. C3a is much less potent than C5a. C3b is very important in opsonisation of immune complexes and invading organisms. C5a increases expression of CD18 on neutrophils and increases P-Selectin expression on endothelium (Foreman et al., 1996; Foreman et al., 1994), contributing to neutrophil accumulation.

Early studies showed that the complement components C1q, C3, C4 and C5 have been identified in infarcted tissue (Pinckard et al., 1980). Early work recognizing the complement cascade as a target for reducing the extent of injury after coronary artery occlusion used cobra venom factor (CVF) to inhibit formation of C3. Maroko and colleagues found that CVF given within 30 minutes of coronary occlusion resulted in a decreased infiltration of neutrophils and a reduction in the size of the infarct as evaluated by measuring Creatine Kinase (CK), (Maroko et al., 1978). Since this study there has been numerous other work attempting to reduce the level of inflammation and damage after myocardial ischaemia by attempting to inhibit parts of the complement cascade. One complement inhibitor which has been used in many organ systems in ischaemia and

reperfusion injury is recombinant sCR1, which inhibits activation of C3, a complement protein common to all pathways of complement activation. This therefore blocks the generation of C3a , C5a and the MAC. sCR1 has been shown to reduce infarct size and reduce accumulation of neutrophils within the infarct area (Zacharowski et al., 1999). This cardioprotective role has been demonstrated by other investigators also in models of myocardial ischaemia (Shandelya et al., 1993a; Weisman et al., 1990). An inhibitor of C1 blocks the classical pathway of complement activation and has been shown to reduce tissue injury in liver, brain and myocardial ischaemia reperfusion injury (Bergamaschini et al., 2001; De Simoni et al., 2003; Horstick et al., 2001). C1 inhibitor has also been used in human post thrombolytic therapy after myocardial ischaemia reperfusion, showing a significant reduction in troponin T cardiac enzyme release in the treated group(de Zwaan et al., 2002).

1.7.1 C5/C5a as a potential target for therapy

C5 and its cleavage product C5a have been extensively studied in experimental models of ischaemia and ischaemia reperfusion. C5a is a potent anaphylotoxin and works in concert with neutrophils. C5 is the final step prior to formation of the terminal MAC complex (which has its own ability to cause direct myocardial injury (Vakeva et al., 1998)) Complement inhibition can be advantageous and disadvantageous as it does have an important role in host defence, particularly C3b in opsonisation of foreign organisms and debris. Hence the C5/C5a axis is a particularly attractive target for anti-inflammatory therapy because of its central role in neutrophil chemotaxis, its role in formation of the terminal MAC complex and because it is downstream of C3, therefore any inhibitor acting at this level would avoid the inhibition of C3 cleavage and formation of the important opsonic fragment C3b.

As reviewed by Gerard (Gerard et al 1994), the receptor for C5a is widely expressed on inflammatory cells, particularly neutrophils with 100000 to 200000 C5a receptors per human neutrophil. C5a reversibly binds to C5a receptor by interaction of the positively charged N-terminal disulphide linked core of C5a and the negative charged N terminal

domain of its receptor and also by the positively charged C-terminal tail of C5a with the interhelical region of its receptor.

1.7.2 Targetting the C5a receptor using small molecules

Kidney

Renal ischaemia/reperfusion is a significant complication of vascular surgery of the aorta and kidney. In this study a peptide antagonist against C5aR was used in rats subject to renal ischaemia for 60 minutes followed by reperfusion for 60 minutes. Effects were measured by measuring tissue levels of myeloperoxidase (MPO) (a measure of neutrophil infiltration), serum creatinine levels (a measure of renal dysfunction) and renal histopathology. The C5aR antagonist was given 15 minutes prior to occlusion of the renal blood vessels IV or by oral gavage 60 minutes prior to occlusion. The antagonist was effective when given orally and IV. Treated animals had a reduced incidence of haematuria, tissue levels of MPO and reduced serum creatinine and less severe ischaemic changes on histopathology (Arumugam et al., 2003).

Small Intestine

The same small molecule antagonist has also been used in ischaemia reperfusion injury in the rat small intestine. Intravenous and oral dosing was used in an ischaemia (30 minutes) reperfusion (120 minutes) model for small intestine. Histological analysis showed markedly reduced mucosal layer damage in treated animals compared to untreated animals. Levels of haptoglobin, an acute phase response protein was significantly reduced in treated animals compared to control and also levels of aspartate aminotransferase (AST), which reflects liver parenchymal cell integrity was reduced in the treated group. Histopathology confirmed the findings of reduced injury in the treated group by demonstrating a reduction in mucosal injury. This demonstrated the importance of C5a in the ensuing injury post ischaemia reperfusion in the small intestine (Arumugam et al., 2002)

Liver

Small molecule peptide C5aR antagonist has also been used in a model of hepatic ischaemia reperfusion. The C5aR antagonist was either given systemically 15 minutes prior to occlusion of the hepatic vessels or orally 60 minutes prior to occlusion. 60 minutes of occlusion was followed by 4 or 24 hours of reperfusion. The levels of liver enzymes AST, ALT and LDH, and also MPO were significantly reduced in the treatment group in comparison to the vehicle treated group. In keeping with this the numbers of circulating neutrophils was significantly reduced in treated animals with evidence of reduced histopathological changes indicating liver necrosis and improved survival (Arumugam et al., 2004)

1.7.3 Targetting C5a using antibody

Heart

An antibody against the complement component C5a has been used in the setting of myocardial ischaemia reperfusion in a porcine model (Amsterdam et al., 1995). Ischaemia was induced by a 50 minute occlusion of the left anterior descending coronary artery (LAD) followed by 3 hours of reperfusion (Amsterdam et al., 1995). The antibody used was shown in vitro to block porcine C5a-induced neutrophil chemotaxis and degranulation. It was administered intravenously 10 minutes prior to occlusion of the LAD. The infarct proportion was calculated by calculating the percent weight of infarcted myocardium as a percentage of the whole heart using triphenyl tetrazolium chloride to identify the infarcted area. Also MPO activity and neutrophil accumulation were used as a measure of neutrophil infiltration. Results from this study showed that although the treated group had a significant reduction of myocardial infarct size, this was not associated with a reduction in neutrophil infiltration. The authors postulate that the fact that the neutrophils were not affected may be due to operation of other pathways such as PAF (platelet activating factor). Note that there is evidence from a study which used an isolated ischaemic heart preparation that neutrophils can accumulate in the myocardium

during reperfusion without causing injury (Shandelya et al., 1993b). In this study, if complement was present or if C5a was provided then there was marked neutrophil mediated damage, indicating the importance of complement in ensuing injury.

1.7.4 Targetting C5aR using a specific C5aR antagonist

Kidney

In this study a specific C5aR antagonist was used in the setting of renal ischaemia reperfusion in a mouse model. Ischaemia was induced for 45 minutes and then the kidney was allowed to reperfuse for 24 hours. Renal dysfunction (assessed by measuring serum creatinine) was significantly improved in the group that received the C5aR antagonist. Infiltration of neutrophils was significantly reduced also in the treatment group. In addition the experiment was repeated in neutrophil depleted mice. Neutrophil depletion did not protect the kidney against ischaemia reperfusion injury, with similar renal function being maintained in neutrophil depleted animals and control treated animals, thus suggesting that neutrophils were not essential for renal dysfunction in the course of renal ischaemia reperfusion injury. However application of the C5aR antagonist protected neutrophil depleted mice from renal failure, indicating that infiltration of neutrophils alone is not sufficient to mediate renal ischaemia reperfusion injury. The results do however give evidence that activation of the complement system and in particular the C5aR pathway is instrumental in induction of renal dysfunction in ischaemia reperfusion injury (de Vries et al., 2003).

1.7.5 Targetting C5 using antibody

Heart

Anti-C5 therapy in the setting of myocardial ischaemia reperfusion in rats resulted in decreased infarct size and reduced neutrophil infiltration. Ischaemia was induced for 30 minutes and reperfusion for 4 hours. Neutrophil analysis was done by measuring MPO,

showing a significant reduction in the group treated with antibody. Creatine Kinase (CK) was used as a biochemical marker of myocardial injury. The group treated with antibody showed a reduction in CK levels indicating attenuation of myocardial damage. Treatment with the anti-C5 antibody 60 minutes prior to occlusion of the left coronary artery showed a significantly reduced infarct size. In addition a group of hearts which were subject to 4 hours of ischaemia and no reperfusion was analysed. This demonstrated also a significant reduction in infarct size. Another group which were reperfused for 7 days showed again a reduced infarct size after 1 bolus injection of the antibody prior to reperfusion (Vakeva et al., 1998).

1.7.6 Clinical studies targeting C5

The first human clinical trial of an antibody specific for the C5 complement product was undertaken in the setting of patients who were being subject to cardiopulmonary bypass as part of a surgical revascularization procedure (Fitch et al., 1999). Cardiopulmonary bypass elicits a systemic inflammatory response that can cause tissue injury and lead to long term clinical co-morbidity (Wan et al., 1997). It is known that exposure of blood to bioincompatible surfaces of the extracorporeal circuit as well as tissue ischaemia and reperfusion associated with the procedure results in activation of humoral pathways of inflammation including complement (Hall et al., 1997). The antibody was delivered prior to initiation of bypass. Serum levels of C3a were no different between treatment and control group, however serum levels of C5b-9 were significantly reduced in the antibody treatment arm. CD11b expression on neutrophils was significantly reduced as was the total CK-MB , an enzyme normally used as a marker of myocardial injury, demonstrating that this C5 specific antibody against C5 was a safe and effective inhibitor of pathological complement activation in patients undergoing cardiopulmonary bypass.

This study was followed by the COMPLY (Mahaffey et al., 2003) and COMMA (Granger et al., 2003) studies which examined the effect of a monoclonal antibody against the complement component C5. A single chain fragment of monoclonal antibody against C5 called Pexelizumab was used. This antibody specifically binds to C5 with high

affinity and prevents cleavage and generation of activated C5a and C5b-9. In this study complement inhibition with pexelizumab as an adjunct to fibrinolysis had no measurable effect on the primary end point infarct size as measured with CK-MB up to 72 hours or on the 90 day clinical endpoint reporting death, congestive heart failure, shock or stroke despite the fact that pexelizumab completely inhibited complement activity for 24 hours by using an infusion . In parallel to the COMPLY study, the COMMA study was carried out (Granger et al., 2003). Pexelizumab was used in the setting of patients with acute MI undergoing primary percutaneous intervention. Infarct size measured by CK-MB was not significantly different between the 2 groups however 90 day mortality was significantly reduced in the group which had received the anti C5 antibody bolus and infusion, suggesting that pexelizumab may benefit patients through alternative mechanisms.

Subsequently a randomized control trial comparing placebo with Pexelizumab in the setting of CABG surgery did not show a significant risk reduction in the endpoints of death or MI, but Pexelizumab was associated with a significant risk reduction 30 days after the procedure (Verrier et al., 2004).

More recently a randomized double blind placebo controlled trial was undertaken using Pexelizumab in patients undergoing primary PCI post MI, which did not show any difference in the composite endpoints of death, shock or heart failure (Armstrong et al., 2007)

In chapter 4 of this thesis the effect of a human C5aR mAb on inflammation and infarct size is tested in the setting of myocardial infarction.

1.8 Overall conclusions and aims

As evidenced by the literature reviewed in this chapter, an ever increasing number of publications have emerged relating to cells in the heart which may be able to contribute to cardiac repair and regeneration. Despite the fact that a number of different cells have been isolated from mammalian heart using different phenotypic strategies which have

shown potential in this respect, there is no consensus as to which cell may be most useful. There is a recent body of evidence however which has documented the involvement of epicardial-derived cells in the regeneration process in zebra fish, and together with the findings that cells expressing PDGFRA are found in the epicardial layer of the mammalian embryo and in the interstitium of adult heart, these cells are an interesting candidate population to investigate in terms of their potential to contribute to cardiac repair and regeneration.

Although putative stem cell populations have been isolated from adult heart, the regenerative ability of the heart has been shown to be poor under circumstances of ischaemic injury. One reason for this could be the harsh inflammatory environment at the time of an acute infarct. It has been shown that targeting this inflammatory response, particularly at the C5/C5a axis, has had mixed results in improving outcomes after myocardial infarction. Hence an antibody against the C5aR which has not been used before in the setting of myocardial infarction was an attractive agent to use.

To tackle these issues a robust model of myocardial infarction was necessary in the mouse particularly as an increasing variety of transgenic models are becoming available, which have proved invaluable in this area of research. Although rodent models of myocardial infarction have been used before, they have been associated with significant levels of death and variability in size of infarct induced (section 3.8)

Aims of this thesis:

1. Develop and characterise a more reproducible, consistent murine model of myocardial infarction with low mortality.
2. Use this to investigate the role of a human C5aR mAb in inflammation as a route to possible therapy.
3. Investigate stem cell activity in the adult heart using a transgenic approach.

Chapter 2

Materials and Methods

2.1 Resin casts to demonstrate coronary vasculature

Mice were anaesthetized and ventilated as described in section 2.2. The left femoral vein was injected with 200IU heparin (BBL HK08264). A thoracotomy was performed as described in section 2.2 and the great vessels to the head and neck were ligated. A total of 5ml methyl methacrylate casting compound (Dow Corning, USA) was then injected into the left atrium. The heart was excised and placed on ice. The heart was then left in 30% potassium hydroxide overnight to digest the tissue, washed in water and air dried for examination under microscopy (Leica MZ6)

2.2 Mouse model of Myocardial Infarction

2.2.1 Anaesthesia

1. Anaesthesia was induced using ketamine (100mg/kg) (Parnell Laboratories, Australia) and xylazine (20mg/kg) (Troy Laboratories, Australia) via intraperitoneal injection. If further anaesthesia was necessary during the procedure, halothane 2% was used.
2. Once fully anaesthetised the left anterior chest wall was shaved.
3. The mouse was intubated using a 20G cannula (Insyte BD) (figure 2.1).
4. Ventilation was set at 110 breaths per minute, with a tidal volume of 0.1-0.2 ml (0.008ml/g) (Harvard Minivent D79232).
5. Oxygen flow was adjusted prior to the procedure to give an inspiratory pressure of approximately 15cm water.
6. The mouse was positioned on a heating pad supine with a slight rotation to its right side (figure 2.2)
7. Moisturising gel (Delvet Pty Ltd, Australia) was applied to the eyes to avoid dehydration.

a)

b)

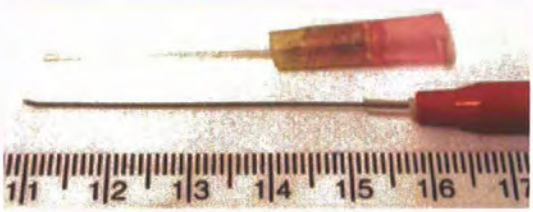

Figure 2.1 Intubation technique.

a) The larynx of the mouse was illuminated from an external light source prior to intubation. (b) A 0.64mm diameter guidewire was used to guide insertion of the 20G cannula. Scale shown in cm.

Figure 2.2 Operative set up showing mouse position and thoracotomy. Scale bar = 1cm.

2.2.2 Surgery

1. The initial transverse incision was made 0.8mm below the left axilla approximately 1.5 cm long
2. Any obvious superficial vessels were coagulated at this stage.
3. A thoracotomy incision 1cm long was made in the 4th intercostal space, and a mini-retractor was used to expose the heart. (figure 2.2) At this stage an intraperitoneal injection of atropine (0.12mg/10g) (Pfizer) was given to counteract the bradycardia induced due to anaesthesia.
4. At all stages meticulous haemostasis was essential due to the small blood volume in the mice.
5. The left coronary artery usually emerges from under the tip of the left atrium and courses towards the apex. The pericardium and associated fat was stripped and stretched over the retractor to suspend the heart in a 'cradle'.
6. A 7/0 prolene suture (Ethicon 8735H) was carefully used to pass around the left coronary artery. The major pitfall to avoid here was intraventricular puncture which would be easy to do especially as the heart beats at between 400-600 beats per minute.
7. This suture was then tied using a 4/0 silk buttress against the myocardial wall, to occlude the left coronary artery (figure 2.3).
8. The chest was then closed in layers. 6/0 prolene (Ethicon 8711H) was used to close the thoracotomy and also the skin.
9. When the thoracotomy was closed positive airway pressure was applied to the lungs to displace air and fluid from the chest cavity to reduce the risk of pneumothorax and haemothorax.
10. Antisedan (atipamezole hydrochloride) (0.05mg/20g) (Novartis Animal Health Pty Ltd)) was given subcutaneously (SC) to reverse effects of anaesthesia.
11. In addition 0.075mg/kg of buprenorphine (Pfizer) was given SC for analgesia and 0.1mg/20g frusemide (Aventis 40N276) SC.
12. The mouse was then observed until it had enough respiratory effort to be detached from the ventilator and extubated.

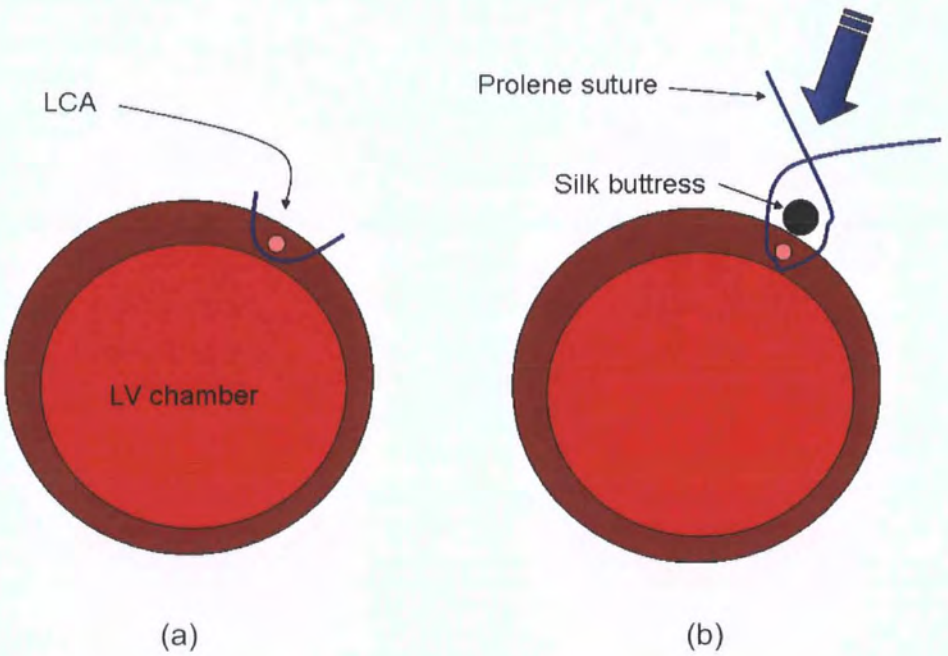

Figure 2.3 Schematic illustration of transverse section through the left ventricle

(a) This demonstrates the relations between the left coronary artery and the prolene suture.

(b) The 4/0 silk buttress suture was used to reduce the chance of the 7/0 prolene cutting through the myocardium. The blue arrow demonstrates the direction the suture is tied to compress the left coronary artery (LCA).

13. Mice were recovered in a warm cage placed on a heating pad with food and water ad libatum.
14. During the procedure monitoring was via continuous observation of limb reflexes, colour of mucous membranes, heart rate and any evidence of spontaneous respiratory effort.
15. On day 1 post surgery a further dose of buprenorphine and frusemide was administered as above.
16. Mice were observed and weighed daily and given daily injections of frusemide for the first 7 days.

2.3 Haematoxylin and Eosin staining

Sections stained had been snap frozen using Optimal Cutting Temperature Compound (OCT) (TissueTek 4583). Sections were initially fixed in 4% paraformaldehyde (PFA) (Sigma P6148) for 5 minutes and then stained for 10 minutes in Haematoxylin stain (Sigma MHS 16) followed by a 10 minute wash in running water. Sections were then immersed in Eosin solution for 2 minutes and then washed in running tap water before being taken through ascending alcohol solutions for 2 minutes each of 80%, 95% and 100% ethanol. The sections were briefly dipped in xylene and air dryed. Sections were mounted with Eukitt mounting solution (Calibrated Instruments Inc. USA) and cover slips added prior to viewing. Nuclei structures stained blue and cytoplasm stained light to dark red.

2.4 Tetrazolium method to demonstrate infarcted tissue

Tetrazolium staining was used to demonstrate infarcted tissue (figure 2.4). Triphenyl tetrazolium chloride (TTC) (Merck 1.08380.0100) is water soluble and colourless. It reacts with dehydrogenase enzymes in actively respiring tissue to form the pigment formazen. Formazen is deposited in healthy tissue and stains it brick red. Infarcted tissue is not actively respiring therefore the tetrazolium salt is deposited, staining the tissue

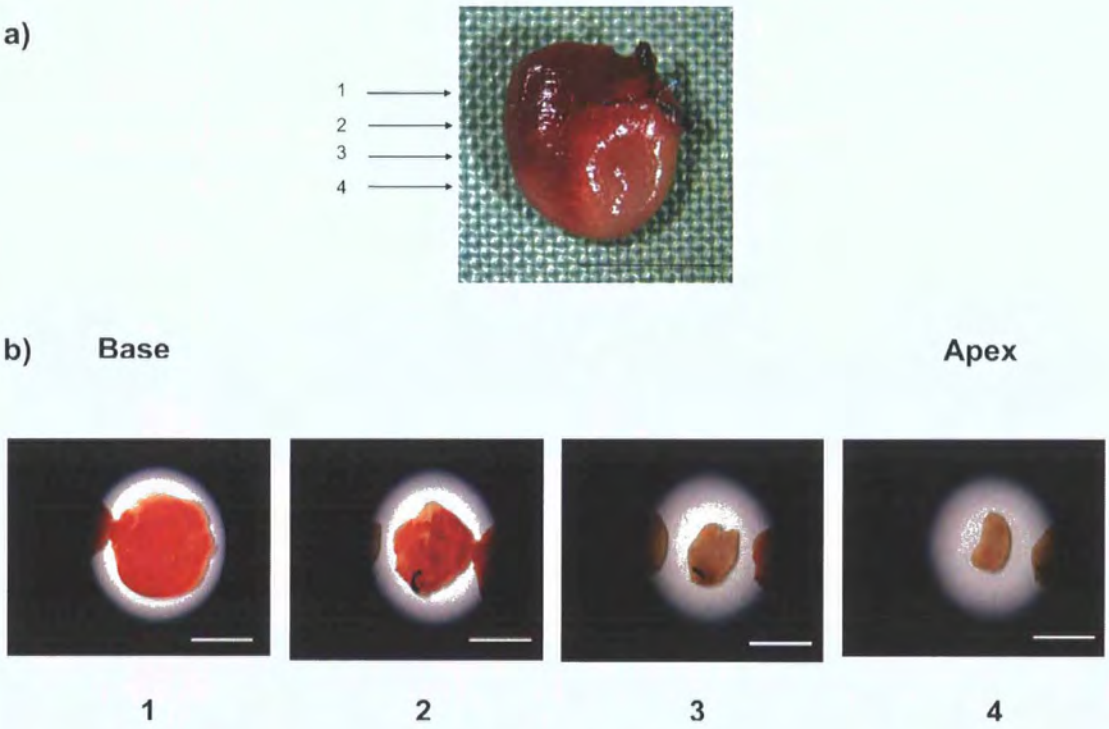

Figure 2.4 Demonstration of tetrazolium staining of the heart post MI.
(a) Schematic showing whole heart prior to sectioning. (b) Series shows serial sections of the heart 7 days post MI. It clearly demonstrates the white infarcted area below the level of the black silk suture which can be seen in panel 2. Scale bar = 5mm.

white (Gao et al., 2000; Michael et al., 1995). The tetrazolium staining method is an adaptation of the method described by Michael et al. (Michael et al., 1995).

1. After harvesting the heart, the atria were excised and the ventricles were wrapped in clear food wrap and placed in a -20^{0}C freezer for 1 hour. The tissues were wrapped to avoid freeze drying. The tissue is easier to cut when it is semi frozen and it also puts the tissue into rigor. If fresh slices are put into TTC the tissue becomes contracted and distorted. Freeze dried tissue will be tetrazolium negative.
2. Specimens were wrapped in Whatman γ1 filter paper and placed in a bowl.
3. 1.5% TTC made in 0.1M phosphate buffer pH 7.4 was poured into the bowl and covered with aluminium foil.
4. These bowls were then incubated for 30 minutes at 37^0. The specimens were turned once at 15 minutes.
5. Infarcted and non infarcted areas of the left ventricle were weighed separately.
6. Infarct size was expressed as a percentage of the left ventricle taking into account the weight of each specimen.

2.5 Myeloperoxidase assay

Myeloperoxidase (MPO) is an enzyme contained in the azurophillic granules in neutrophils and in the lysosomes of monocytes. It is released when the cells are activated. Monocytes contain only one third of the MPO contained in neutrophils (Askari et al., 2003). Activity of MPO was measured by an adaptation of the method described by Bradley et al and Zhao et al (Bradley et al., 1982; Zhao et al., 1997).

At all times except the final analysis, solutions and tissue were kept at 4^{0}C.

1. Heart tissue samples which had been stained were homogenised (4 x 10 seconds) (Polytron Homogeniser) in 0.1M potassium phosphate buffer pH 6 containing

5mM EDTA (10%w/v). The volume of buffer used (ml) was the tissue weight in grams multiplied by 7.

2. The homogenised sample was then centrifuged at 40000g for 15 minutes at 4^0C (Beckman Optimax TLX Centrifuge).
3. The supernatant was discarded and the pellets resuspended in the same potassium phosphate buffer with the addition of 0.5% hexadecyltrimethylammonium bromide to dissolve the myeloperoxidase.
4. The sample was homogenised (4 x10 seconds) and then sonicated (3 x 10 seconds) (Branson Ultrasonic Sonifier 250).
5. The sample was centrifuged again at 40000g for 15 minutes at 4^0C.
6. The final supernatant was collected and kept at 4^0C for MPO activity analysis as below.
7. An aliquot of 50µl of supernatant was mixed with 14500µl of 50mM phosphate buffer pH 6 containing 0.167mg/ml of O-dianisidine dihydrochloride and 0.0005% hydrogen peroxide. This phosphate buffer and the aliquot were kept at room temperature.
8. The change in absorbance at 460nm was measured using a spectrophotometer for 5 minutes at 10 second intervals.
9. For each specimen the units of MPO were calculated in the well assuming that 1 µmole hydrogen peroxide results in a change in absorbance of 1.13 X 10^{-2} (Bradley et al., 1982).
10. The final calculation was made per 1000g of tissue so the result for each sample could be compared.

2.6 Gr-1 Immunohistochemistry

Gr-1 antibody reacts with the epitope Gr-1 which is expressed on granulocytes (neutrophils and eosinophils) and monocytes. Sections were cut at 6µm and fixed in acetone for 4 minutes. They were then air dried and washed in 0.05% Tween (Sigma P1379) made up with PBS (Sigma P4417). A 1% bovine serum albumin (BSA) (Sigma A2153), 1% goat serum (Sigma G9023) blocking solution made up in PBS was then

applied to each slide and incubated for one hour at room temperature. Primary Gr-1 antibody (BD Pharmingen 550291) was then applied to each slide (1:200) made in the blocking solution. For the control sections an isotype control antibody (BD Pharmingen 559478) was used at the same dilution. Primary antibody was applied and left overnight in a humidified chamber. Slides were then washed three times for 5 minutes in 0.05% Tween made up in PBS. Secondary antibody (Invitrogen A11006 goat anti-rat) was applied to all slides (1:500) and incubated for 30 minutes in the dark at room temperature. Slides were washed again 3 times in Tween (0.05%) and mounted with immunofluore mounting medium containing Hoechst (1:100) (Sigma D9564).

2.7 Fluorescence microscopy of *Pdgfra*$^{GFP/+}$ hearts

Hearts were embedded in OCT by snap-freezing using isopentane. 6 μm sections were cut and mounted on slides at -20C. Specimens were fixed in 4% paraformaldehyde (Sigma P6148) for 2 minutes at 4^{0}C and then washed 3 times in PBS (Sigma P4417). A pap pen was used to encircle each specimen and Hoescht staining was applied to each section for 10 minutes. The Hoescht staining (1:100) was made up in 1%BSA (w/v) (Sigma A2153) in which was 3% goat serum (w/v) (Sigma G9023) and 0.3% triton (w/v) (Sigma 234729). Specimens were then examined using a ZeissM1 Axio fluorescent microscope.

2.8 Preparation of heart for Flow cytometry

Mice were killed by cervical dislocation and the heart was carefully dissected out and washed in cold PBS (Sigma P4417). The heart was minced using a scalpel in 1ml 2% foetal calf serum (FCS) (w/v) (Gibco 10082170) before being transferred into a specimen pot with 5ml of pre-filtered (0.2μm) 0.1% collagenase type 2 (Gibco 17101015) (w/v) in PBS (Sigma P4417). The pot was then placed in a shaking water bath at 37^{0}C. At 10 minutes the supernatant was taken and inactivated by pipetting into neat FCS at 4^{0}C. The remaining heart tissue was re-suspended in 5ml fresh 1% collagenase type 2 and digested again for 10 minutes. The supernatant was collected as before and the process repeated

one more time. The supernatant was filtered with a 40μm filter then centrifuged for 10 minutes at 300g. The supernatant was then discarded and the pellet re-suspended in 2% FCS . This was centrifuged for 10 minutes at 300g, the supernatant was discarded and the pellet re-suspended in red cell lysis buffer. After standing for 1 minute at room temperature, it was centrifuged and re-suspended in 2% FCS. The specimen was then washed again by centrifuging at 300g for 10 minutes. The specimen was then subject to MACS® dead cell removal as per manufacturers instructions (MACS® Miltenyi Biotech Gladbach, Germany) which negatively selects for the viable cells. The cell suspension was then centrifuged and re-suspended in 100μl 2% FCS. This was then centrifuged at 300g for 10 minutes and re-suspended in 100μl 2% FCS in preparation for addition of antibodies. Antibodies were now added according to the specific experiment (see table 2.1 for antibodies used) and incubated at 4^0C for 30 minutes. Specimens were then centrifuged and re-suspended in 2% FCS two more times to wash. 5μl 7 Amino-Actinomycin D (7AAD) (eBioscience 006993) (which was used to gate out any remaining dead cells) were added to the specimens prior to analysis by flow cytometry. Flow cytometry enabled separation of populations according to size and surface epitopes. Prior to loading samples to be analysed, compensation samples were taken using fluorochromes being used in each experiment. Isotype control samples were used in each experiment to enable accurate gating. Cell sorting was used to obtain cell preparations of high purity which had been sorted based on the desired surface markers. Cells were sorted using the BD FACS Aria™ Cell Sorter (BD Biosciences) and FACS DiVA SE™ software (BD Biosciences). FlowJo software (TreeStar, Oregon, USA) was used for flow cytometry data analysis.

2.9 Preparation of bone marrow for Flow cytometry

Mice were killed by cervical dislocation and tibia and femur were carefully dissected out and washed in cold PBS (sigma P4417). The bone marrow was then flushed out using 2% FCS (w/v) (Gibco 10082170) before being centrifuged at 0.3rcf for 10 minutes and re-suspended in 1ml 2% FCS. The sample was then centrifuged again at 0.3rcf for 10

Antibody and Fluorochrome	Cat. number	Company	Isotype	Cat. number	Company
Sca PE	553108	BD bisoscience	PE IgG2a	553930	BD bioscience
PECAM APC	551262	BD bioscience	APC IgG2a	553932	BD bioscience
PECAM APCCy7	25031182	ebioscience	PECy7 IgG2a	254321	ebioscience
ckit APC	553356	BD bioscience	APC IgG2b	55391	BD bioscience
CD45 APCCy7	557659	BD bioscience	APCCy7 IgG2b	552773	BD bioscience
CD90 PE	ab24904	abcam	PE IgG2c	ab37368	abcam
CD44 APC	559250	BD bioscience	APC IgG2b	553991	BD bioscience

Table 2.1 Antibodies used in flow cytometry (all were used at a dilution of 1:100)

minutes. Supernatant was discarded and cells were resuspended in red cell lysis buffer. Preparation of samples were now identical to that of heart described above.

2.10 Primary CFU-F assay

Once cells had been isolated using flow cytometry, 5000 cells were plated into separate tissue culture plates in 2ml of 20% Foetal calf serum (v/v) (Valley Biomedical BS3038) made up with minimum essential medium (MEM) (Invitrogen 12571063) containing penicillin (100μg/ml)/streptomysin (250ng/ml) and incubated in an incubator in humid air at 37^0C with 5% CO2. Media was changed the next day then every 3 days. At media change the plates were initially washed twice using sterile PBS (Sigma Australia P4417) before replenishing media. At day 12 the plates were stained with crystal violet (section 2.12) so that colonies could be counted. For the serial dilution assay, cells were plated into separate plates in an incremental dilution.

2.11 Secondary and tertiary CFU-F assay

Primary micro colonies, small colonies and large colonies were isolated using an O-ring at day 12 in culture and cells were re-plated after trypsinisation into individual plates (1 cell/well) with 20% foetal calf serum (v/v) made up with MEM as above (section 2.10), to assess the ability to form secondary and tertiary colonies. Counts were done at 12 days after plating. Continual passaging was also done by taking a secondary colony from a primary colony of each size and plating these cells into a 75cm flask. Before confluency was achieved the cells were trypsinised and 20000 cells were re-plated into another flask. This process was repeated for as long as the cells continued to passage.

2.12 Crystal Violet staining

Old media was discarded and plates were washed twice with PBS (Sigma P4417), then once with 50% ethanol (v/v) and left in ethanol for 15 minutes. The ethanol was then

aspirated and plates were left to air dry. Crystal violet (0.5% in 50% ethanol (v/w)) (Sigma Australia C6158) was then added and left to stain for 30 minutes. Dishes were washed with distilled water and colonies counted. Colonies were scored as being a micro colony, small colony or a large colony. Micro colonies contained 5-25 cells, small and large colonies were made up of >25 cells with small colonies being <2mm diameter and large colonies being>2mm diameter. A Zeiss Axiovert 25 microscope was used to view the cells.

2.13 Differentiation assays

Cells were initially allowed to attach to the tissue culture plates and start to form colonies, and after 5 days were then subject to specific tissue culture conditions detailed below. The control groups continued to have the usual MEM media described above.

2.13.1 Cardiomyocyte differentiation

At day 5 post plating, after aspiration of media and washing, the media used was changed to 10% FCS (v/v) (Valley Biomedical BS3038) made up with Dulbecco's Minimum Essential Medium high glucose (Invitrogen Australia 10938025) containing penicillin (100μg/ml) /streptomycin (250ng/ml). Added to this was 10μmol/l 5-azacytidine (Sigma A2385), 10μg/l fibroblast growth factor (RND Systems 3139FB025), 0.25mg/l amphotericin (Sigma A9528). After 24 hours the media was changed to one without amphotericin and thereafter every 4 days (Makino et al., 1999). At 14 days the cells were stained for α-sarcomeric actinin.

2.13.2 Smooth muscle differentiation

At day 5 post plating, after aspiration of media and washing, the media was changed to 2% FCS (v/v) (Valley Biomedical BS3038) made up with Dulbecco's Minimal Essential Medium high glucose (DMEM HG) (Invitrogen 10938025) containing penicillin (100μg/ml)/streptomycin (250ng/ml). Added to this was 50ng/ml Platelet derived growth

factor BB (PDGF-BB) (Invitrogen PMG0044) (Yamashita et al., 2000; Yoon et al., 2005). Media was changed every 4 days. At 14 days cells were stained for smooth muscle myosin heavy chain.

2.13.3 Endothelial differentiation

At day 5 post plating, after aspiration of media and washing, the media was changed to 1% FCS (v/v) (Valley Biomedical BS3038) made up with Iscove's modified Dulbecco's Medium (Invitrogen 12440046) containing penicillin (100μg/ml)/streptomycin (250ng/ml). Added to this was 10ng/ml vascular endothelial growth factor (VEGF) (Yoon et al., 2005). Media was changed every 4 days. At 14 days cells were stained for PECAM1 (CD31).

2.13.4 Adipogenic differentiation

At day 5 post plating, after aspiration of media and washing, the media was changed to adipogenic differentiation media which consisted of 10% FCS (v/v) (Valley Biomedical BS3038) made up with Dulbecco's Minimal Essential Medium high glucose (DMEM HG) (Invitrogen 10938025) containing penicillin (100μg/ml)/streptomysin (250ng/ml) and 0.5μM isobutyl methylxantine (Sigma), 1μM dexamethasone (sigma D4902), 10 μM insulin (sigma I0516), 200μM indomethacin (Sigma 17378) (Romanov et al., 2003). Media was changed every 4 days and cells were examined at 14 days, staining with oil red O for adipocytes (Romanov et al., 2003). Oil red O stock was made with 0.7g oil red O (sigma O0625) and 200ml isopropanolol. 10% formalin (v/v) was added to the cells for 5 minutes, then plates were washed with 60% isopropanolol (v/v). A 60% oil red O solution (v/v) was made up from the oil red stock, using distilled water and this was used to stain the cells for 10 minutes. The plates were then washed with distilled water. Lipid droplets were visible inside cells stained red with the oil red O solution.

2.13.5 Osteogenic differentiation

At day 5 post plating, after aspiration of media and washing, the media was changed to osteogenic differentiation media which consisted of 10% FCS (v/v) (Valley Biomedical BS3038) made up with Dulbecco's Minimum Essential Medium low glucose (Invitrogen 11885) containing penicillin (100μg/ml)/streptomysin (250ng/ml) and 0.1μM dexamethasone (Sigma D4902), 50μM βGlycerol (Sigma 50020), 50μM ascorbic acid (Biochemika 49752) (Romanov et al., 2003). Media was changed every 4 days and cells were examined at 14 days for staining with alizarin red which complexes with calcium (Aikawa et al., 2007; Lee et al., 2003). 2g of alizarin red (Sigma A5533) was added to 100ml distilled water. The pH was adjusted to 4.1-4.3 using 0.5% ammonium hydroxide. The culture plates were incubated in this solution for 10 minutes and then washed with distilled water. Any calcium deposits complex with the alizarin red, visible as an orange/red stain.

2.14 Immunostaining

Media was aspirated from tissue culture plates and washed 3 times in PBS (Sigma P4417) with 1% Bovine albumin (BSA)(w/v) (Sigma A2153) washing solution. The cells were then fixed with 2% PFA (w/v) (Sigma P6148) with 0.1% Tween-20 (v/v) (Sigma P1379) for 10 minutes at room temperature. The plates were washed again 3 times in the washing solution. Blocking solution PBS with 1% BSA (w/v)(Sigma A2153), 3% goat serum (Sigma G9023) (w/v), 0.1% tween-20 was added for 1 hour. Cells were then stained with the primary antibody made up to the required concentration (table 2.2) in PBS, 1%BSA (w/v), 0.1% Tween-20 (v/v) overnight at 4^0C. Next the plates were washed with the washing solution 3 times and stained with the appropriate secondary antibody made up to the required concentration (table 2.2) in PBS, 1%BSA(w/v) 0.1% Tween-20 (v/v) for 30 minutes at room temperature. Hoechst (invitrogen H3569) was used to stain nuclei (10mg/ml) 1% (v/v) made up in blocking solution . Cells were mounted with immunofluore mounting medium (ICN, Aurora USA).

	Primary antibody Manufacturer/ Cat number/ Host (dilution)	**Secondary antibody** Manufacturer/ Catalogue/ Host (dilution)
Alpha sarcomeric actinin	Sigma/ A7811/ mouse (1:500)	Goat anti-mouse 555 Invitrogen A21424 (1:300)
Smooth muscle myosin heavy chain	Santa Cruz/ SC6956/ mouse (1:300)	Goat anti-mouse 555 Initrogen A21424 (1:300)
PECAM1	BD/ 550274/ rat (1:50)	Goat anti-rat 555 Invitrogen A21434 (1:300)

Table 2.2 Antibodies used in differentiation assays and the dilutions

2.15 Analysis

Analysis of results from flow cytometry used FlowJo software (TreeStar, Oregon, USA). Comparison of means was analysed using t-test, and standard error was used as the measure of spread unless indicated otherwise. GraphPad Prism version 4 was used for statistical analysis.

2.16 Buffers

Potassium Phospate Buffer 0.1M

	ml/l
1M Dipotassium hydrogen orthophosphate 174.18g/l	132
1M Potassium Dihydrogen Orthophosphate 136.09g/l	868

Phosphate Buffer 0.1M

	ml/l
0.1M Disodium hydrogen orthophosphate 14.2g/l	774
0.1M Sodium dihydrogen orthophosphate 12.0g/l	226

Ethylene Diamine Tetra Acetic Acid (EDTA) 0.5M

	g/l
EDTA	186.12
10M Sodium Hydroxide	60ml

Make up to volume with MilliQ water. Add Sodium Hydroxide and heat. The EDTA dissolves at pH 8.0.

Chapter 3

Establishing a mouse model of Myocardial Infarction

3.1 Introduction

Animal models of myocardial infarction (MI) have proved to be very valuable in determining the complex pathophysiology of ischaemic heart disease (Hasenfuss, 1998). Experimental models of MI in rats have been used for a long time to provide information concerning structural, biochemical and haemodynamic changes after coronary artery occlusion and the effect of therapies. Surgical coronary ligation is a useful experimental technique to induce reproducible myocardial infarction. It has been shown that the vessel ligated and the coronary anatomy of the given animal model determines the extent of the resulting MI and its functional impact (Liu et al., 1997). Coronary artery ligation in Lewis in-bred rats has been shown to produce large infarcts, with progressive left ventricular (LV) dysfunction (Liu et al., 1997). Despite the technical advantages of operating on larger animals and the potential for chronic instrumentation, the mouse has started to emerge as an important animal to base disease models in especially due to the wide variety of transgenic models available, short gestation times, breeding capabilities and ease of housing due to their size, and especially with the accelerated interest in regenerative medicine over the last ten years it has become apparent that this model is an essential tool to facilitate investigation into this field (Beltrami et al., 2003). As documented in Chapters 4 and 5 the intention in this thesis was to investigate the role of a monoclonal antibody against C5a receptor and examine its effects on MI, and also to explore putative stem cell and progenitor populations in normal hearts and hearts post infarct, therefore it was essential to set up a model of MI in the mouse, which was consistent, reproducible and did not result in excessive mortality.

3.2 Pathophysiology of acute MI

Ischaemic heart disease is characterised by coronary atherosclerosis. An atherosclerotic plaque is composed mainly of fibrous tissue and lipid laden foam cells. Acute MI is associated with plaque rupture. This results in platelet aggregation and activation, thrombin generation and thrombus formation. The resulting thrombus interrupts the

myocardial blood supply. If this persists there is an imbalance between supply and demand of oxygen which results in myocardial necrosis (Braunwald, 2001).

Acute MI can be divided into transmural infarcts (myocardial necrosis involves the full thickness of the ventricular wall) and subendocardial (where the necrosis just involves the subendocardium, the intramural myocardium or both without extending all the way through to the epicardium).

Gross pathological changes can be seen 6-12 hours after the onset of necrosis in humans. Initially the myocardium in the affected area looks pale. Approximately 18 to 36 hours after the onset of the infarct the myocardium looks reddish purple due to trapped erythrocytes. During the first few days the myocardial wall in the region of the infarct thins as necrotic tissue is removed by inflammatory cells. Eventually in humans fibrous tissue is layed down over the course of the next 8 to 12 weeks.

If reperfusion is not instituted irreversible changes can be seen in some cells between 20 minutes and 2 hours after the onset of ischaemia. Under electron microscopy, cells irreversibly damaged by ischaemia are usually swollen with an enlarged sarcoplasmic space. The sarcolemma can peel off the cells and the mitochondria become fragmented. On light microscopy, a pattern of wavy myocardial fibres can sometimes be seen 1 to 3 hours after onset of myocardial infarction. By 8 hours there is interstitial oedema and infiltration of neutrophils. Muscle cell nuclei undergo karyolysis and small blood vessels undergo necrosis. Neutrophils continue to accumulate and by day 4 post infarct there is an infiltration of macrophages which remove necrotic debris. Over the next few weeks there is continued accumulation of fibroblasts and the infarcted area becomes converted into a firm connective tissue scar with some interspersed intact muscle fibres (Fishbein et al., 1978).

3.3 Ventricular remodelling

Initially after myocardial infarction there is an acute reduction in the ejection fraction in proportion to the size of the myocardial infarct. To compensate, there is an acute distension of the viable myocardium and operation of the Frank-Starling mechanism, as well as augmentation of chronotropic and inotropic activity through adrenergic receptor stimulation. All of these changes help to maintain pump function despite the loss of contractile tissue (Pfeffer and Braunwald, 1990).

After the acute phase described above, there are architectural changes in the wall of the myocardium which were initially described as 'infarct expansion' (Hutchins and Bulkley, 1978). This is defined as 'dilatation and thinning of the area of infarction not explained by additional myocardial necrosis'. Histology shows that this thinning of the infarcted region is due to slippage between muscle bundles. As previously explained, during the course of healing there is an accumulation of fibroblasts. The laying down of connective tissue scar connects the disrupted myocyte fibres and provides resistance to further stretching (Pfeffer and Braunwald, 1990). Infarct expansion is observed most frequently after large transmural infarcts and results in an increased likelihood of left ventricular aneurysm formation, congestive heart failure and myocardial rupture.

3.4 Differences in mouse and human coronary anatomy

The mouse and human both have a right and left coronary artery, however the mouse left coronary artery does not divide proximally into the left anterior descending coronary artery (LAD) and circumflex. It courses obliquely across the left ventricular free wall and branches in a variable fashion. The septal artery arises either from a separate ostia from the right sinus of valsalva or as a proximal branch of the right coronary artery (Kumar et al., 2005). The mouse coronary arteries are intramyocardial as opposed to epicardial (figure 3.1), therefore are more difficult to visualise than in the human and the right coronary artery is invariably small and non-dominant (Gan et al., 2004).

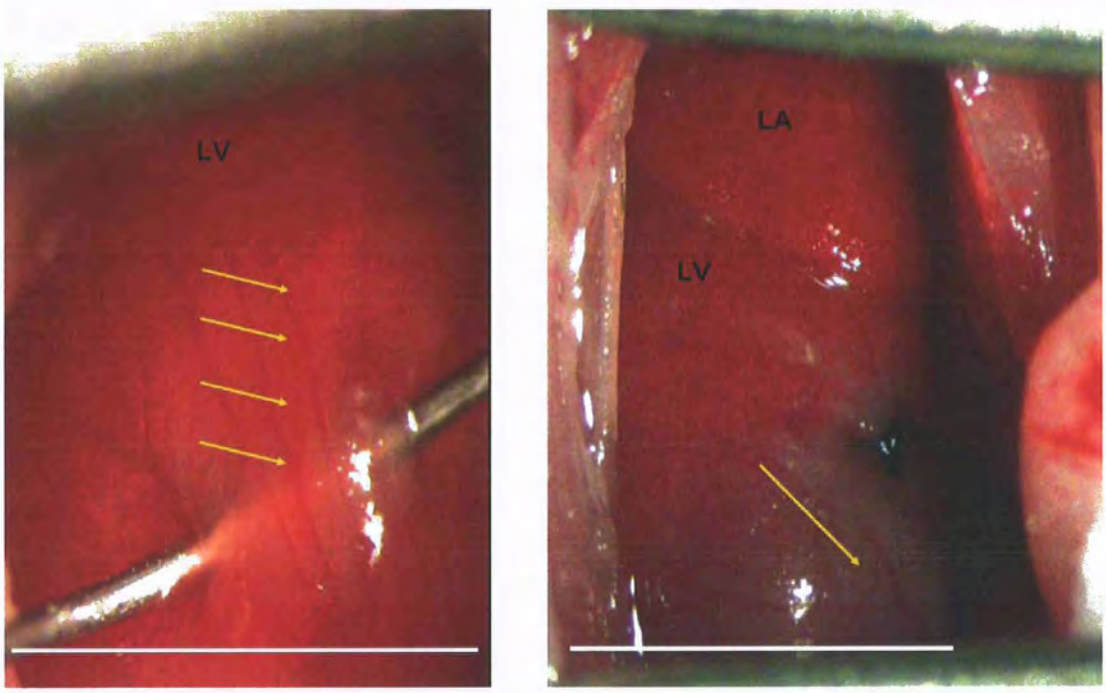

Figure 3.1 Mouse coronary anatomy

(a) This shows the intramyocardial course of the left coronary artery (arrows) and demonstrates how difficult it is to visualise, particularly when the heart is beating at 400-600bpm. (b) Post ligation there is blanching of the area distal to the ligation (arrow). Left atrium (LA). Left ventricle (LV). Scale bar = 5mm.

Immediate mortality in the left coronary ligation procedure has been quoted as high as 50% in the rat (Muders and Elsner, 2000), the main difficulties being the small size of rodents and the technical difficulties associated with this and other physiologic parameters. Some physiologic differences between mice and humans are outlined in table 3.1 (Barbee et al., 1992). In mice the procedure is inherently difficult, not only due to the small size of the heart and thoracic cavity, but also because physiologic parameters such as its very small blood volume and heart rate of 600 beats per minute, combined with a ventricular wall thickness of less than 1mm, and intramyocardial coronary arteries provide no margin for error in this technically demanding procedure.

Although myocardial infarction in mice has been used as a platform in the investigation of cardiac biology (Hsieh et al., 2007; Wang et al., 2006), no complete protocol is documented for this procedure, therefore it was established from basic principles as detailed in the Methods section. The first step in this process was to determine the vascular structure of the coronary tree.

3.5 Visualisation of the coronary tree

Due to the fact that the coronary arteries in the mouse are intramyocardial and therefore difficult to visualise, 5 mice were initially used to make acrylic resin casts to assess the coronary tree and its variability in the C57B6 mouse strain. An example of one of the casts is shown in figure 3.2. This illustrates how the mouse coronary arterial tree does not have a well developed collateral circulation. Due to this, the infarct produced after ligation of the left coronary artery in the mouse typically provided a sharply delineated and reproducible area of ischaemic damage (figure 3.3). Unfortunately for the same reason, as discussed below, if the left coronary artery is ligated close to its origin the infarct produced is extensive due to the fact there is no collateral protection, commonly resulting in early mortality.

	Human (70kg)	**Mouse (20g)**
Heart rate (bpm)	80	600
Blood volume (ml)	5000	1.6
Cardiac Output (l/min)	5	0.016
Tidal volume (ml)	500	0.15
Respiratory rate (breaths/min)	12	110

Table 3.1 Comparison of haemodynamic variables in mice and humans

In particular note the small blood volume and tidal volume in the mouse

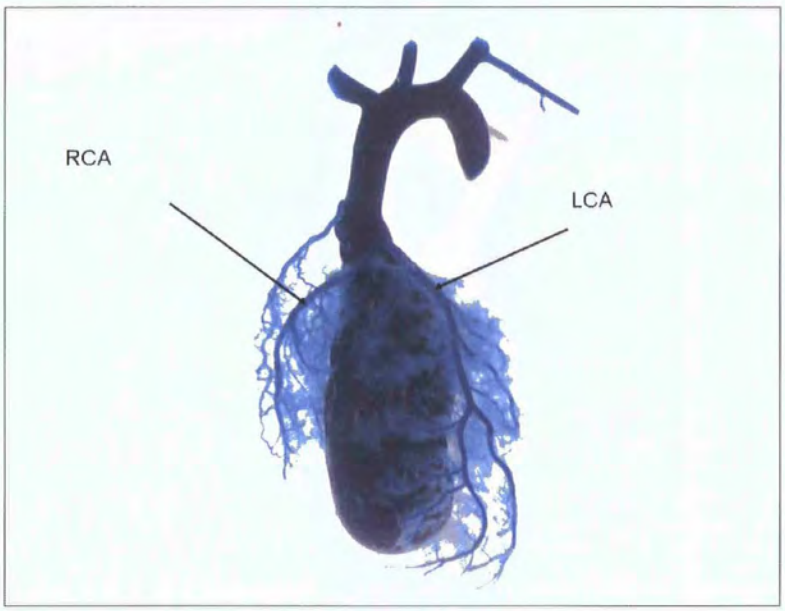

Figure 3.2 Acrylic resin cast of mouse coronary arterial tree.

Anterior view of the heart demonstrates the right (RCA) and left (LCA) coronary arteries. The right coronary artery was always less dominant than the left. The left coronary artery traversed over the left ventricle with multiple small branches and bifurcated towards the apex of the heart.

Figure 3.3. Whole heart at 5 days post infarct stained with triphenyl tetrazolium chloride.

Healthy tissue is stained red and infarcted tissue is stained white. This is typical of the sharply delineated and reproducible area of ischaemic damage resulting from this technique. The atria have been removed. Scale bar = 5mm.

3.6 Initial mortality and other complications

Initially the procedure was set up as detailed in the Methods section. Although this procedure resulted in myocardial infarction, it was associated with complications of mortality due to technical errors, left ventricular rupture and heart failure. Figures 3.4 and 3.5 demonstrate the appearance post MI of the infarcted area of the myocardium at different time points. Early technical errors were part of the learning curve and involved misplacement of the suture either too superficial causing damage to the left coronary artery , or too deep so it pierced the left ventricle. Both of these resulted in excessive blood loss and death. The other common technical error in the early stages was misplacement of the endotracheal tube resulting in inadequate ventilation. Once these technical errors were overcome with practice, the mortality for the procedure was 46% at day 7 post infarct (figure 3.6). Sham operated controls were used as a comparison. In the control mice a needle was passed through the myocardium without ligating the left coronary artery. No difference was found between female and male mice. Sub analysis of the mortality data showed the trend in figure 3.7. There was an initial peak at day 1 and 2 followed by another peak between day 3 and 5 post infarct. Post mortems on those mice which died at day 1 and day 2 post infarct showed evidence of acute heart failure. Prior to death these mice showed respiratory distress and on careful examination were found to have an increased lung weight/body weight ratio as evidence of pulmonary congestion (figure 3.8). There was no difference in heart weight/body weight ratios between sham and those with infarct which reached the 7 day endpoint. The mice which died at day 3 to day 5 post surgery were invariably found to have left ventricular rupture, a known complication of MI (figure 3.9). Left ventricular rupture is known to be a consequence of large transmural myocardial infarction and is associated with left ventricular aneurysm formation (Pfeffer and Braunwald, 1990).

(a)

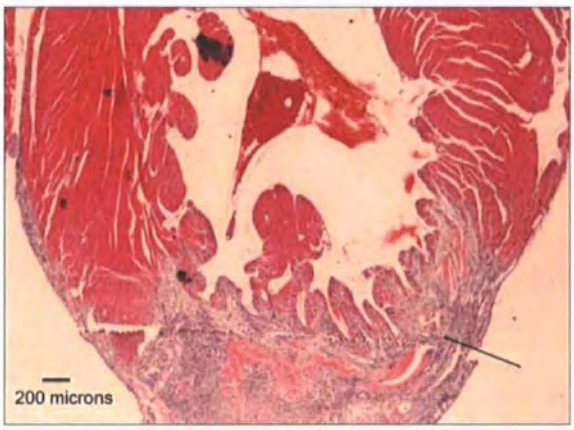

(b)

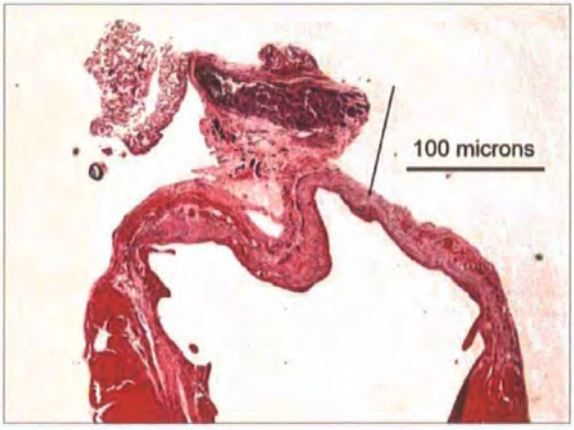

Figure 3.4 Histological demonstration of appearance of infarct area with time.

(a) H and E stained transverse section through the infarct area at 24 hours post infarct demonstrating loss of normal myocyte architecture in the infarct region (arrow) and replacement by inflammatory cells. (b) H and E stained transverse section through the infarct area 6 weeks post infarct demonstrating loss of normal myocyte architecture and replacement by fibrotic scar (arrow).

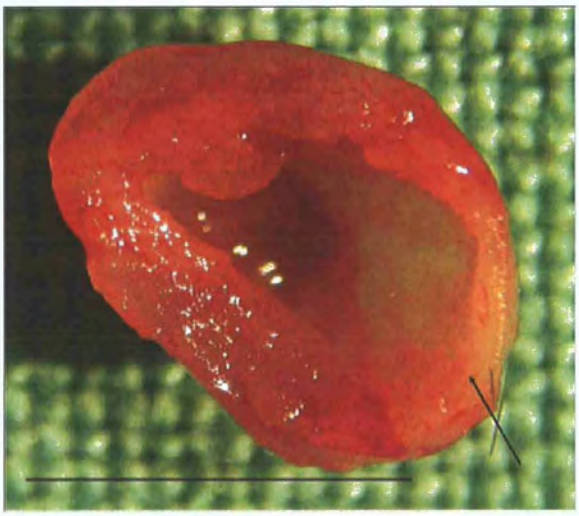

Figure 3.5 Transverse section through the ventricle below the level of the atrioventricular valves at 5 days post infarct.

This demonstrates the pale thin infarcted LV wall (arrow) associated with dilatation of the left ventricular cavity. Scale bar = 5mm.

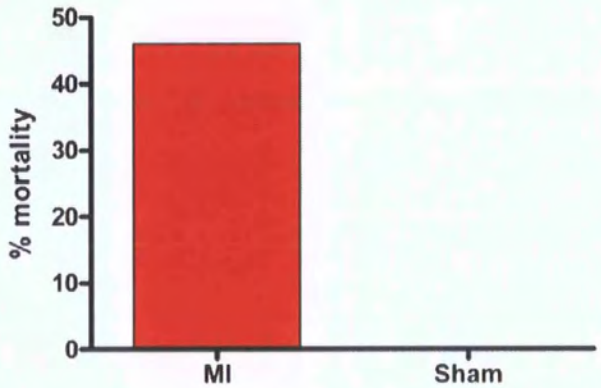

Figure 3.6 Mortality within the first 7 days after surgical ligation of the left coronary artery

Mortality was 45% at this stage of development of the model of MI. This is similar to that quoted for rat models of myocardial infarction. There was no mortality in the sham operated group. N = 50 in each group.

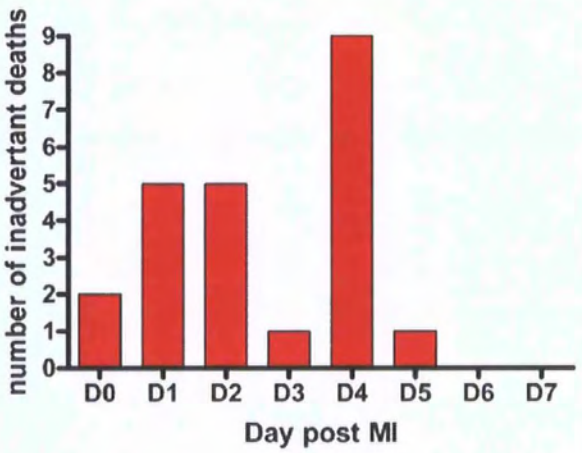

Figure 3.7 Sub analysis of mortality data over time

This showed 2 peaks of mortality, one within the first two days post MI and another significant increase at day four post MI. N= 50.

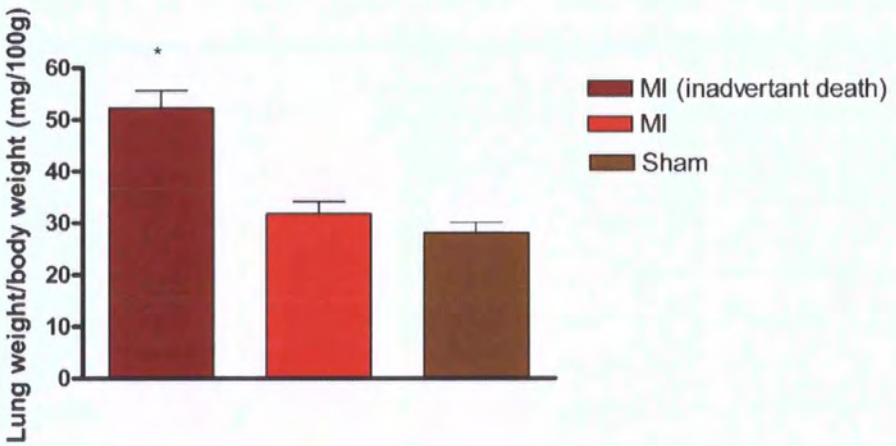

Figure 3.8 Comparison of lung weight/body weight (mg/100g)

Lung weight/body weight ratios of those mice which had an inadvertant death within the first 2 days of surgery are shown compared with mice which had MI and no inadvertant death within the first 2 days, and also sham operated mice at equivalent time points. * signifies $p<0.05$.

(a)

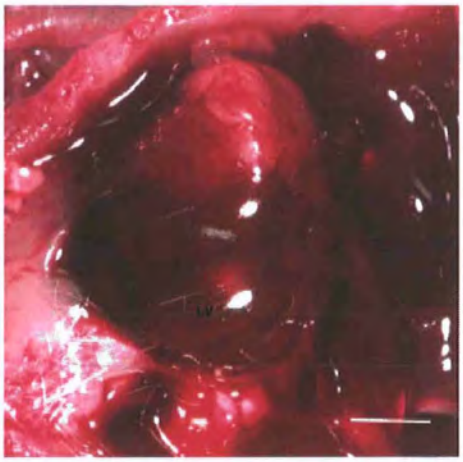

(b)

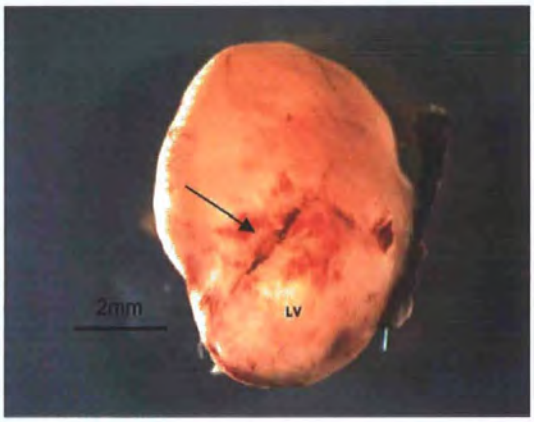

Figure 3.9 Diagnosis of left ventricular rupture

This was identified at post mortem by identification of haemopericardium and haemothorax (the pleura was often opened at the time of surgery). Figure 3.9(a) shows the heart within the thoracic cavity post rupture. Figure 3.9(b) demonstrates localisation of the point of rupture (arrow). Left ventricle (LV). Scale bar = 2mm.

3.7 Optimisation of the model

3.7.1 Reduction of early mortality

There were a very small proportion of mice which died at day 0. Some of these were initially due to bleeding or misplacement of the endotracheal tube. However it was noticed that there were some deaths without either of these 2 occurrences. On examination of these mice which had died on the day of surgery, post mortem revealed very small petechial haemorrhages in the lungs and occasionally tears at the bifurcation of the bronchi were found. This was thought to be due to barotrauma as a result of over ventilation . At the time the only ventilator available was one normally used for rats which could deliver a minimum of 0.8ml tidal volume. For this reason another ventilator with the ability to deliver small tidal volumes of 0.1-0.3ml was acquired (Harvard Minivent D79232). Mortality associated with these petechial haemorrhages was not seen once the ventilatory strategy was changed.

In order to address the deaths due to pulmonary congestion noted above, frusemide (0.1mg/20g) was given on a daily basis from the day of surgery. Two groups of 50 mice were each subject to surgery. One group received frusemide (0.1mg/20g intraperitoneal) daily, the other group received instead a daily intraperitoneal injection of the equivalent volume of saline. For each group there was an equivalent sham group which either received a daily injection of intraperitoneal frusemide or saline. This resulted in an overall reduction in 7 day mortality from 40% in the group which had an infarct and saline to 32% in the group which had an infarct and frusemide. This was not significant using the chi squared test. There were no deaths in sham operated animals in the frusemide or saline group. The actual numbers of deaths each day is shown in figure 3.10. Note that the proportion of early deaths (within 2 days) was reduced when frusemide was used ($p<0.05$). Late deaths at day 4 post infarct were similar and all of these were found to have rupture of the left ventricle.

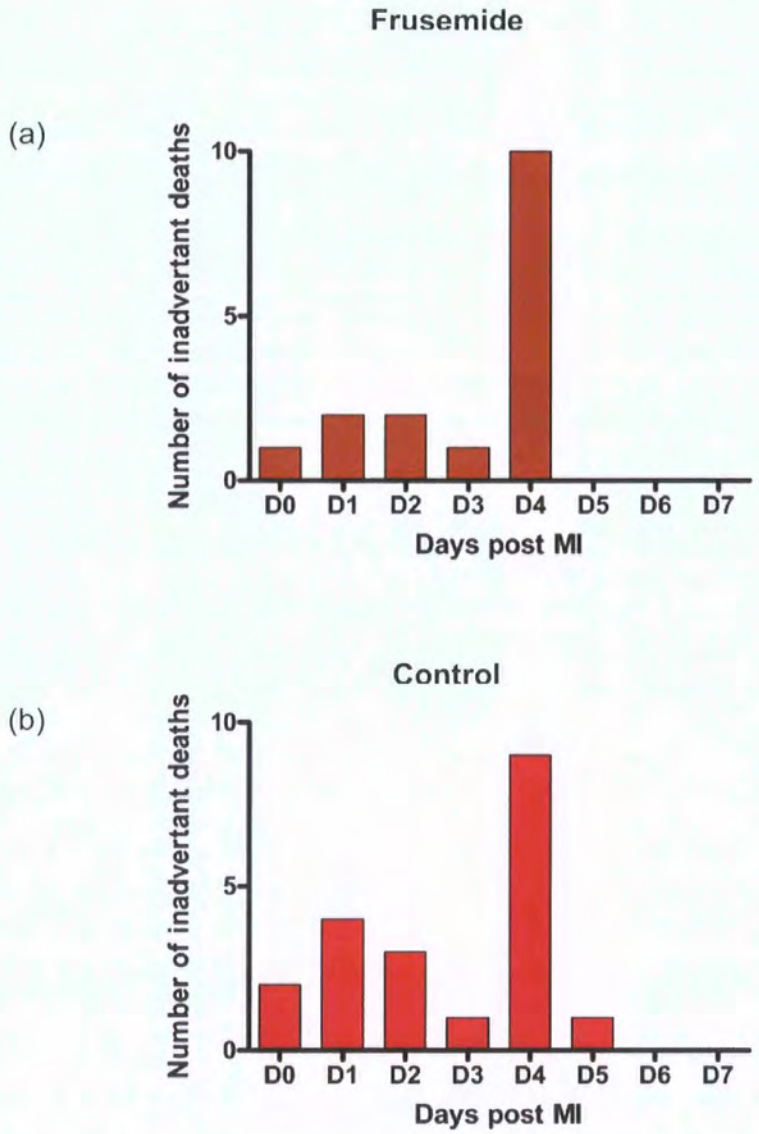

Figure 3.10 Effect of intraperitoneal frusemide injection on early mortality post MI

(a) Daily intraperitoneal frusemide injection resulted in a decrease in overall mortality from 40% to 32% ($p = 0.05$)) (Chi squared test). Primarily early death (D0-D2) was reduced as illustrated ($p<0.05$), which has been previously attributed to acute pulmonary congestion post MI. (b) Control group received an equivalent volume of saline. N=50 in each group.

3.7.2 Reduction of late mortality

Although use of frusemide and change of ventilation strategy reduced early inadvertent death, overall mortality was still found to be 32%, with most of the deaths resulting from LV rupture. In the experiments described above, the mean infarct size was 45% (± 1.44). As infarct size is related to risk of ruptue (Pfeffer and Braunwald, 1990), it was important to attempt to decrease infarct size so as to further improve survival in this model of MI. Originally the left coronary artery was ligated just proximal to where it emerges from the tip of the left atrium. It was thought this may be resulting in the large infarct , which led to high mortality from LV rupture. Therefore the strategy was changed and 2 groups of 50 mice were again subject to surgery, one group having ligation of the left coronary artery as above, and the second group subject to ligation 2mm distal to the point at which the left coronary artery emerges from under the tip of the left atrium as shown in figure 3.1 (b) . Sham operated controls consisted of mice which were subject to thoracotomy without ligation of the left coronary artery. The results in infarct size produced can be seen in figure 3.11. Re-positioning of the ligation point of the left coronary artery resulted in a significant decrease in infarct size from 42% ± 1.98 to 31% ± 1.70 ($p<0.05$). The impact of this on overall mortality is demonstrated in figure 3.12. Seven day mortality was reduced in this experiment from 34% in the group which had proximal ligation of the left coronary artery to 18% with the new more distal level of ligation of the left coronary artery (($p<0.05$) using chi squared test). There was a concomitant drop in LV rupture from 24% to 14% (($p<0.05$) using chi squared test). Note that all groups received frusemide daily in this experiment. There were no deaths or evidence of infarct in the sham group.

Although the risk of death from pulmonary congestion and LV rupture was now decreased within the first seven days, there was still evidence of the usual post infarct pathophysiology of thinning of the myocardial wall and LV aneurysm formation as shown in figure 3.13, however as the infarct size was smaller this evidently resulted in decreased risk of large aneurysm formation which could lead to death from LV rupture.

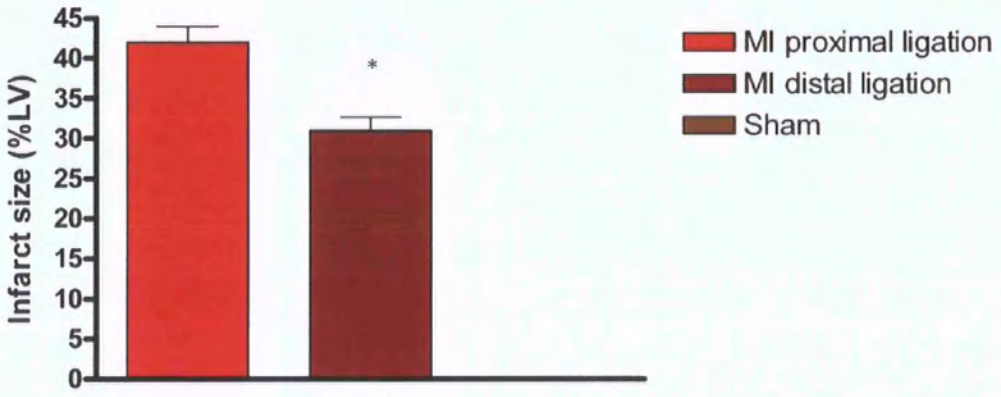

Figure 3.11 Change in infarct size with level of ligation.

Infarct size with the new more distal ligation of the left coronary artery resulted in a significant reduction in infarct size from 42% (± 1.98) to 31% (± 1.70) $p<0.05$. N=50 in each MI group. N=20 in sham group. * signifies $p<0.05$.

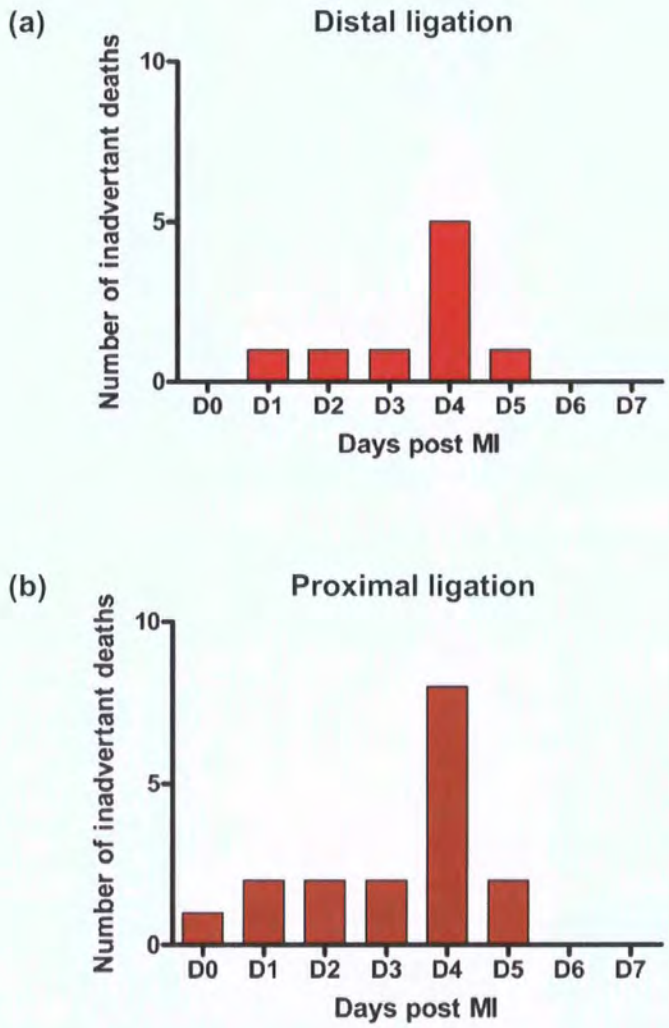

Figure 3.12 Reduction of mortality by changing level of ligation of the left coronary artery

(a) A more distal ligation strategy of the left coronary artery resulted in smaller infarct size ($p<0.05$) and also impacted on the overall mortality as shown compared to a proximal ligation strategy (b). Overall mortality decreased from 24% to 14% (($p<0.05$) using chi squared test). All groups received frusemide daily (0.1mg/20g). There was no mortality in the sham operated group. N=50 in each MI group.

Figure 3.13 Apical LV aneurysm in the heart.

This small aneurysm at seven days post infarct is delineated by the blue line at the inferior aspect of the heart. Scale bar = 2mm.

3.8 Discussion

Models of myocardial infarction have been used for some time to provide information on pathophysiologic and haemodynamic changes post infarct (Hasenfuss, 1998). Much of the small animal work in this field has been based on rats. Reports of surgical induction of MI in rats have shown mortality rates of up to 50% in the initial 24 hours post procedure and infarct size varying between 4-59% of the left ventricle(Gu et al., 1998; Pfeffer et al., 1979). However, with the expansion of interest in regenerative medicine it is apparent that a mouse model of infarct is essential in this field of study, partly because of their ease of housing and breeding capabilities but more importantly due to the fact there is an increasing variety of transgenic models becoming available together with technology allowing conditional expression of transgenes (Hsieh et al., 2007), which would help to facilitate the understanding of the endogenous biology surrounding events post infarction (Santini et al., 2007; Zhou et al., 2008), and also the isolation of putative stem and progenitor cells and tracing their derivatives. Additionally, unlike larger rodents and other animals, murine electrophysiology dictates that they have a lesser likelihood to develop fatal ventricular arrythmias, hence improving their chance of survival after ischaemic events (James et al., 1998). This thesis aims to explore events surrounding myocardial infarction, including inflammation (Chapter 4) and also aims to explore a putative stem and progenitor cell population (Chapter 5), hence a robust and efficient murine model was vital to set up. Although mouse models of MI are being used, it is apparent that they are technically very difficult to establish (Kajstura et al., 2005; Li et al., 1997a; Santini et al., 2007) and there are limited guidelines or protocols to safely, and efficiently achieve this goal with consistent results. Although cryoinjury has been used as a means of inducing myocardial injury (Leferovich et al., 2001) and is technically much simpler, it may not mechanistically be comparable to clinical occlusion of the coronary artery as occurs in human disease and hence physiologic mechanisms which follow may not be an accurate representation of what may occur after ligation of the coronary artery. This discrepancy was noted by Abdullah and colleagues (Abdullah et al., 2005) who used a coronary occlusion model in the MRL mouse strain, and Lefevorich et al (Leferovich et al., 2001)who used cryoinjury in the same mouse strain. The MRL mouse strain has been

reported to be able to have a unique capacity for wound healing after ear punch injury (Clark et al., 1998), reminiscent of that shown in amphibian regeneration, however in repect to the heart, this regenerative ability was shown to be the case only after cryoinjury. After coronary occlusion, this regenerative response was not found (Abdullah et al., 2005).

Guidelines to establish a model of murine myocardial infarction were pursued in this chapter to achieve a model which resulted in a reproducible, consistent infarct with a relatively low mortality. This study has demonstrated some important differences between the human and mouse coronary tree in a similar way to work by Kumar et al (Kumar et al., 2005), particularly the limited collateral circulation and reliance primarily on the dominant left coronary artery, which helps to explain the consistency of infarct achievable, but also the concomitant high mortality in this procedure, reported to be as high as 40-50% (Kumar et al., 2005; Muders and Elsner, 2000). Mortality associated with coronary ligation in mice have been reported at 50-60% at 24 hours (Li et al., 1997a; Li et al., 1997b) and 57-70% at 7 days post infarct (Li et al., 1997b). Ruptue of the LV has not been described in the literature in other species, however analysis of post infarct rupture by Gao and colleagues found the incidence to be 27%, which is similar to the 24% found in the present study prior to changing the point of ligation (Gao et al., 2005). Gao and colleagues showed a 24 hour mortality of 8% with a range in infarct size of 10-62% in comparison to the consistent infarct size generated in the present study of 31% $\pm$ 1.70.

In summary a step wise approach to limiting the degree of physiologic insult has been developed in this study so as to reduce 7 day mortality to 18% by limiting pulmonary congestion, lung barotrauma, making the procedure as simple as possible to reduce anaesthesia time and limitation of death from ventricular rupture. A robust model was now available to continue the study of inflammation and stem cells in cardiac ischaemic injury.

Chapter 4

Use of a C5a receptor antibody in Acute Myocardial Infarction

4.1 Introduction

As previously described in Chapter 1, the C5/C5a axis is a key mediator of the inflammatory process involved in myocardial ischaemia and is an important candidate for anti-inflammatory based therapy. Many different approaches have been used to target the inflammatory pathway but due to its pivotal role in ischaemic injury the C5/C5a axis has been a popular target using small molecules and specific antibodies.

The complement system is central to defence against harmful stimuli, however because it cannot discriminate between self and non-self, inappropriate complement activation can cause tissue inflammation in many circumstances such as rheumatoid arthritis, sepsis, inflammatory bowel disease and ischaemia.. The complement cascade, activated via classical, alternative and lectin pathways converge at complement proteins C3 and C5 (Wang, 2006). This is illustrated in the schematic figure 4.1.

C3 and C5 are cleaved by multi-subunit convertases. Once C5 is cleaved, this generates C5a, a potent anaphylotoxin and chemotactic mediator for neutrophils, monocytes and macrophages, and C5b which initiates assembly of the C5b-9 membrane attack complex which can cause direct cellular injury. C3 is cleaved to C3a and C3b. C3a has similar properties to C5a but is less potent, C3b is critical for innate defence against infection and immune complexes due to its role in opsonisation prior to phagocytosis (Wang, 2006). There is in addition another pathway through the coagulation system (specifically thrombin) which acts on C5 but not C3 (Huber-Lang et al., 2006).

Recent work from Rosenthal et al has postulated that in a transgenic mouse line where mIGF-1 is over expressed in the heart , the early resolution of inflammation at the site of injury may allow processes to occur which facilitate tissue repair (Santini et al., 2007), making the inflammatory response and its resolution a very attractive target for repair post cardiac injury.

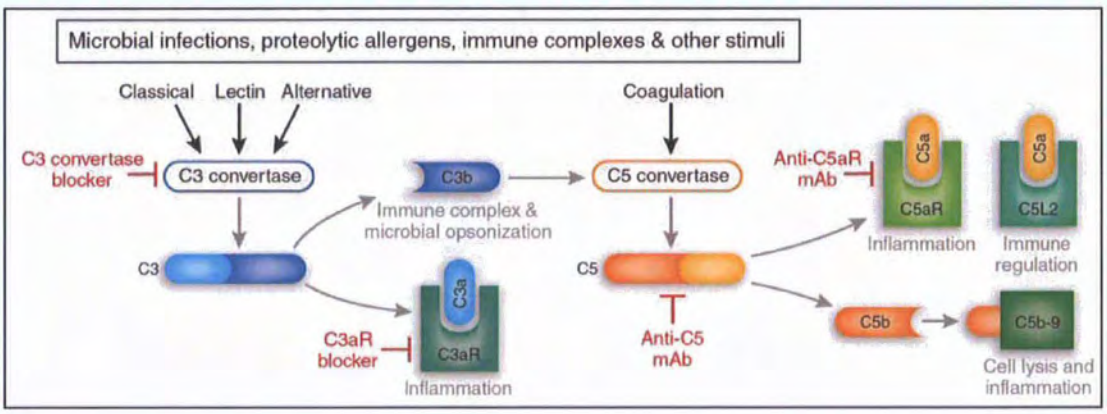

Figure 4.1 The central role of C3 and C5 in the complement activation cascade.

Schematic figure of the complement activation cascade showing that C3 and C5 are critical convergence points of four activation pathways and indicates potential targets of anti-inflammatory drugs. Inhibitors targetting C5 may impact activation of all four pathways and offer advantages over C3b inhibitors, most notably the generation of C3b, a key component of the innate immune response. Reprinted by permission from (Wang, 2006).

Hence a collaboration with Mackay et al (Lee et al., 2006) enabled the testing of a monoclonal antibody against human C5a receptor (hC5aR) in the setting of myocardial ischaemia to assess the effect of this antibody on its potential role in limiting myocardial injury and possibly to observe the effects of enhanced repair. Prior to this a specific monoclonal antibody against the human C5aR had not been tested in this environment. As previously documented, small molecules and antibodies have been used at the C5/C5a axis however with varying results (see Chapter 1).

When considering the optimal site for complement blockade, it seemed appropriate to focus on products which are common to each of the activation pathways. C5/C5a has in recent years been the target of choice so as to avoid blocking C3b which is a critical player in opsonisation and therefore innate immunity. Monoclonal antibodies are a rapidly growing class of therapeutics due to their predictable pharmacokinetic properties, high success rate in the clinic and their ability to inhibit interactions between large proteins such as a receptor and its protein ligand (Reichert et al., 2005). However poor cross-reactivity of certain monoclonal antibodies between humans and rodents often complicates the use of the same drug in pre-clinical studies, in animals as well as for human trials due to interspecies differences in receptors. To overcome this Mackay et al generated mice in which the native C5a receptor had been replaced by its human counterpart (Human C5aR mice), hence not only having a model for use at the benchside but also one where the same reagents could be translated into use in human clinical trials. As well as this, human C5aR mice could be used to produce high affinity monoclonal antibodies which were able to target the C5a receptor and reverse inflammation (Lee et al., 2006). Mice homozygous for the human C5aR transgene (*hC5aR1*$^{+/+}$) had neutrophils with high expression of human C5aR as shown by flow cytometry (Lee et al., 2006). Mouse and human C5a bound to human C5aR with similar affinities. Also human C5aR was functional in mice, in that neutrophils from *hC5aR1*$^{+/+}$ mice migrated in response to both human and mouse C5a *in vitro* in a similar fashion (Lee et al., 2006). Human C5aR was shown to be expressed at high levels on neutrophils, eosinophils, basophils and monocytes, but was absent from memory, effector T cells and B cells. At this time the antibody available was named 7F3 mAb. Mackay et al went on to test this antibody in a

mouse model of rheumatoid arthritis. Transfer of serum containing autoantibodies from arthritic K/BxN mice to healthy mice induces a joint specific inflammatory reaction that mimics the disease which develops spontaneously in K/BxN mice (Reichert et al., 2005). After serum was transferred from K/BxN mice the *hC5aR1*$^{+/+}$ mice pretreated with control antibody or saline showed typical clinical arthritis with joint swelling and inflammatory infiltrates consisting of primarily neutrophils whereas mice which were pre-treated with 7F3 mAb were completely free of inflammation clinically and histologically (Lee et al., 2006). Also when the antibody was given 5 days after induction of the disease there was complete reversal of the inflammation (figure 4.2). 7F3 mAb showed only a modest effect on neutrophil depletion. Anti-C5 mAb has been used to inhibit arthritis in mice before, however the doses which were required were much greater than that required for 7F3 mAb. One reason that could be postulated that much greater concentrations were needed for anti-C5 antibody is because of the high concentration of C5 present in blood. In addition 7F3 mAb was shown not to recognize C5L2 (Lee et al., 2006) which is a second C5a binding receptor that provides inhibitory signals on C5a binding(Gerard et al., 2005).

4.2 Efficacy of the 7F3 mAb on neutrophil infiltration and effect on infarct size

In view of the efficacy of 7F3 mAb in combating inflammation associated with rheumatoid arthritis, this antibody was then assessed in the setting of acute myocardial infarction. Chapter 3 illustrates the development of a mouse model of myocardial infarction by surgical ligation of the left coronary artery. Initially *hC5aR1*$^{+/+}$ mice were used to establish that infarct size induced using the methods established were consistent with that established using the C57B6 mice initially used to establish this model. *hC5aR1*$^{+/+}$ are on a background of C57B6 therefore although no anatomical differences were expected it was important to establish the consistency of the technique in this mouse. No significant difference in infarct size was found between C57B6 and *hC5aR1*$^{+/+}$ (figure 4.8).

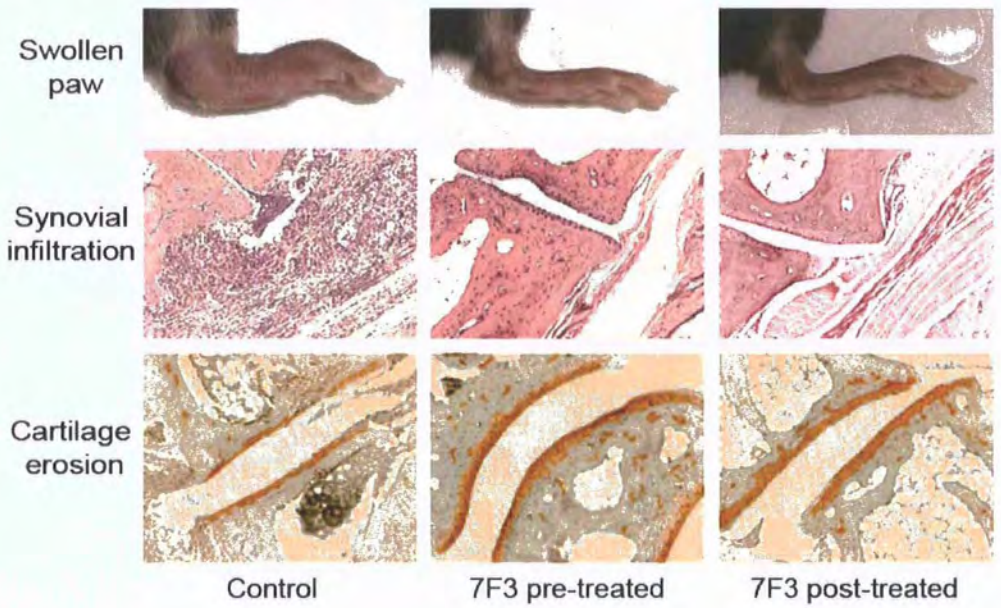

Figure 4.2 Anti-C5aR antibody can suppress inflammation in a model of rheumatoid arthritis.

Representative photographs and sections of hind paws from *hC5aR1*+/+ mice treated with10mg/kg isotype control antibody (left) or 7F3 mAb (centre) in a regime where the antibody was given prior to development of arthritis. The figure on the right shows the result of giving 3mg/kg 7F3 mAb after arthritis had developed. Haematoxylin and Eosin staining shows cellular infiltration to the joint and severity of histological arthritis. Safranin O staining shows cartilage structure. Original magnification x 100. Reprinted with permission (Lee et al, 2006).

The *hC5aR1*$^{+/+}$ mice were used for all studies. A schematic representation of the experimental outline is shown in figure 4.3. Groups were divided into an antibody treatment arm and a control arm. The 7F3 mAb was used by Mackay et al at 1mg/kg, 3mg/kg and 10mg/kg. Effective outcomes were achieved with intraperitoneal delivery. Both 3mg/kg and 10mg/kg were found to be highly effective in reducing the clinical signs of inflammation of the joints (Lee et al., 2006). When 3mg/kg was used the mice were injected twice per week to keep the signs of joint swelling quiescent. (personal communication Dr P Whitfield, Garvan Research Institute, Sydney). In this present study an initial dose of 10mg/kg intraperitoneal injection was used 20 minutes prior to surgery in an attempt to achieve an adequate systemic load before manipulation of the heart. After surgery 3mg/kg were given as a daily intraperitoneal injection until the 3rd day post surgery when the hearts were harvested and analysed. The rationale behind giving a greater dose than that used in the rheumatoid arthritis model was because the intention was that any effect of the antibody on inflammation would be manifest at this dose and there was an increased likelihood of the anti-inflammatory effects of the 7F3 mAb to be clinically effective as had been shown in the rheumatoid arthritis model. The intention was to perform dose titrations in later experiments. Hearts were harvested at 3 days post surgery as previous studies have reported a peak in neutrophil infiltration post infarct in rodent models at day 3 post MI (Smith et al., 1988). The Control arm used an IgG2a isotype control.

4.2.1 Pre-operative characteristics

As shown in table 4.1 there were no significant demographic differences between the treatment group and the control group.

4.2.2 Neutrophil infiltration analysis

In initial pilot studies Haematoxylin and Eosin stained sections were used to estimate the neutrophil infiltration, however neutrophils were difficult to distinguish from other granulocytes (figure 4.4), also this technique did not incorporate the whole of the heart to

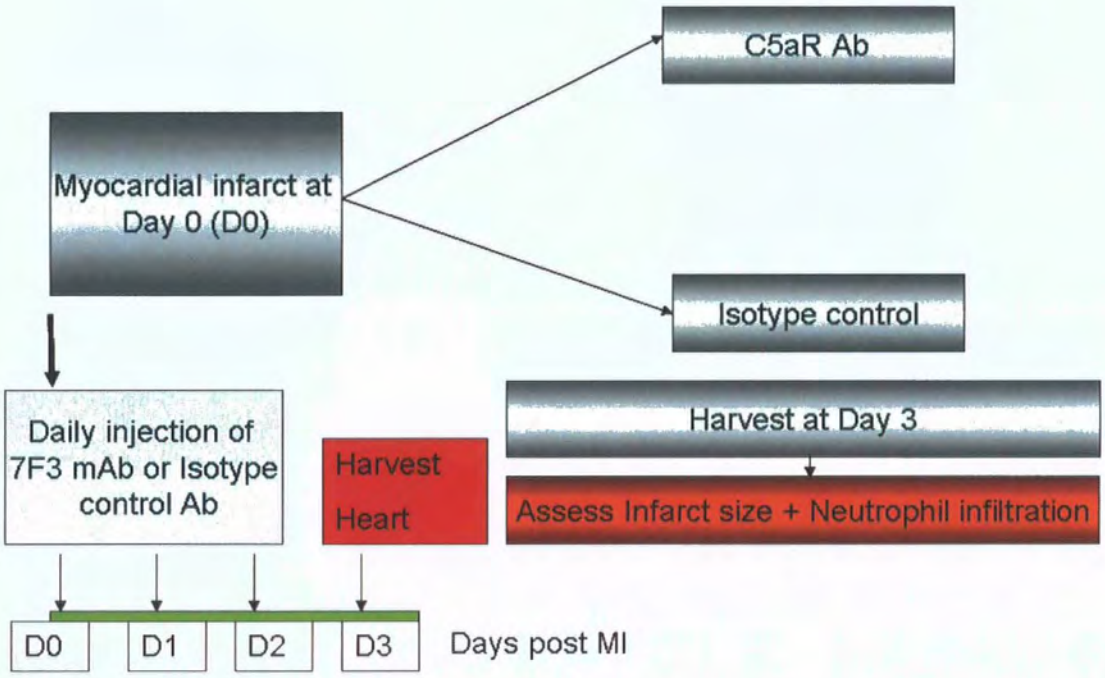

Figure 4.3 Schematic representation of the experimental outline.

Mice were given a 10mg/kg intraperitoneal injection of 7F3 mAb or isotype control Ab 20 minutes prior to surgery, and then 3mg/kg daily until hearts were harvested on day 3 post MI.

	7F3 mAb N = 25 Mean ± SE	**Isotype Control** N = 25 Mean ± SE
Age (weeks)	10.4 ± 0.5	10.2 ± 0.5
Weight (g)	21.9 ± 0.6	21.2 ± 0.6
% male	16	20

Table 4.1 Populations of mice employed in this study.

The experimental and isotype control groups showed no significant difference in respect of age, mass or sex ratio prior to protocol start.

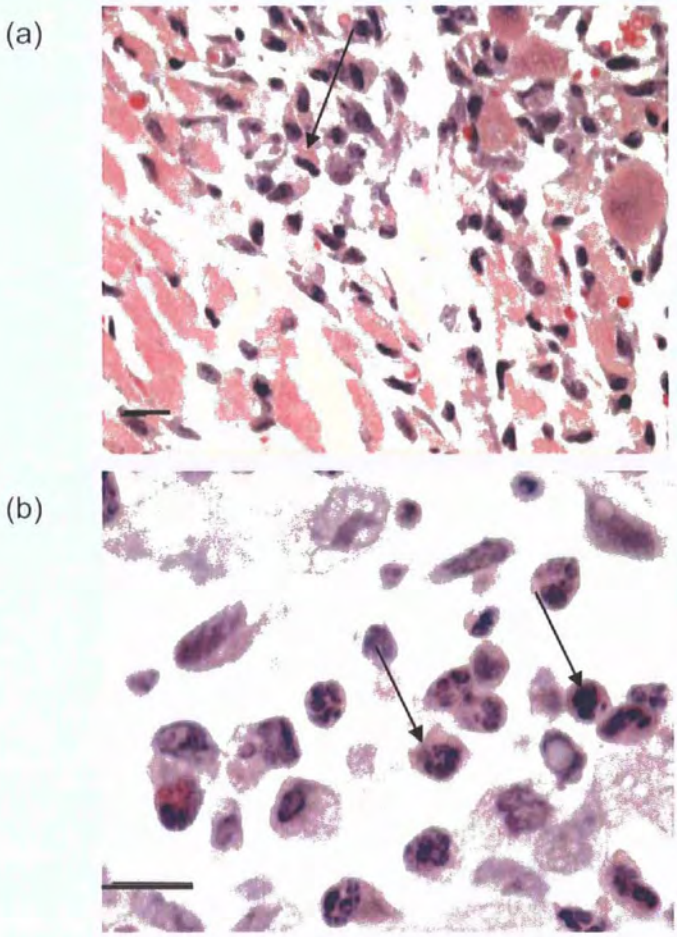

Figure 4.4 Haematoxylin and Eosin stained transverse sections of mouse left ventricle 3 days post infarct.

This demonstrates influx of neutrophils. (a) Arrows indicate infiltration into the infarct and peri-infarct area post MI. (b) Arrow indicates characteristic muliti-lobed nucleus of neutrophils. (a) and (b) are low and high magnification images respectively. Scale bar = 20μm.

be examined or permit measurement of infarct size in the same specimen. Due to this, myeloperoxidase (MPO) activity was used as the measure of neutrophil infiltration. Briefly, any myeloperoxidase present in the tissue reacts with hydrogen peroxide, releasing a free radical. This free radical oxidizes a substrate O-dianisidine dihydrochloride resulting in a change in colour of the specimen. This change in colour is detected by a spectrophotometer. From changes in the spectrophotometer reading, the units of MPO per specimen are calculated. Results of initial experiments to show low level of interassay variance are shown in figure 4.5. Photomicrographs of myocardial sections stained with Gr-1 antibody (recognizes neutrophils, eosinophils and monocytes) are shown in figure 4.6 together with images of the spectrophotometer wells illustrating the change in colour. As can be seen from the immunohistochemistry, in an uninjured heart there were very few neutrophils seen after sectioning and staining. This was also reflected in the MPO assay. In each experiment an uninjured heart was used as a negative control and the spleen was used as a positive control for neutrophils. Using this technique to detect neutrophil prescence in tissue permits measurement of infarct size using the triphenyl terazolium chloride technique described in Chapter 2. Smith et al have shown a concordance between tissue MPO activity and histologic determination of neutrophils in infarcted myocardium (Smith et al., 1988). Having determined that MPO was an appropriate tool to examine neutrophil infiltration, the MPO activity in the infarcted hearts from 7F3 mAb treated or isotype control treated animals was examined. As can be seen in figure 4.7 the 7F3 mAb treated animals had a significantly reduced neutrophil infiltrate 3 days post MI compared with control treated animals (416.8 $\pm$ 52.6U MPO/1000g and 590.3 $\pm$ 55.6 U MPO/1000g respectively). As discussed earlier, infiltrating neutrophils associated with inflammation are associated with poorer outcomes post MI. Hence the size of infarct after 7F3 mAb and control Ab was also examined.

4.2.3 Infarct size analysis.

This was done on day 3 post MI prior to analysis for MPO activity in the same manner as described in Chapter 3 using triphenyl tetrazolium chloride to mark the infarcted area. Initially C57B6 mice and *hC5aR1*$^{+/+}$ mice were infarcted in parallel to ensure the infarct

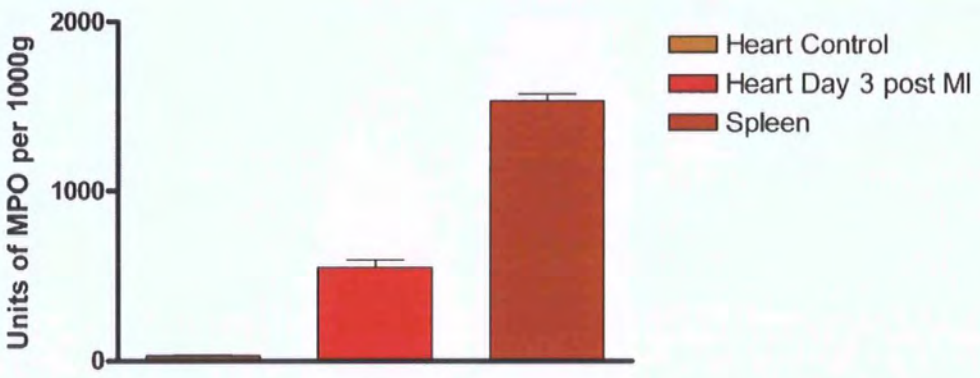

Figure 4.5 Use of MPO assay to monitor neutrophil infiltrate into the infarcted heart.

The MPO assay was able to detect neutrophil prescence in hearts at 3 days post MI. Note comparatively low level of inter-assay variance in these samples. Spleen was used as a positive control. Coefficient of variation calculated to be 24.5% and 8.4% for heart post MI and spleen respectively. N = 10 per group.

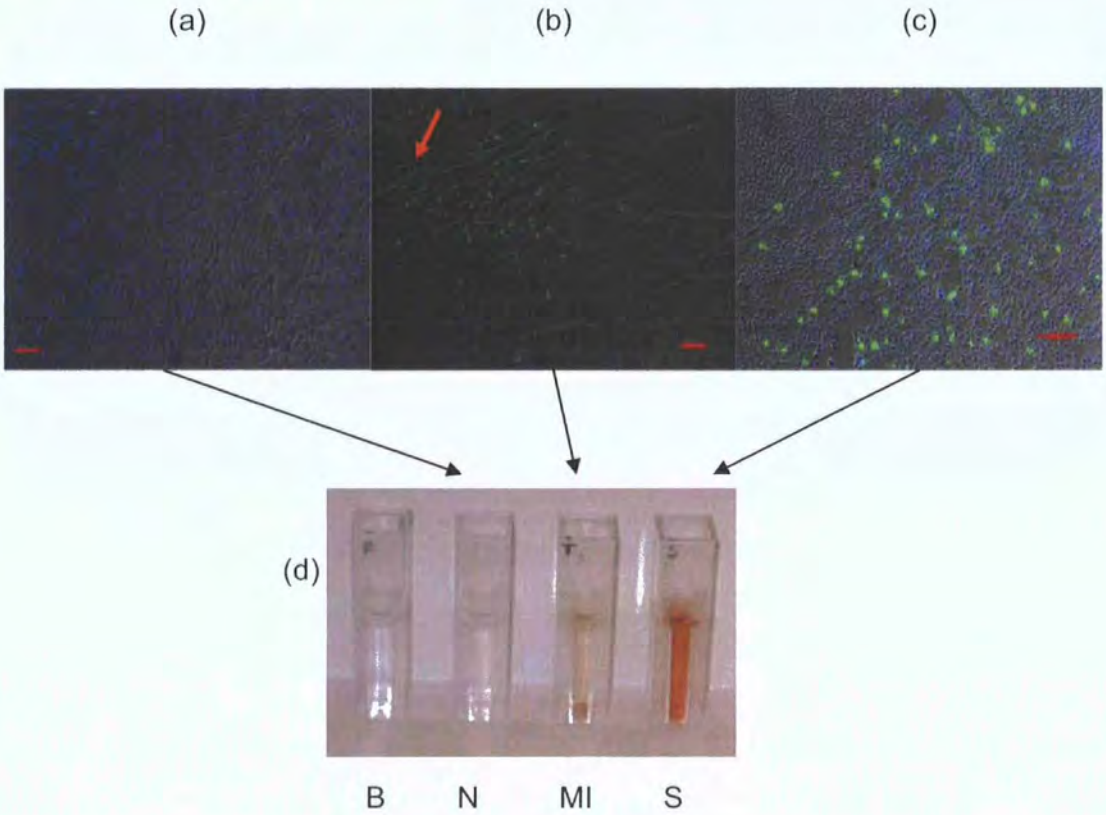

Figure 4.6 Detection of infiltrating neutrophils by immunofluorescence.and MPO assay

(a) – (c) show staining of transverse sections of the heart using Gr-1 antibody to detect infiltration of neutrophils post MI. (a) Normal heart. No Gr-1 staining indicating normally there are few, if any, neutrophils residing in the interstium of the heart. (b) 3 days post MI the Gr-1 stained neutrophils can be seen primarily in the peri-infarct area recognisable by the junction between normal architecture of myocardium and infarct area (arrow indicates infarct area). (c) Spleen tissue used as a positive control due to the abundance of neutrophils. Gr-1 is stained green. Nuclei are stained blue with Hoechst.
(d) Demonstrates the change in colour in the myeloperoxidase assay in relation to the neutrophil content of the specimen, illustrating that the MPO assay shows broad concordance with numbers of neutrophils determined by immuofluorescence. Blank specimen contained no tissue. B = Blank, N = Normal heart, MI = 3 days post MI, S = Spleen. Scale bar = 50μm.

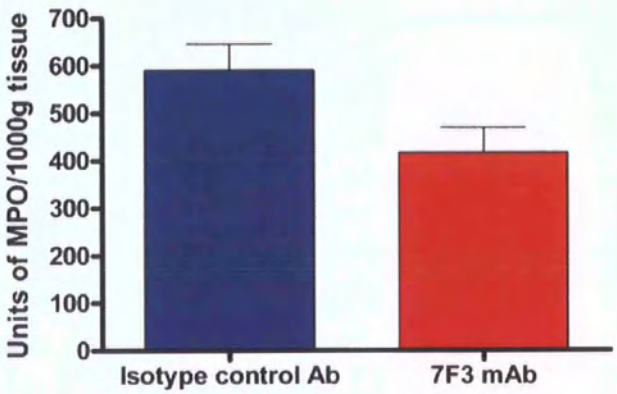

Figure 4.7 MPO assay of neutrophil accumulation in 7F3 mAb and isotype control Ab hearts post MI

Neutrophil accumulation was assessed by MPO activity. Those animals treated with 7F3 mAb had a significantly reduced level of MPO activity compared with control treated animals ($p<0.05$). N=23 and 24 for 7F3 mAb and control groups respectively.

technique resulted in consistently uniform infarcts in both types of mice and to ensure the transgenic mouse did not have any inherent differences which would affect the outcome of coronary ligation.. Infarct size was similar in both groups with the technique used, as shown in figure 4.8. Once establishing that the infarct technique gave a consistent result, the 7F3 mAb was tested in comparison to the isotype control. These results are shown in figure 4.9, demonstrating that there was no significant difference in infarct size between the treated (32.6% $\pm$ 2.98) and control Ab (34.3% $\pm$ 2.61) groups ($p<0.05$).

To ensure differences observed between infarct size and MPO were not due to changes in total heart mass, each heart was weighed at the time of harvest. No significant difference was found between the 7F3 mAb treated and control groups. The mean weight of the hearts which had received 7F3 mAb and control were 0.11 $\pm$ 0.02g and 0.11 $\pm$ 0.02g respectively.

Although there was no significant difference in infarct size, this does not measure all of the physiological effects of 7F3 mAb treatment. In order to assess this, mice were observed and weighed during the period leading up to the 3 day endpoint.

4.2.4 Physiological observations

Mice were checked and weighed daily. Surgical induction of myocardial infarction has a significant physiologic impact on the mouse and this is usually reflected in some weight loss in the first week post procedure. The weight loss documented at day 3 post infarct was not significantly different in the 7F3 mAb treated group and the control group (13.6% $\pm$ 1.42 and 10.7% $\pm$ 1.63 respectively) as illustrated in figure 4.10.

Although there were no peri-operative deaths the cause of all deaths which occurred prior to elective harvesting of the hearts were investigated at post mortem. All deaths prior to harvest were found to be due to rupture of the left ventricle. Each group started with 25 mice in each group. 23 mice reached the 3 day end point in the group which received 7F3 mAb and 24 hearts reached the end point in the control group. All deaths were due to left

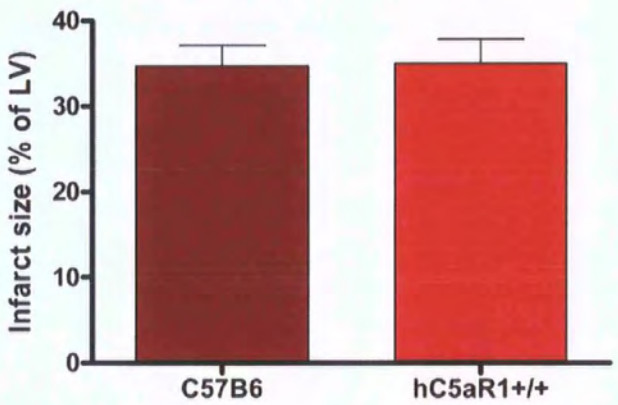

Figure 4.8 Comparison of infarct size induced in C57B6 and *hC5aR1*+/+ mice.

There was no significant difference in the size of infarcts induced in the *hC5aR*$^{+/+}$ mice compared with C57B6 mice. No antibody treatment was used in either group (p = ns). N=10 in each group.

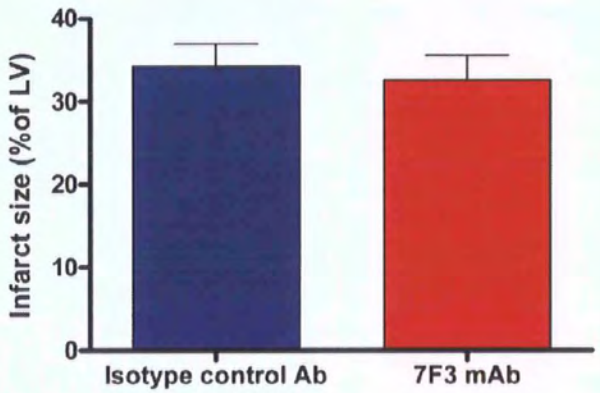

Figure 4.9 Effect of hC5aR mAb on infarct size at day 3 post MI.

There was no significant difference in the size of infarct in the 7F3 mAb treated group compared with the control (p = ns). N=23 and 24 for 7F3 mAb and control groups respectively.

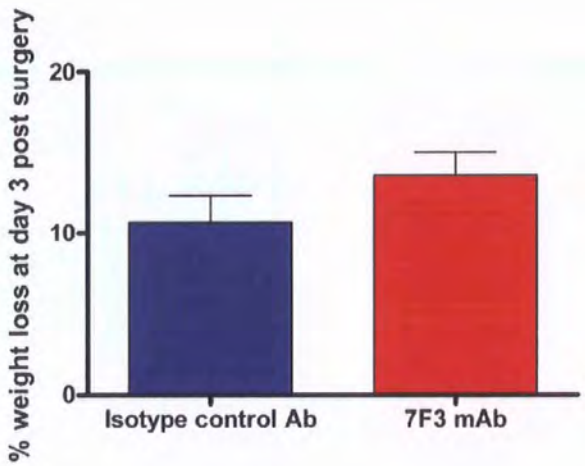

Figure 4.10 Weight loss in mice post MI as percentage of original weight.

There was no significant difference in weight loss post MI in the 7F3 mAb treated group and control animals (p = ns). N=23 and 24 for 7F3 mAb and control groups respectively.

ventricular rupture. Incidence of left ventricular rupture was very low in both groups, being 8% in the 7F3 mAb group and 4% in the control mAb group. This difference was not significant, using the chi squared test (p = ns). There were no complications of local infection or sepsis.

4.3 Discussion

This study examined the effect of complement inhibition in a murine model of acute myocardial infarction. The complement pathway was inhibited using a monoclonal antibody against human C5aR (7F3 mAb) in a transgenic mouse in which human C5aR had been knocked in (*hC5aR1*$^{+/+}$) (Lee et al., 2006).

Inflammation is known to contribute to cell damage during ischaemia (Frangogiannis et al., 2002). Initial attempts to inhibit inflammation with corticosteroids (Hammerman et al., 1983a)or non steroidal anti-inflammatory drugs (Hammerman et al., 1983b) have not shown to improve outcome after MI. Neutrophil depletion or inhibition of function has been shown to limit infarct size underlying their importance in myocyte injury after an ischaemic event (Amsterdam et al., 1993; Mullane et al., 1984), however it would be useful to specifically reduce neutrophil mediated damage at the site of inflammation. Hence antibodies or antagonists targeted at C5/C5a/C5aR have been an attractive candidate for reduction of ischaemic damage due to the importance of this part of the complement pathway in neutrophil chemotaxis and also in generation of the C5b-9 membrane attack complex. Additionally targeting this part of the complement pathway does not affect C3b which is a critical for opsonisation in its role in innate immunity. A number of animal studies and human studies in this regard have already been described in Chapter 1, which have shown varying efficacy. This is the first time the 7F3 mAb has been used in the setting of myocardial infarction.

In the present study in a murine model of infarction, 7F3 mAb was given prior to infarction and the hearts were analysed after 3 days. In contrast, the majority of previous studies have used antagonists or antibodies at the C5/C5a axis in models of ischaemia

reperfusion and have usually been analysed within hours. A number of different methods have been used previously to assess outcomes including assessment of neutrophil infiltration by MPO assay and measurement of myocardial injury by measuring infarct size using triphenyl tetrazolium chloride, biomarkers such as CK-MB, functional studies including echocardiography and long term survival data.

In this study on the effect on myocardial infarction, neutrophil infiltration was assessed by MPO activity in the heart at 3 days post infarct. This time point was chosen as the most appropriate point for assessment as it has been shown to correlate with the peak of neutrophil infiltration after coronary artery occlusion (Smith et al., 1988). Assessment of MPO activity demonstrated that treatment with the 7F3 mAb resulted in a significant reduction in the MPO activity in the heart. MPO activity has previously been shown to correlate well with neutrophil infiltration after ischaemia. (Smith et al., 1988). Despite this reduction in neutrophil infiltration, surprisingly there was no significant change in infarct size after using the 7F3 mAb despite the outstanding clinical results demonstrated when using this antibody in a murine model of rheumatoid arthritis (Lee et al., 2006).. Despite the encouraging results of other studies in using an inhibitor or antibody at the C5/C5a axis, one reason a significant change in infarct size was not demonstrated here could be the mechanism of ischaemia employed. No reperfusion was instituted here, whereas in the majority of previous studies reperfusion was instituted after a much shorter time of ischaemia (Amsterdam et al., 1995; Vakeva et al., 1998). Although this reperfusion time will be involved in contributing to myocardial injury in response to complement activation and cytokine release, it also may allow enough blood to perfuse to salvage some of the damage resulting from the initial ischaemic insult, thereby affecting the final outcome. The results in the present study reflect those in the COMPLY and COMMA trials where no change in infarct size was observed (Granger et al., 2003; Mahaffey et al., 2003). There is a possibility that modulating the inflammatory pathway by using the 7F3 mAb in the setting of myocardial infarction might enhance outcomes in a manner which is not detectable from measuring infarct size at such an early time point of 3 days post MI. The COMMA trial showed that despite the fact that myocardial injury (measured using CK-MB) was no different in the treated and control group, there was a

beneficial effect in the treatment group evident at 90 days with a reduction of mortality. Hence even thought no difference using the antibody has been noted in the present study there is a possibility that its anti-inflammatory effect may affect ventricular remodeling and affect long term survival in this manner.

In summary, the findings from this study demonstrated the use of a human C5aR mAb (7F3 mAb) in a human C5aR knock in mouse in the setting of acute myocardial infarction. Use of 7F3 mAb resulted in a significant reduction in neutrophil infiltration at 3 days post infarct, but no difference in infarct size at that time point. There were no infective complications or differences in ventricular rupture between the two groups. This data supports an important role for 7F3 mAb in reducing inflammation when administered prior to onset of myocardial infarction, however it also suggests other mechanisms of potential regenerative and repair strategies must be studied to try to elucidate mechanisms which may be available in cardiac repair. Hence an investigation was carried out into the phenotype of a putative stem cell population found in the adult heart.

CHAPTER 5

In vitro characterization of a putative stem cell population in the adult heart

5.1 Introduction

A disease model of myocardial infarction in mice was initially established in order to have an *in vivo* model for investigating regenerative activity in the heart (Chapter 3). This model was used to assess the efficacy of reduction in the inflammatory response after an ischaemic insult, by using an antibody directed against the C5a receptor (Chapter 4). It was suggested that cells extrinsic to the heart, such as inflammatory cells may not play a complete role in infarct recovery. Recent studies have highlighted the potential role of cardiac resident cells that may be capable of regenerating the heart (Chapter1) however their nature, role and phenotype is as yet not completely understood. One approach to finding a cardiac resident stem cell population is to look for those cell types present within the developing embryo which may also be present in the adult. One such candidate cell population is that expressing platelet derived growth factor receptor alpha (PDGFRA). PDGFRA expressing cells have been found in the developing mouse embryo in the region of the proepicardial organ at E9.0. These cells are also found on the epicardial surface of the heart at E9.0 to E10.5. From E12.5 they appear in the interstitium of the myocardium. PDGFRA also co-localises with Wilms tumour protein (Wt1) which has been reported as being an expression marker for the epicardium of the heart (Perez-Pomares et al., 1998) (personal communication, Owen Prall, Victor Chang Cardiac Research Institute, Sydney). Epicardial derived cells are known to invade the cardiomyocyte layer by a process called epithelial to mesenchymal transformation (EMT) and contribute to endothelium, smooth muscle and fibroblasts of the developing coronary vasculature. Soriano et al generated a mouse with a targeted null mutation of the *Pdgfra* locus using a histone H2B-eGFP fusion reporter protein construct knock in (Soriano, 1997). Heterozygous mice show that GFP reproduced the PDGFRA expression pattern (Orr-Urtreger et al., 1992; Takakura et al., 1997). Further, Hamilton et al showed by flow cytometry analysis of cells from $Pdgfra^{GFP/+}$ mice that H2BGFP and the wild type PDGFRA are expressed in the same population of cells, further supporting the idea that $Pdgfra^{GFP}$ faithfully reproduces the native wild-type PDGFRA expression pattern (Hamilton et al., 2003). Homozygous *Pdgfra-null* mice die by E10.5 showing multiple defects which include cardiac defects such as aortic arch malformations, persistent

truncus arteriosus, atrial and ventricular septal defects, myocardial wall thinning and abnormal atrio-ventricular valves and dilatation of the pericardium (personal communication, Dr O Prall, Victor Chang Cardiac Research Institute, Sydney).

The anatomical location of the PDGFRA expressing cells in the heart, coupled with the phenotypic changes in the *Pdgfra-null* mice, suggest that this population may exhibit stem cell activity in the adult. In order to address this an assay for stem cell activity was needed. *In vivo* reconstitution is arguably the strongest and most robust assessment (Seaberg and van der Kooy, 2003), however *in vivo* models are very time consuming and demand very large numbers of animals. An alternative initial approach is to characterise the stem cell properties of a candidate population *in vitro*, assessing self renewal, proliferation and differentiation (Potten and Loeffler, 1990). An assay needed to be chosen which may isolate a stem/progenitor cell population, to show *in vitro* self renewal and proliferation potential. The assay chosen was a Colony Forming Unit Fibroblast (CFU-F) assay. This was initially demonstrated by Friedenstein and colleagues (Friedenstein et al., 1970) where they plated whole bone marrow in plastic culture dishes, discarding the non-adherent (typically haematopoietic) cells after 4 hours. The remaining adherent cells were found to form colonies and further work established that these cells were also multi-potent being capable of differentiating into osteoblasts, chondrocytes and adipocytes (Digirolamo et al., 1999). Due to their self renewal ability, proliferative capacity and ability to differentiate into multiple mesenchymal lineages they were known as Mesenchymal Stem Cells (MSCs). Amongst all the stem cell assays described it seemed appropriate to choose a simple robust assay which not only is capable of revealing key *in vitro* features of self renewal and proliferation but also one which has been shown to allow isolation or enrichment of stem cells.

This chapter (Chapter 5) will assess mononuclear cell populations in the murine adult heart for expression of PDGFRA and examine their stem cell status using a CFU-F assay *in vitro*.

5.2 Initial characterization of *Pdgfra*$^{GFP/+}$ mice

The reporter mice, carrying a *Pdgfra*^{GFP} knock-in/knockout allele, were maintained as heterozygotes (*Pdgfra*$^{GFP/+}$). There were no detectable differences in development, growth or fertility between WT littermates and heterozygous *Pdgfra*$^{GFP/+}$ knock-in mice, an observation confirmed by others (personal communication, Dr O Prall, Victor Chang Cardiac Research Institute, Australia; Professor P Soriano, Fred Hutchinson Cancer Research Centre, Seattle). In order to confirm that GFP expression in these *Pdgfra*$^{GFP/+}$ mice faithfully reflected endogenous PDGFRA expression, cells from the hearts of these mice were subjected to flow cytometry. As can be seen in figure 5.1, expression of native PDGFRA was coincident with GFP expression. Having confirmed the validity of the model, the relationship of these GFP^{+} cells with expression of other stem cell markers and their stem cell status was investigated using a CFU-F assay.

5.3 CFU-F in the heart and enrichment of Sca1^{+}/PECAM1^{-} /PDGFRA^{GFP+} population

Initial experiments demonstrated that the proportion of GFP positive mononuclear cells in the *Pdgfra*$^{GFP/+}$ adult heart was approximately 14% (figure 5.1). In order to refine this comparatively large population prior to CFU-F analysis, additional surface markers characteristic of stem cells needed to be employed. As outlined in chapter 1 there are a number of candidate surface antigen markers. Sca-1 was selected as there are a number of independent reports indicating its expression on candidate stem cells (Matsuura et al., 2004; Oh et al., 2003; Pfister et al., 2005), and unlike other markers (for example c-kit), it is less sensitive to enzymatic degradation (Li et al., 2008; Pfister et al., 2005). Mononuclear cell fractions from the heart were therefore subjected to sequential cytometry and sorting based on the expression of surface antigen markers and/or GFP. A schematic diagram showing organization of the gating by the flow cytometry used in these series of experiments is shown in figure 5.2. All specific fluorescent antibody

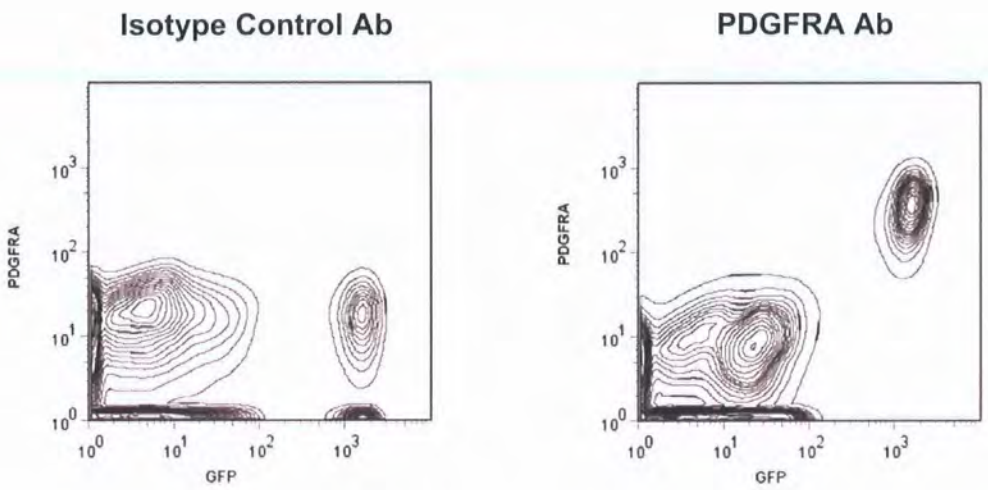

Figure 5.1 Flow cytometry plot demonstrating co-expression of PDGFRA^{GFPHIGH} and PDGFRA Ab in adult *Pdfgra*$^{GFP/+}$ heart.

Expression of native PDGFRA was coincident with GFP expression in the *Pdgfra*$^{GFP/+}$ heart

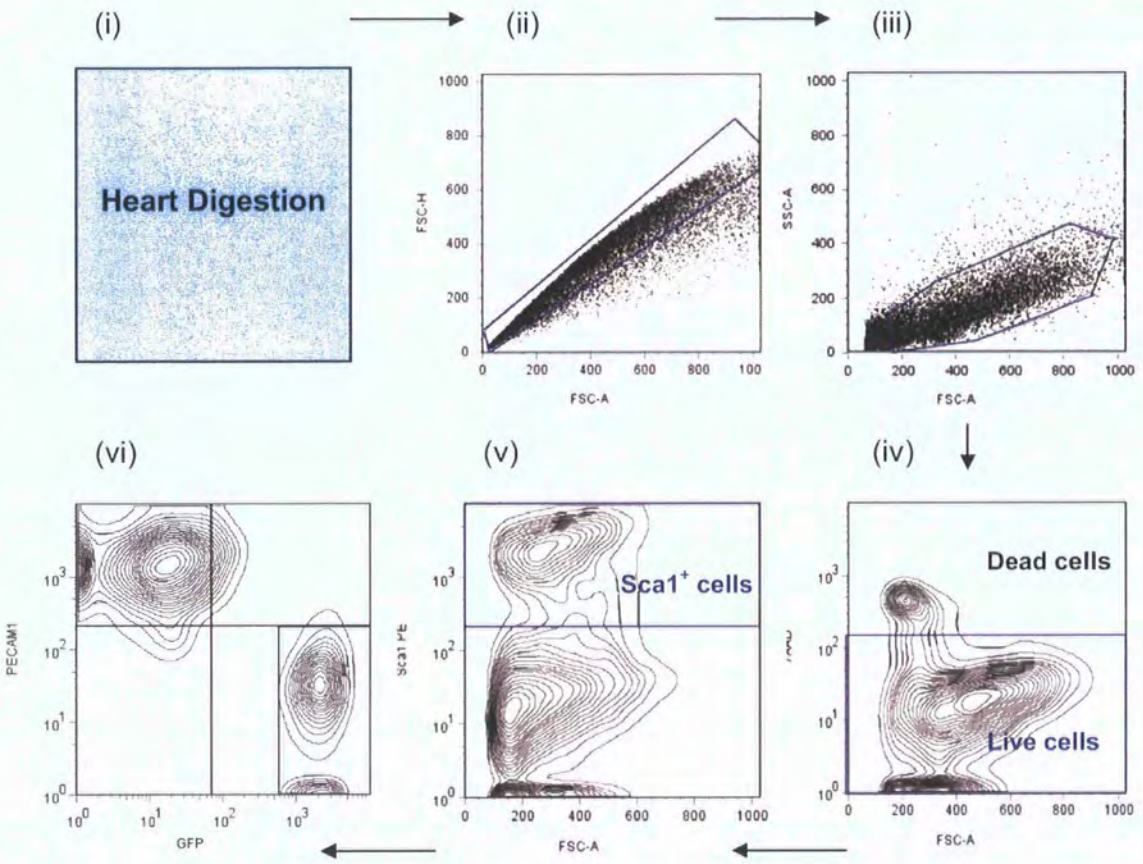

Figure 5.2 Schematic diagram showing the gating strategy used in flow cytometry.

i) The heart was initially digested.(ii) Forward Scatter Height/ Forward Scatter Area gate shown aims to reduce aggregates (iii) Side Scatter/Forward Scatter demonstrates isolation of cells excluding cell fragments. (iv) 7AAD was used to gate out dead cells. (v) Sca-1^{+} cells were isolated using Ab. (vi) Finally PECAM1 Ab and GFP were used to isolate the PECAM1^{-}/PDGFRA^{GFP+} fraction from Sca-1^{+} cell fraction in *Pdgfra*$^{GFP/+}$ hearts.

labeling was confirmed by isotype matched negative control antibodies. The sorted populations were then assessed for colony forming activity.

Although the present study concentrated on a $PDGFRA^{GFP+}$ population, the numbers of colony forming cells in whole unfractionated heart was first addressed, and then in order to enrich for this population the mononuclear cell population was fractionated on the basis of expression markers which have been found to be associated with stem cells. Hearts from adult mice aged between 8 to 12 weeks were digested and the unfractionated mononuclear fraction plated out in a CFU-F assay. In three independent experiments 0.39% $\pm$ 0.014 of the unfractionated heart mononuclear cells demonstrated colony forming ability (figure 5.3).

Primary CFU-F assays demonstrated a heterogeneity in the size of colonies formed. This is consistent with other reports of similar assays (Louis et al., 2008). Louis et al found in a neural colony forming assay that different size colonies had different re-plating abilities enabling the authors to make conclusions as to the putative progenitor or stem cell status of a selection of cells. The progenitor cells which formed the smaller colonies were found to have limited self-renewal potential and also a restricted differentiation potential compared to the cells which formed the larger colonies (putative stem cells) which had a greater potential for self renewal and differentiation. In a similar way in the present study colonies formed could be scored into different size categories, micro (<2mm diameter with 5-25 cells), small (<2mm diameter with >25 cells), large (>2mm diameter with >25 cells). In initial experiments only small (<2mm) and large (>2mm) colonies were quantitated but once the $PDGFRA^{GFP+}$ fraction was subject to CFU-F assay, micro colonies were also quantitated. When assessed by size, the numbers of colonies formed from the whole heart were broadly equivalent, 0.20% $\pm$ 0.015 and 0.19% $\pm$ 0.020 for small and large colonies respectively (figure 5.4).

Having established that CFU-F could be detected, the association of this activity with surface antigen expression was investigated. The mononuclear cell fraction from adult mouse hearts was FACS sorted into Sca-1 positive and negative fractions in ten

Figure 5.3 Photograph of a typical large primary colony. Stained with crystal violet. Scale Bar = 2mm.

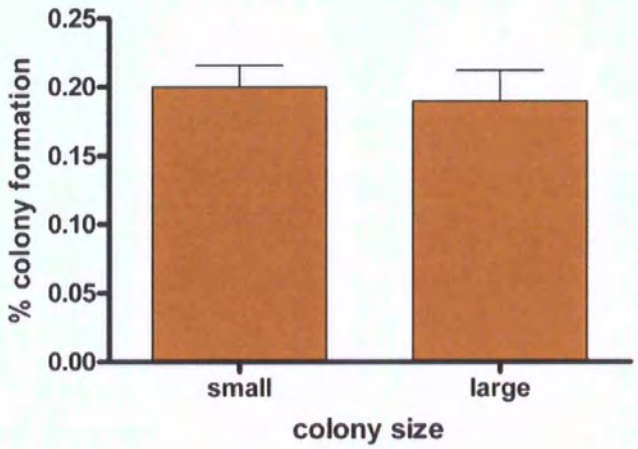

Figure 5.4 Whole heart percentage colony formation after selection for live cells

Numbers of colonies formed from the whole heart were broadly equivalent, 0.20% $\pm$ 0.015 and 0.19% $\pm$ 0.020 for small and large colonies respectively. (p = ns). N=10 per group.

independent experiments, and the isolated cells plated out in a CFU-F assay. 52.3% ± 3.03 of live mononuclear cells expressed high levels of Sca-1 (Figure 5.5a). When plated out in a CFU-F assay, this Sca-1$^+$ fraction contained all of the detectable colony forming activity (figure 5.5b), a result which was statistically significant ($p<0.05$). However the proportion of cells giving rise to colonies was still comparatively low, 0.33% ± 0.016 for small colonies and 0.30% ±0.037 for large colonies. In order to enrich this population further the expression of PECAM1 (CD31) was investigated, as this has been used previously by Pfister et al to enrich the yield of putative stem cell populations in the heart. Pfister and colleagues showed that from a side population (SP) group of cells isolated from the heart, only those Sca-1$^+$/CD31$^-$ cells showed any cardiomyogenic potential (Pfister et al., 2005). The digested heart specimens were therefore subject to Sca-1 and PECAM1 dual staining and analysed by flow cytometry. 25.1% ± 3.2 of the Sca-1$^+$ cells were PECAM1 negative (figure 5.6), and in three independent experiments it was found that all of the detectable CFU-F activity was found in this Sca-1$^+$PECAM1$^-$ sub-population (data not shown).

Having established that 100% of detectable CFU-F activity in the heart segregated with the Sca-1$^+$PECAM1$^-$ population the expression of Sca-1$^+$/PECAM1$^-$/PDGFRA^{GFP} was examined. Figure 5.7a shows the flow cytometry contour plot for PECAM1 and PDGFRA^{GFP} from the Sca-1$^+$ fraction of cells. As can be seen, there was a distinct PDGFRA^{GFPHIGH} population that was PECAM1 negative. Note that from now on it can be assumed that PDGFRA^{GFP} population refers to the Sca-1$^+$/PECAM1$^-$ /PDGFRA^{GFP+} subfraction. There was a small shoulder of PECAM1$^+$ cells which appeared to demonstrate a GFP fluorescence greater than that seen in the negative control. Gates were set up to identify all of these populations as shown in figure 5.7b. All of the seven populations were assessed for CFU-F activity, however only the PDGFRA^{GFPHIGH} fraction possessed any detectable colony forming ability. In this experiment which incorporated data from 8 hearts, colony forming ability was 0.18% ± 0.022 for small colonies and 0.7% ± 0.036 for large colonies. This represented an enrichment of small and large colony forming efficiency from using just the whole heart. Figure 5.8 summarises the CFU-F proportions for the small and large colonies and also micro

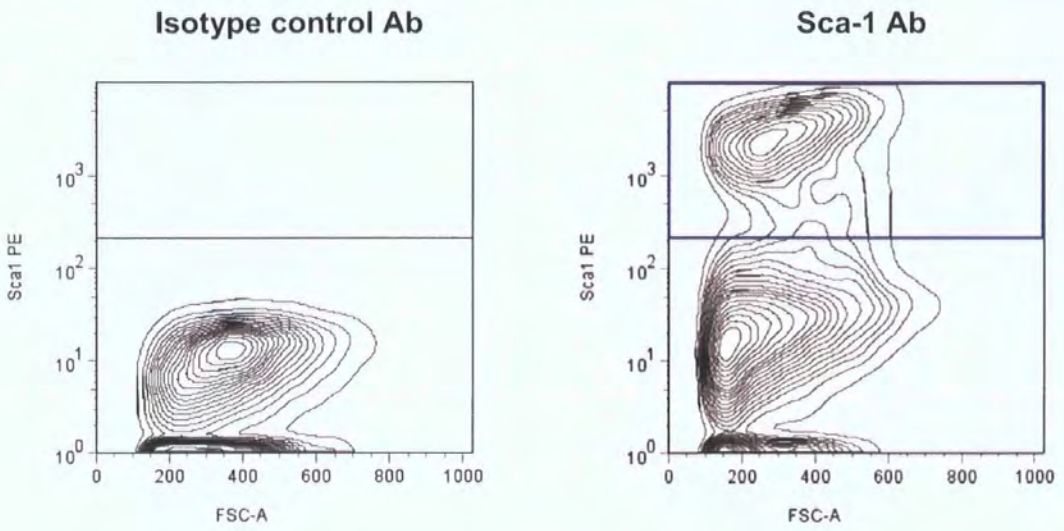

Figure 5.5 (a) Flow cytometry plot showing gating strategy for Sca-1^{+} cells.

52.3% $\pm$ 3.03 of live mononuclear cells expressed high levels of Sca-1+. N=20.

Figure 5.5 (b) Percentage colony formation in the heart according to Sca-1 status.

All the detectable CFU-F activity in the heart was shown to be in the Sca1^{+} fraction. N=10 in each group

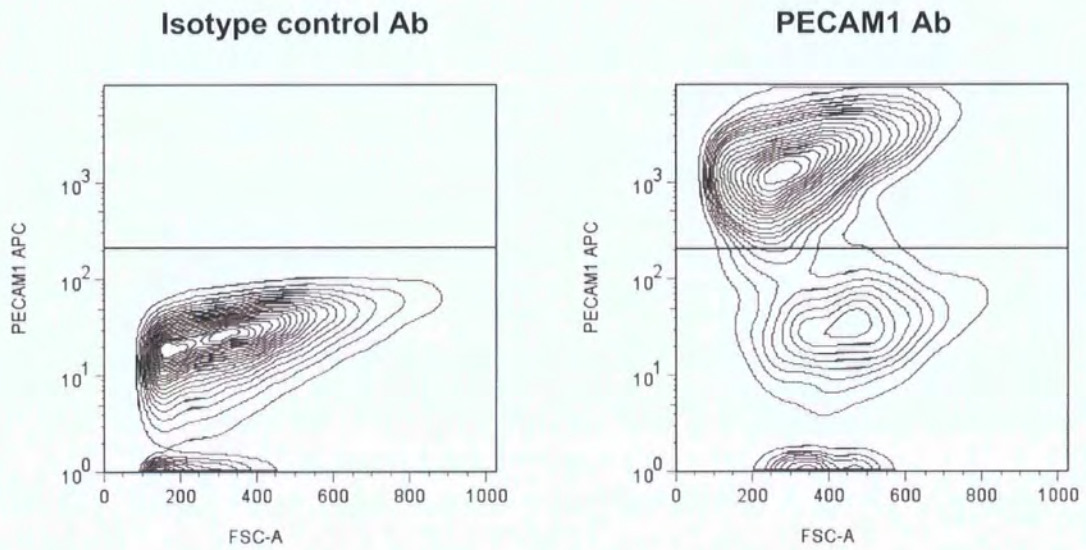

Figure 5.6 Flow cytometry plot demonstrating the PECAM1 gate.

25.1% $\pm$ 3.20 of the Sca-1^+ fraction were negative for PECAM1 and when plated out in the CFU-F assay, this negative fraction contained all of the detectable colony forming activity.

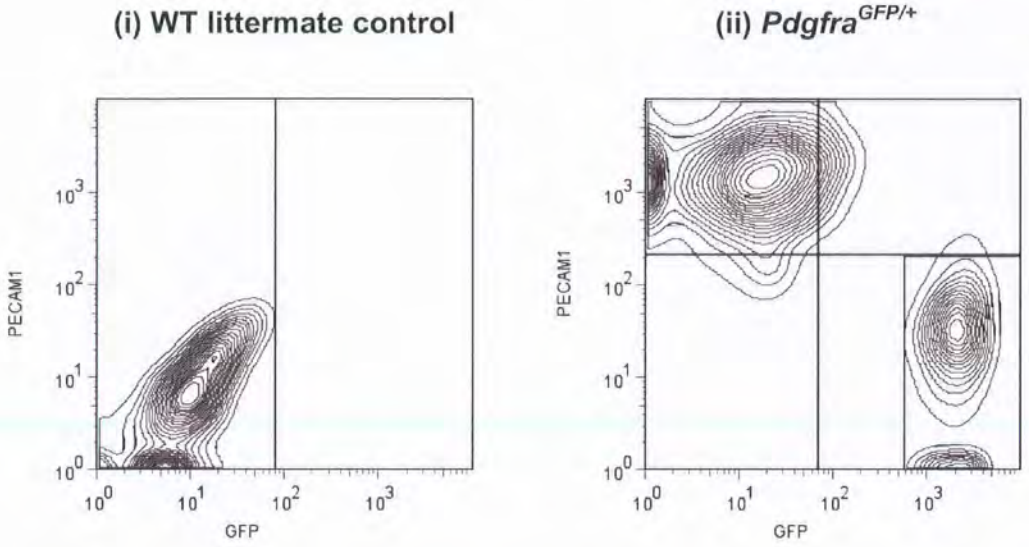

Figure 5.7(a) Flow cytometry plot of examination of GFP expression

(i) WT heart demonstrating gating strategy (ii) *Pdgfra*$^{GFP/+}$ heart. 10.2% $\pm$ 1.37 of the Sca-1+ population was found to be PECAM^{-}/GFP^{HIGH} in *Pdgfra*$^{GFP/+}$ hearts. All of the CFU-F activity was contained in this population. This plot was divided into the gates shown in figure 5.7b and the same strategy was used in further analyses.

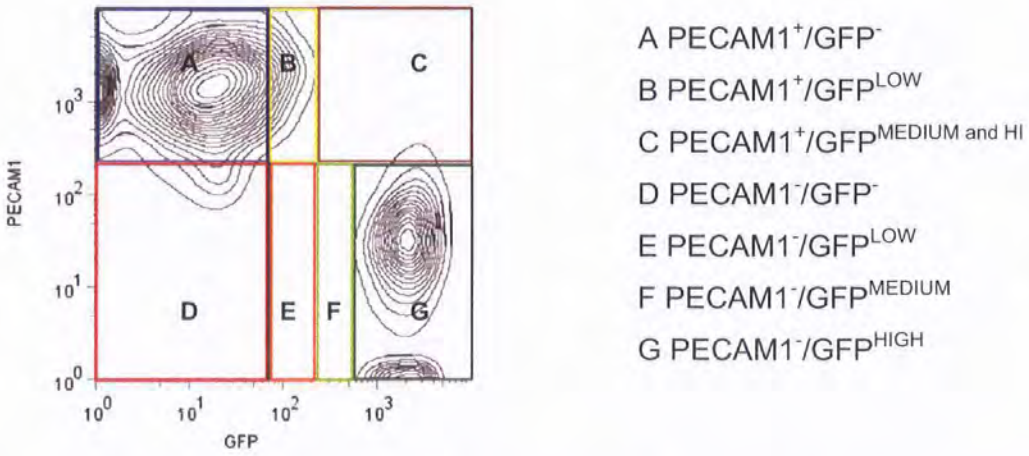

Figure 5.7(b) Gating strategy used in flow cytometry prior to CFU-F assay

Each of these seven populations (A-G) were assessed for colony forming activity.

Figure 5.8 Primary colony formation from PDGFRA^{GFPHIGH} cells.

Colonies were divided into micro, small and large sizes. The percentage colony formation of each of these was significantly different from each of the others ($p<0.05$). N = 8 hearts. 5 plates counted for each colony type per heart.

colonies . In addition to analyzing colony formation in a cell population it was important to examine colony formation at the single cell level to assess whether there was any effect of cell – cell interaction on colony formation. Figure 5.9 demonstrates the results from a serial dilution assay showing consistency of colony formation at the single cell level of $PDGFRA^{GFPHIGH}$ cells.

Now that it had been established that CFU-F activity was present in the adult heart and that this CFU-F activity was exclusively associated with the $PDGFRA^{GFPHIGH}$ fraction of cells, it was important to establish any changes in these populations in diseased states and also characterize further their self renewal capacity.

5.4 Quantification of $Pdgfra^{GFP+}$ cells in a diseased heart- Myocardial Infarction

As shown in Chapter 3 a murine model of myocardial infarction had been established for the purpose of investigating the diseased heart. In this experiment, sham operated mice were used as controls, where the mice were anaesthetized and thoracotomy performed, but there was no manipulation of the heart. Figure 5.10 depicts an annotated outline of the experimental events.

Murine hearts, 5 days and 12 days after surgical ligation of the left coronary artery were digested and subject to flow cytometry to delineate the cell fractions on the basis of expression of Sca-1, PECAM1 and $PDGFRA^{GFP}$. Figure 5.11 demonstrates the contour plots of PECAM1 and $PDGFRA^{GFP}$ for the Sca-1 positive fraction of both sham operated and those subject to MI. The gates used were those already established (figure 5.7b). Compared with the sham operated mice the mice subject to MI demonstrated the appearance of an increased number of cells in fractions F and G, a result consistently seen across 18 experiments. In order to examine the CFU-F activity of each of these populations the cells from all fractions shown in figure 5.11 from both sham operated and MI mice were plated out in a CFU-F assay. Only cells from fractions F and G ($Sca\text{-}1^{+}/PECAM1^{-}PDGFRA^{GFPHIGH}$ and $Sca\text{-}1^{+}/PECAM1^{-}/PDGFRA^{GFPMEDIUM}$) contained cells

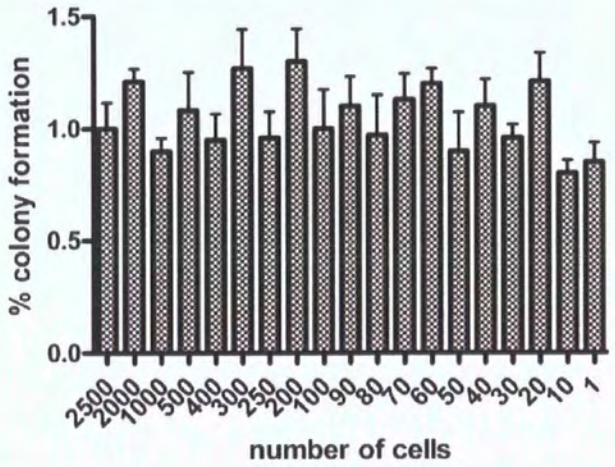

Figure 5.9 Serial dilution assay using PDGFRA^{GFPHIGH} cells from *Pdgfra*$^{GFP/+}$ heart.

Total colony formation percentage is shown demonstrating consistency of total colony formation down to the single cell level. N = 3 hearts.
Assay performed by Dr V Chandrakanthan (Victor Chang Cardiac Research Institute, Australia)

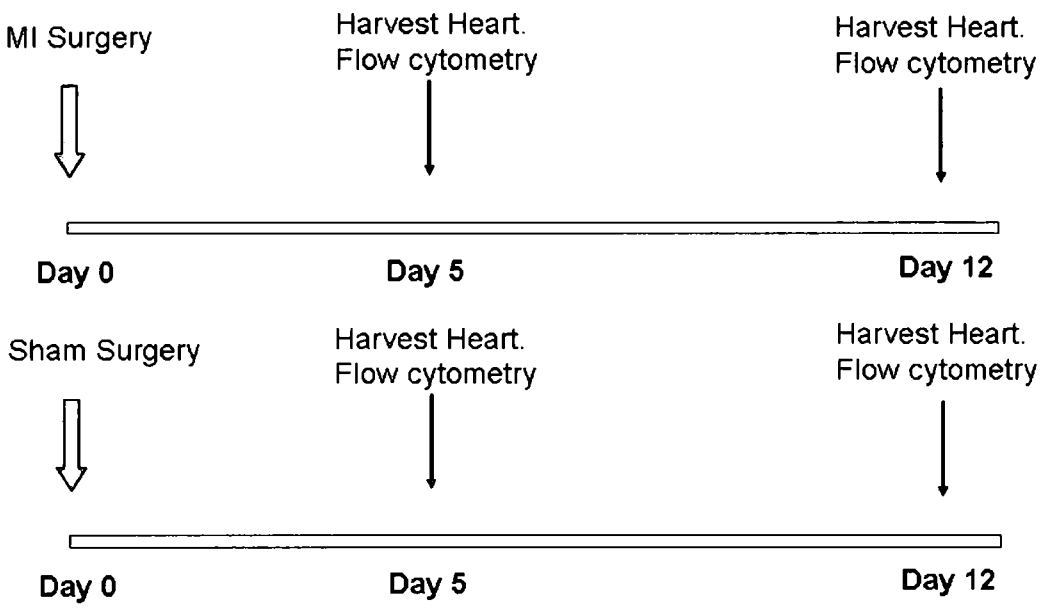

Figure 5.10 Experimental outline of events prior to analysis

This shows timepoints of surgery and flow cytometry analysis in *Pdgfra*$^{GFP/+}$ mice.

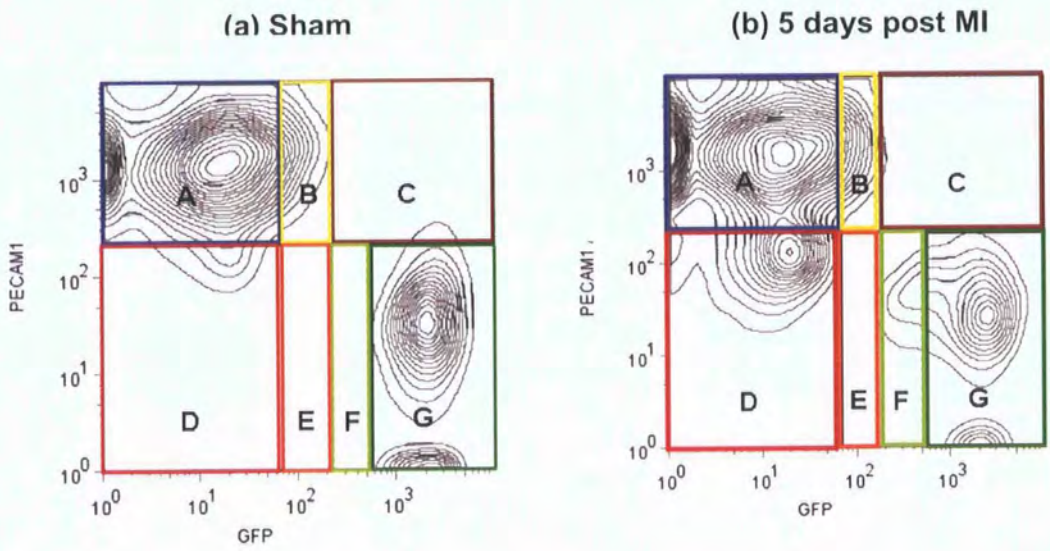

Figure 5.11 Flow cytometry plot of *Pdgfra*$^{GFP/+}$ heart comparing sham and MI.

This demonstrates the change in proportions of the colony forming fractions in (a) sham and (b) 5 days post MI. Note that post MI, cells could be isolated from Gate F, a PDGFRA^{GFPMEDIUM} population which formed colonies. Only cell fractions F and G formed colonies.

which formed colonies. There were very few PDFGFRA^{GFPMEDIUM} cells isolated from the sham operated mouse therefore it was only after MI that enough of these cells could be obtained for plating. Change in the proportion of PDGFRA^{GFPMEDIUM} and PDGFRA^{GFPHIGH} cells after MI is illustrated in figures 5.12a and 5.12b. The PDGFRA^{GFPHIGH} fraction post MI was significantly increased (17.40% $\pm$ 1.08) compared to the same population in the sham operated control (8.10% $\pm$ 1.37) ($p<0.05$). The PDGFRA^{GFPMEDIUM} population also changed post infarct increasing from a mean of 1.50% $\pm$ 0.09 to 4.70% $\pm$ 0.51 ($p<0.05$). Note also from figure 5.11b there was an increase in the proportion of cells in gate D post MI ($p<0.05$). There was a similar pattern as that just described found in hearts at day 12 post infarct. The PDGFRA^{GFPHIGH} fraction increased significantly from a mean of 9.47% $\pm$ 0.38 in the sham to 13.3% $\pm$ 0.58 post MI ($p<0.05$). The PDGFRA^{GFPMEDIUM} population increased nearly 5 fold from a mean of 1.45% $\pm$ 0.37 to 6.91% $\pm$ 0.12 ($p<0.05$) (figure 5.12a,b).

These changes in proportion of PDGFRA^{GFPHIGH} and PDGFRA^{GFPMEDIUM} populations could be due not to an increase in absolute number, but a diminution of the other populations. In order to address this, the absolute numbers were assessed (figure 5.13). In correlation to the increase in proportions, actual cell number for these 2 populations increased post MI . Indeed, the absolute increase was even greater than that suggested by the proportional analysis. The proportions calculated by flow cytometry showed an increase at 5 days post MI in PDGFRA^{GFPHIGH} population by a factor of 2.1 and an increase in the PDGFRA^{GFPMEDIUM} population by a factor of 3.1, whereas when cell numbers were analysed the increase for PDGFRA^{GFPHIGH} population was 2.5 and for the PDGFRA^{GFPMEDIUM} population was 4.8. This may be because the increase in proportion calculated on flow cytometry may be 'diluted' by an influx of inflammatory cells post MI (this may account for the increase in gate D). Indeed, the PECAM^{-}PDGFRA^{GFP-} fraction (labeled as D in figure 5.11) was shown to stain positive for CD45, a marker of haematopoietic cell types (figure 5.14b), which would be consistent with this expanded population reflecting an influx of extra-cardiac inflammatory cells, such as neutrophils, part of the post infarct inflammatory response (Frangogiannis et al., 2002). However, this raised the question of whether the increased populations of PDGFRA^{GFPHIGH} and

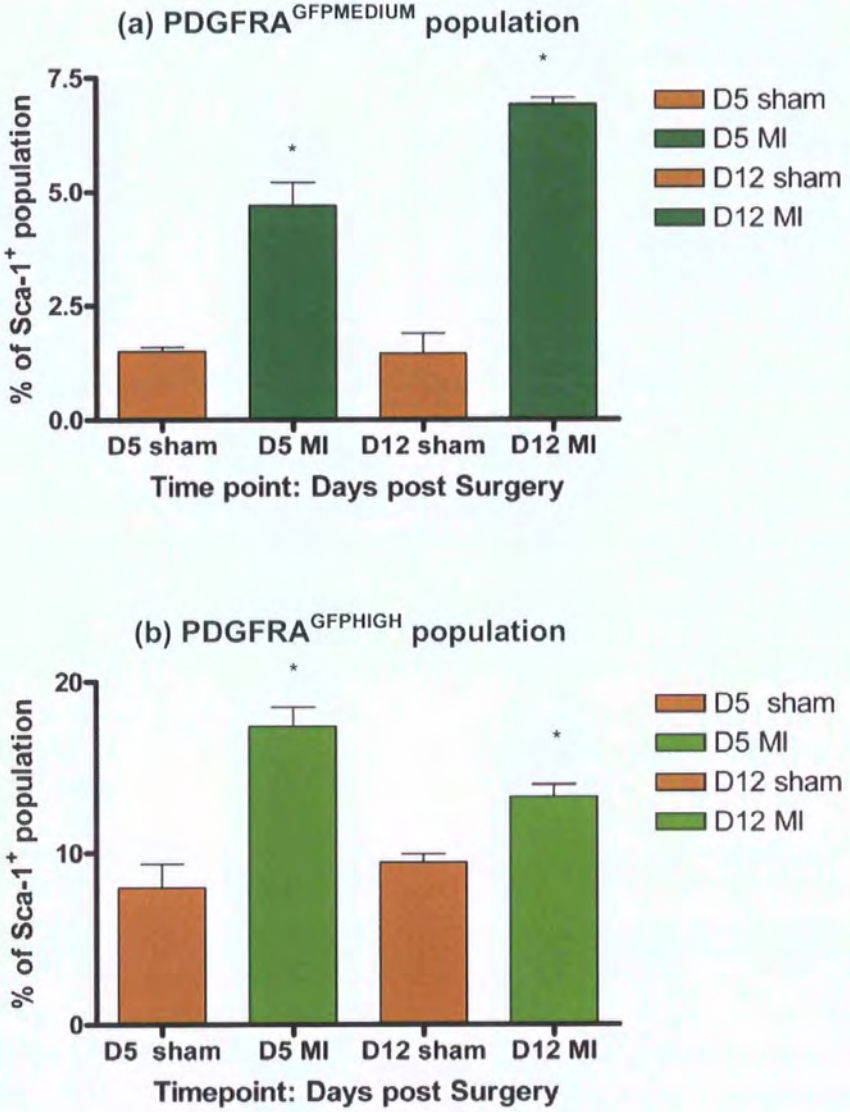

Figure 5.12 Histogram demonstrating the change in (a) PDGFRA^{GFPMEDIUM} and (b) PDGFRA^{GFPHIGH} populations at Day 5 and 12 post MI in comparison to sham.

Note the significant increase in percentage of PDGFRA^{GFPMEDIUM} and PDFGRA^{GFPHIGH} populations post MI. * denotes $p<0.05$. N = 18 in each Day 5 (D5) post surgery group. N = 3 in each Day 12 (D12) post surgery group.

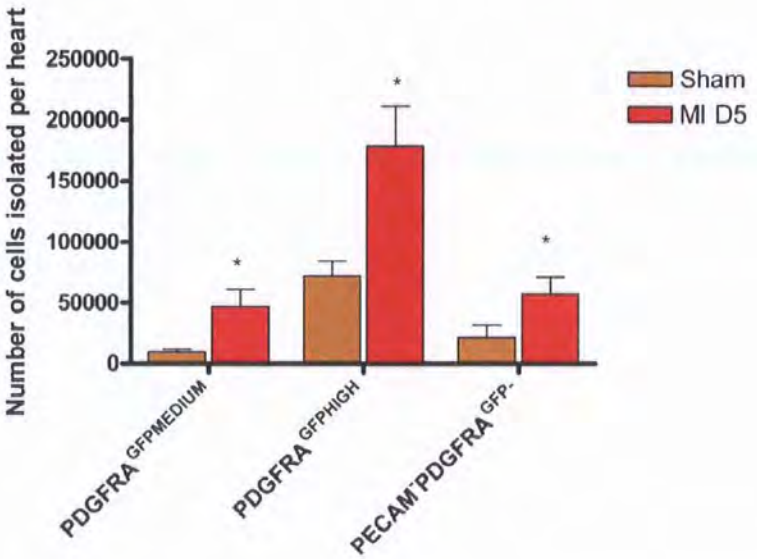

Figure 5.13 Comparison of actual cell numbers per heart isolated by flow cytometry for PDGFRA^{GFPMEDIUM} and PDGFRA^{GFPHIGH} cells in sham hearts and day 5 post MI (MI D5); *Pdgfra*$^{GFP/+}$ hearts.

Numbers of PDGFRA^{GFPHIGH} and PDGFRA^{GFPMEDIUM} cells increased significantly post MI ($p<0.05$). Also shown is the increase in PECAM$^-$/PDGFRA^{GFP-} fraction (labelled as D in figure 5.11) ($p<0.05$). The increase in this PECAM$^-$PDGFRA^{GFP-} fraction could be represented by an influx of cells from the bone marrow post infarct- see section 5.5 on CD45 status.* denotes $p<0.05$. N = 8 hearts.

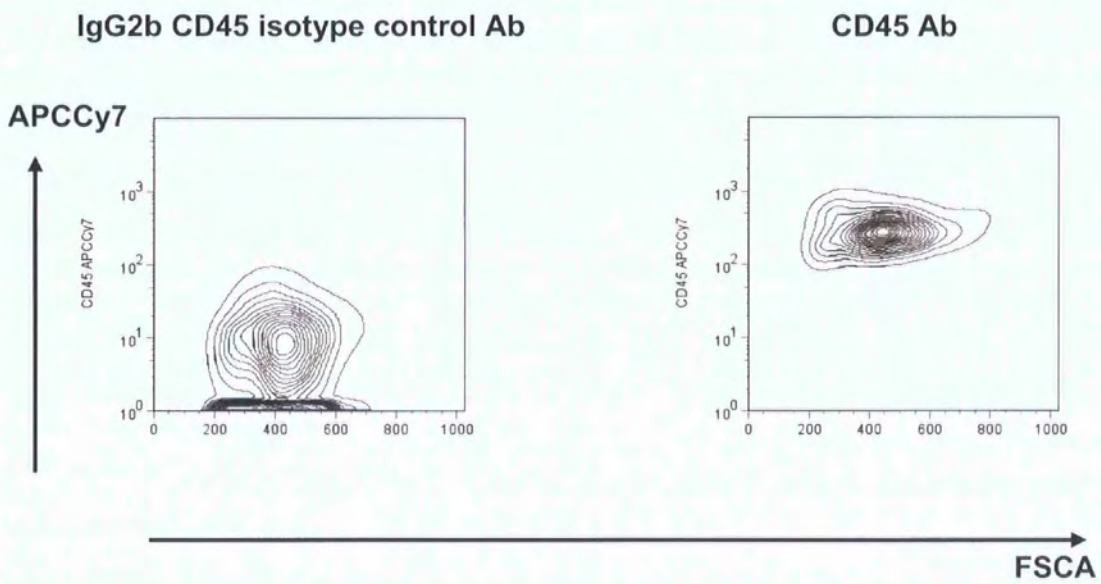

Figure 5.14 (a). Flow cytometry of bone marrow from a WT mouse
This demonstrates that the CD45 antibody and its isotype were effective

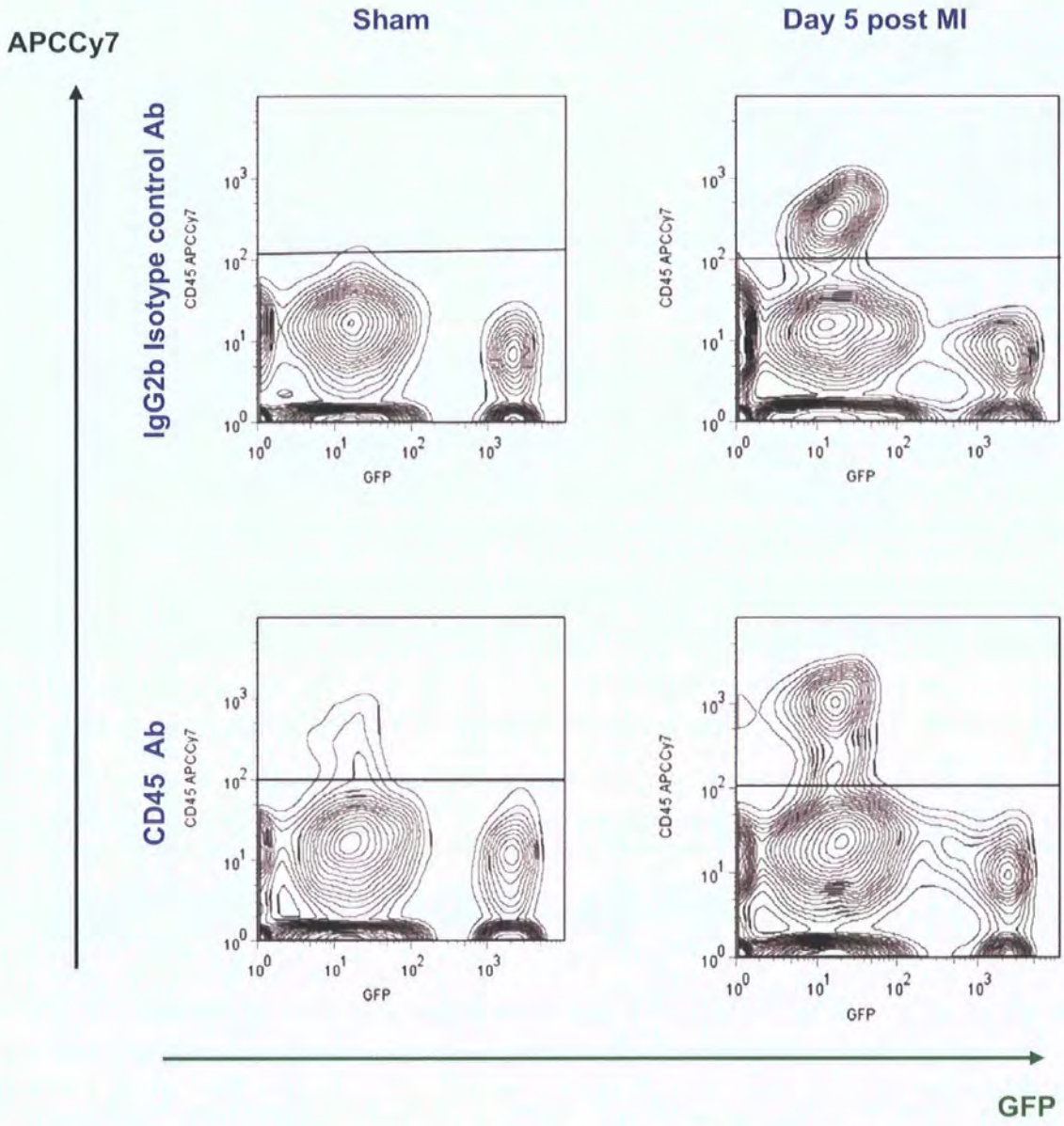

Figure 5.14 (b) Interrogation of the Sca-1^{+} population in *Pdgfra*$^{GFP/+}$ hearts for CD45 expression.

The PDGFRA^{GFPHIGH} and PDGFRA^{GFPMEDIUM} populations were negative for CD45. The PDGFRA^{GFP-} fraction however was shown to contain CD45^{+} cells in sham operated hearts and post MI. See main body of text section 5.5 for interpretation of isotype. control.

PDGFRA ^{GFPMEDIUM} cells similarly reflected an infiltration of exogenous haematopoietic cells. In order to address this, the CD45 status of these populations was assessed.

5.5 CD45 status

In an effort to assess whether the increase in the candidate cell populations which formed colonies (PDGFRA^{GFPMEDIUM} and PDGFRA^{GFPHIGH}) may have been due to an influx of haematopoietic cells, the cells were interrogated with antibody against CD45. The results of this are shown in figure 5.14b. The PDGFRA^{GFPHIGH} and PDGFRA^{GFPMEDIUM} cells were negative for CD45 reducing the possibility that there had been any influx of haematopoietic cells into these populations. The initial gating was performed using the IgG2b isotype for CD45 in the sham. The positivity for the isotype control in the MI is likely to be due to activation of and influx of inflammatory cells in the heart. It is known that Fcγ receptors are found on most effector cells of the immune system, notably monocytes, macrophages, natural killer cells, mast cells, eosinophils and neutrophils. FcγR1 is expressed on the surface of neutrophils, monocytes, granulocytes and macrophages and binds the Fc portion of IgG with high affinity (Raghavan and Bjorkman, 1996). All of these cells are activated as part of the post infarct inflammatory response and hence are likely to bind to the IgG isotype control as shown in figure 5.14b.

Having determined that the PDGFRA^{GFPHIGH} and PDGFRA^{GFPMEDIUM} populations were unlikely to be haematopoietic, the nature of the colonies that these cell types could produce was examined.

5.6 Primary colony formation from *Pdgfra*$^{GFP/+}$ mice post MI

In a manner similar to non-infarcted mice, there was heterogeneity in the size of the primary colonies formed by PDGFRA^{GFP+} cells isolated 5 days after either MI or sham operation. However, although there was no significant difference in the frequencies of the different sizes of colony formed from un-operated mice compared to the sham operated

controls, there were substantial changes in the colony forming ability post MI, as shown in figure 5.15. PDGFRA^{GFPMEDIUM} cells formed very few small and large colonies, however they formed significantly greater numbers of micro colonies compared to the PDGFRA^{GFPHIGH} population ($p<0.05$). Also interestingly, post MI there was a significantly greater colony forming ability of the PDGFRA^{GFPHIGH} cells for micro, small and large colonies ($p<0.05$). These differences in colony size could reflect a different potential of the initiating cell. In order to address this, the ability of cells from these different populations to form secondary and tertiary colonies was assessed.

5.7 Secondary and tertiary colony formation from *Pdgfra*$^{GFP/+}$ mice

Individual primary colonies were disaggregated and re-plated in a secondary CFU-F assay and numbers and size of new colonies assessed. Micro colonies did not demonstrate any ability to form secondary colonies of any size. Similarly, colonies formed by PDGFRA$^{GFP\ MEDIUM}$ cell population from either the sham or post MI mice did not produce secondary colonies. However colonies did form from small colonies and large colonies from the PDGFRA^{GFPHIGH} cell population as illustrated in figure 5.16a and 5.16b. The small and large primary colonies gave rise to all sizes of secondary colony, however large colonies predominated. There were no significant differences between the groups which were sham operated or five days post MI in the percentage colony forming ability from any one particular primary colony size. The large primary colonies from the PDGFRA^{GFPHIGH} cell population generated a greater percentage of large secondary colonies in comparison to that from small primary colonies ($p<0.05$). Small primary colonies gave 12% $\pm$ 1.84 large colonies in the sham and 12% $\pm$ 1.18 large colonies post MI. Large primary colonies gave 16% $\pm$ 1.00 large colonies in the sham and 13% $\pm$ 1.67 post MI. These data suggested that the numbers of CFU-F present in the different PDGFRA^{GFP+} populations within the sham and MI mouse differed, the phenotype of individual CFU-F groups appeared broadly similar for sham and post MI, with secondary colony formation of large colonies being greatest from large primary colonies. Production of secondary colonies is evidence for self-renewal of a CFU-F initiating cell, but this

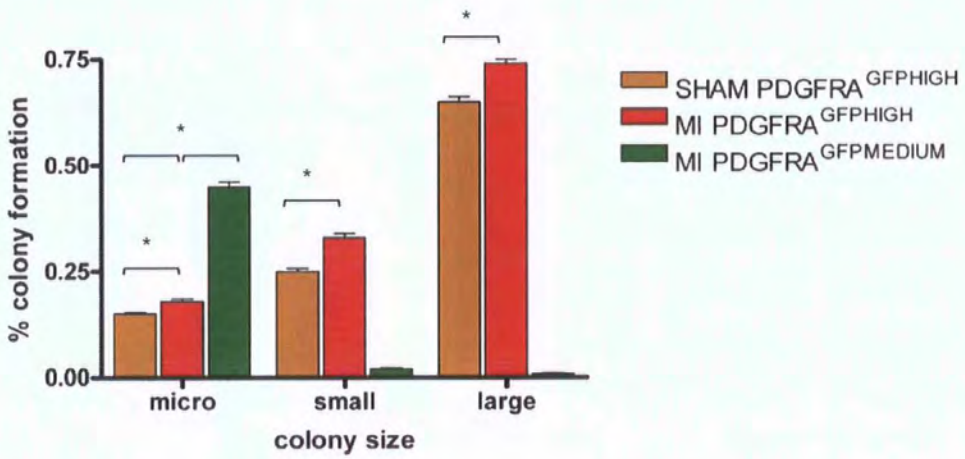

Figure 5.15 Primary colony formation in *Pdgfra*$^{GFP/+}$ hearts in sham and 5 days post MI.

PDGFRA^{GFPMEDIUM} cells formed very few small and large colonies, however they formed significantly greater numbers of micro colonies compared to the PDGFRA^{GFPHIGH} population ($p<0.05$). Post MI there was a significantly greater colony forming ability of the PDGFRA^{GFPHIGH} cells for micro, small and large colonies ($p<0.05$). * denotes $p<0.05$. Total of 16 hearts used in this analysis for Sham and MI and 5 plates counted per population per heart.

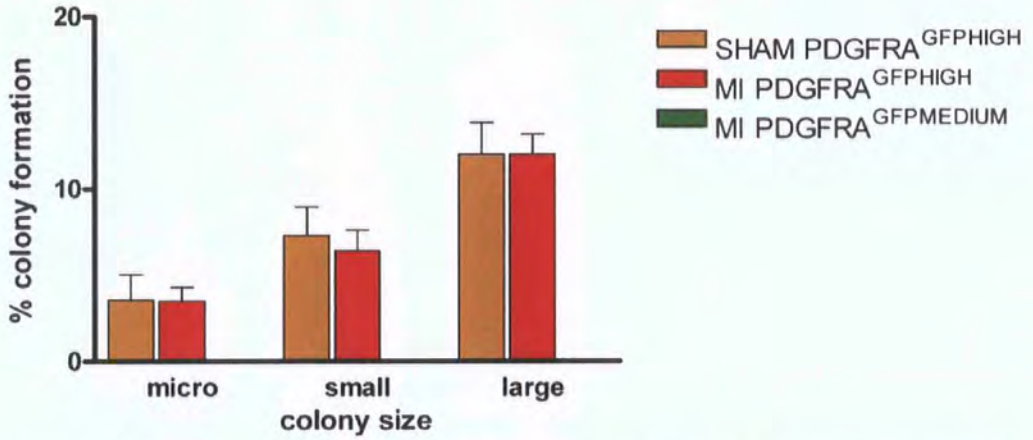

Figure 5.16 (a) Secondary colony formation from small primary colonies in *Pdgfra*$^{GFP/+}$ hearts.

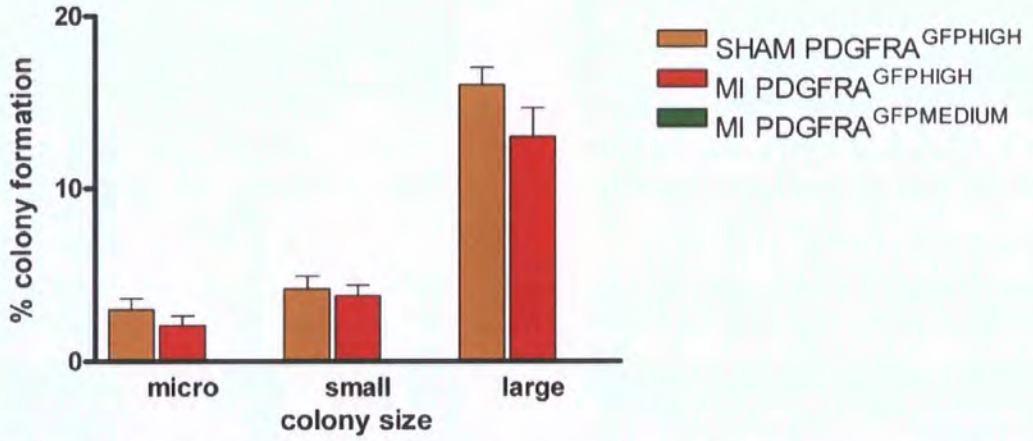

Figure 5.16 (b) Secondary colony formation from large primary colonies in *Pdgfra*$^{GFP/+}$ hearts.

Small and large primary colonies gave rise to all sizes of secondary colony, however large colonies predominated. There were no significant differences between the groups which were sham operated or five days post MI in the percentage colony forming ability from any one particular primary colony size. The large primary colonies from the PDGFRA^{GFPHIGH} cell population generated a greater percentage of large secondary colonies in comparison to that from small primary colonies in the sham heart ($p<0.05$). Total of 12 hearts were used in this analysis for Sham and MI and 30 colonies counted for each colony type per heart.

does not address whether such self renewal is maintained. In order to examine this individual secondary colonies were disaggregated and assessed for the formation of tertiary colonies.

Tertiary colonies were not formed from micro colonies. Tertiary micro, small and large colonies were produced from small and large secondary colonies, the predominant colony type being large. Small secondary colonies gave rise to 8.7% $\pm$ 1.80 large colonies in the sham and 9.5% $\pm$ 1.68 large colonies post MI (p = ns). Large secondary colonies generated 16% $\pm$ 1.47 large colonies in the sham and 14% $\pm$ 1.68 large colonies post MI (p = ns). Note that the percentage of large tertiary colonies was greater from large secondary colonies compared to small secondary colonies in sham and post MI ($p<0.05$). This data is brought together in figure 5.17 so that direct comparisons can be made. There was a significantly greater percentage of tertiary small and micro colonies from small secondary colonies post MI ($P<0.05$) compared to the percentage from small secondary colonies in a sham heart. These data suggested that the size of the initial colony was a strong predictor of both proliferative capacity (size of secondary/tertiary colonies) and self-renewal ability (numbers of colonies formed). If this was the case, then the ability of the different sized colonies to support extended culture in vitro should show a similar correlation. In separate experiments, the clonal passagability of the small and large colonies were assessed, showing that the small primary colonies did not passage beyond passage 4. At this end-stage they were predominantly non-adherent and although occasional cells were seen , no further colonies formed (data not shown). Cultures established from large colonies however showed no such limit, and have been cultured out to passage 15 with no phenotypic change, suggesting that their growth may extend beyond this. One possibility is that rather than showing a different proliferative/self renewal capacity, cells from large colonies may show a greater sensitivity to cellular transformation and/or tissue culture adaptation, which might also extend their *in vitro* life span. However, such transformation is normally associated with marked changes in cell cycle time. As can be seen from figure 5.18, the population dynamics of cultures from large colonies remained essentially constant through the entire period. That the population doubling time at the very oldest passage was the same as that at passage 1

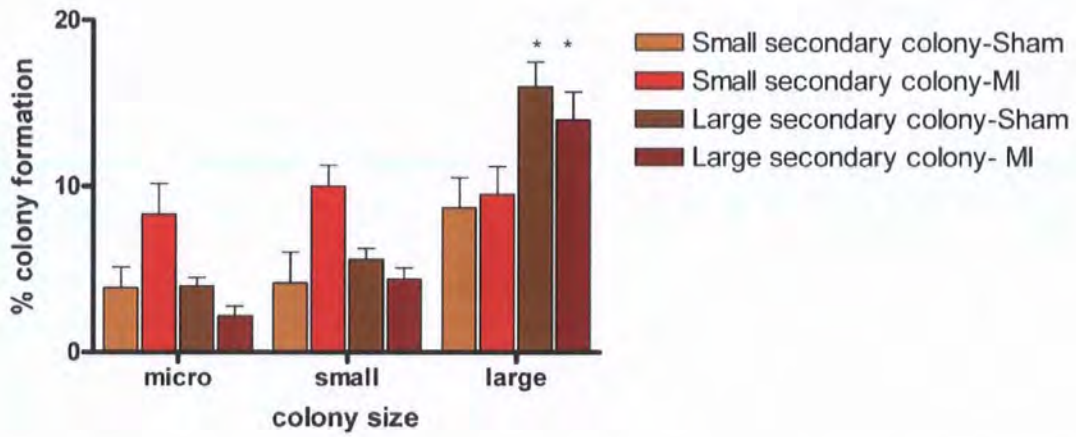

Figure 5.17 Tertiary colony formation from small and large secondary colonies derived from PDGFRA^{GFPHIGH} cells 5 days post sham surgery and post MI.

Tertiary colonies were not formed from micro colonies. Tertiary micro, small and large colonies were produced from small and large secondary colonies, the predominant colony type being large. Small secondary colonies gave rise to 8.7% $\pm$ 1.80 large colonies in the sham and 9.5% $\pm$ 1.68 large colonies post MI (p = ns). Large secondary colonies generated 16% $\pm$ 1.47 large colonies in the sham and 14% $\pm$ 1.68 large colonies post MI (p = ns). Note that the percentage of large tertiary colonies was greater from large secondary colonies compared to small secondary colonies in sham and post MI ($p<0.05$), indicated by *. Total of 6 hearts were used in this analysis for sham and MI and 30 colonies counted for each colony type per heart.

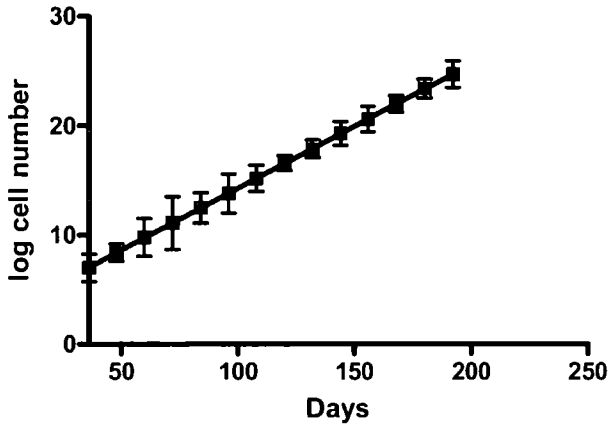

Figure 5.18 Serial passage growth curve for PDGFRA^{GFPHIGH} cells from a primary large colony (*Pdgfra*$^{GFP/+}$ heart).

Population dynamics of cultures from large colonies remained essentially constant through the entire period suggesting that substantial cellular transformation was unlikely.

(Reproduced with permission from Dr V Chandrakanthan, Victor Chang Cardiac Research Institute, Sydney)

suggests that substantial cellular transformation was very unlikely, and that the phenotypic differences between small and large colonies were indeed likely to be a function of their self renewal/proliferative capacity. MI is an acute, degenerative event, which promotes a number of responses, including inflammatory (see section 1.6). One hypothesis is that the PDGFRA^{GFP+} populations with CFU-F activity are changing as a component of a potential repair/regenerative response . If that is the case, these numbers should also be altered in mouse models which show a propensity for cardiac repair/regeneration. One such model is the α-MHC/mIGF-1 transgenic mouse.

5.8 Quantification of Pdgfra^{GFP+} cells in a proregenerative model

αMHC/mIGF-1 transgenic mice have been engineered to express an isoform of IGF-1 (Insulin like growth factor1) under the control of the αMHC promotor (Santini et al., 2007). Injury of mammalian tissues induces a transient production of locally acting IGF-1 isoforms that control growth, survival and differentiation (Goldspink, 2002). Tissues which over express IGF-1 could be predicted to show enhanced regenerative abilities. Indeed, a recent study has shown that the αMHC/mIGF-1 transgenic mice have an enhanced ability to recover heart functionality after cardiac injury, as outlined in chapter 1 (Santini et al., 2007). In order to examine whether this enhanced ability reflected changes in the Sca-1^{+}/PECAM1^{-}PDGFRA^{GFP+} population, the αMHC/mIGF-1 transgene was crossed onto the *Pdgfra*$^{GFP/+}$ background and the resulting double transgenics maintained as heterozygotes (*Pdgfra*$^{GFP/+}$*;mIGFtg*). These mice will be refered to as *Pdgfra*^{GFP}*/mIGF.*

The hearts of *Pdgfra*^{GFP}*/mIGF* mice were assessed by flow cytometry for the expression of Sca-1, PECAM1 and PDGFRA^{GFP}, using the same gating strategy as described in section 5.3. There were no detectable differences in the profiles of the sham and un-operated mice (data not shown), a result identical to that seen in the *Pdgfra*$^{GFP/+}$ mouse, suggesting that over expression of IGF-1 had no direct effect on numbers of PDGFRA^{GFP} cells. However, induction of MI changed this profile (figure 5.19). As in the *Pdgfra*$^{GFP/+}$ mice, there was an increase in the proportion of cells in the PDGFRA^{GFPMEDIUM} gate (gate

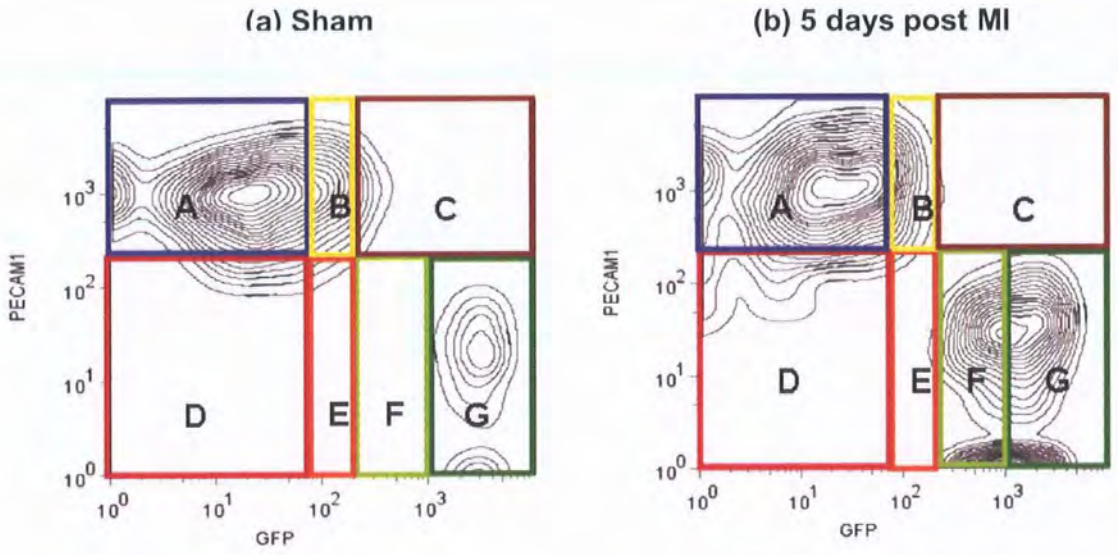

Figure 5.19 demonstrating the change in proportions of the colony forming fractions in (a) sham and (b) 5 days post MI in the *Pdfra*^{GFP}*/mIGF* mouse.

Most notably post MI, cells could be isolated from Gate F aswell as gate G. Gate F was a PDGFRA^{GFPMEDIUM} population which formed primary colonies . Only cells from gates F and G showed colony forming ability.

F) and the PDGFRA^{GFPHIGH} gate (gate G) post MI (figure 5.19b), however this increase in PDGFRA^{GFPMEDIUM} cells was significantly greater ($p<0.05$) than for the *Pdgfra*$^{GFP/+}$ mice post MI (figure 5.20). Having demonstrated that the proportions of PDGFRA^{GFP+} cells increased in the proregenerative model, absolute numbers of cells isolated at 5 days post infarct were also quantitated as for *Pdgfra*$^{GFP/+}$ hearts (section 5.4.1) (figure 5.21). As in the *Pfgfra*$^{GFP/+}$ mice the PDGFRA^{GFPHIGH} and PDGFRA^{GFPMEDIUM} cell population in *Pdgfra*^{GFP}*/mIGF* mice was CD45 negative (data not shown). The phenotype of the colonies present within the PDGFRA^{GFPHIGH} and PDGFRA^{GFPMEDIUM} populations were then addressed for the *Pdgfra*^{GFP}*/mIGF* mouse.

5.9 Primary colony formation from *Pdgfra*^{GFP}*/mIGF* hearts post MI

Data from the *Pdgfra*$^{GFP/+}$ mouse demonstrated that the PDGFRA^{GFPHIGH} and PDGFRA^{GFPMEDIUM} populations showed quantitative and qualitative differences in the respective CFU-F. Thus these two populations were sorted from the hearts of *Pdgfra*^{GFP}*/mIGF* hearts and assessed for CFU-F activity. First the PDGFRA^{GFPHIGH} population will be considered. Although there was an increase in colony forming ability post infarct for *Pdgfra*^{GFP}*/mIGF* hearts as previously described for *Pdgfra*$^{GFP/+}$, the increase was only significant for small colonies (increasing from 0.18% $\pm$ 0.004 to 0.34% $\pm$ 0.005, $p<0.05$) and large colonies (increasing from 0.76% $\pm$ 0.007 to 1.02% $\pm$ 0.010, $p<0.05$). The increase in colony forming activity from large colonies post MI in the *Pdgfra*^{GFP}*/mIGF* hearts was particularly pronounced (figure 5.22) and was significantly greater than in the equivalent population from *Pdgfra*$^{GFP/+}$ ($p<0.05$). The results for the PDGFRA^{GFPMEDIUM} population are shown in figure 5.23 . As for the *Pdgfra*$^{GFP/+}$ hearts, PDGFRA^{GFPMEDIUM} cells from *Pdgfra*^{GFP}*/mIGF* hearts formed primarily micro colonies, with few small and large. However the percentage colony formation in *Pdgfra*^{GFP}*/mIGF* hearts was significantly higher for small and large colonies ($p<0.05$). The self-renewal and proliferative capacity of these colonies was then assessed by secondary and tertiary re-plating studies.

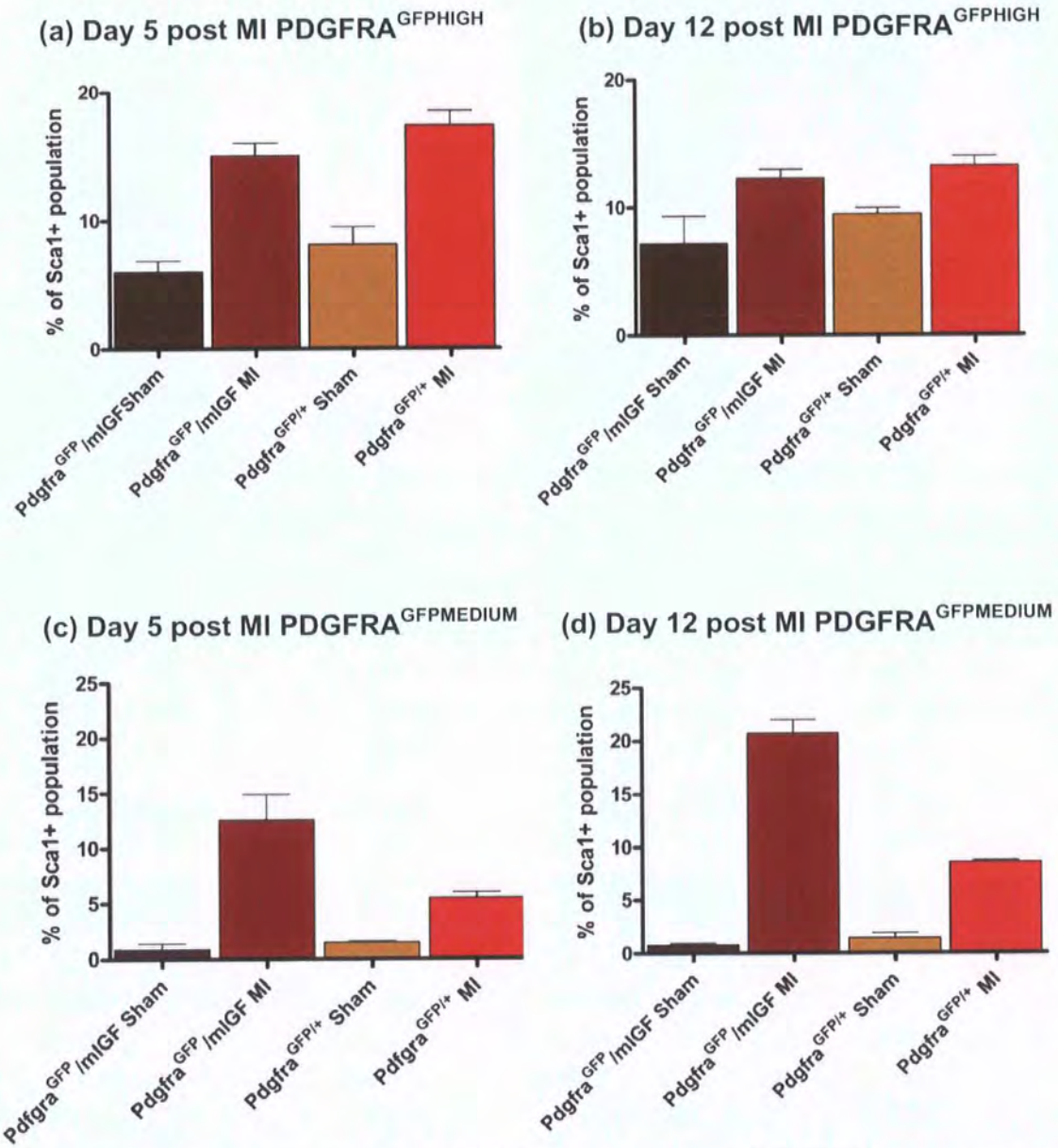

Figure 5.20 Change in PDGFRA^{GFPHIGH} and PDGFRA^{GFPMEDIUM} populations in *Pdgfra*$^{GFP/+}$ and *Pdgfra*^{GFP}*/mIGF* hearts at day 5 and day 12 post MI.

There was an increase in percentage of cells in all populations post MI, however the increase in PDGFRA^{GFPMEDIUM} fraction was significantly greater at day 5 post MI and day 12 post MI in the *Pdgfra*^{GFP}*/mIGF* heart ($p<0.05$) than for the *Pdgfra*$^{GFP/+}$ heart. N= 6 per group.

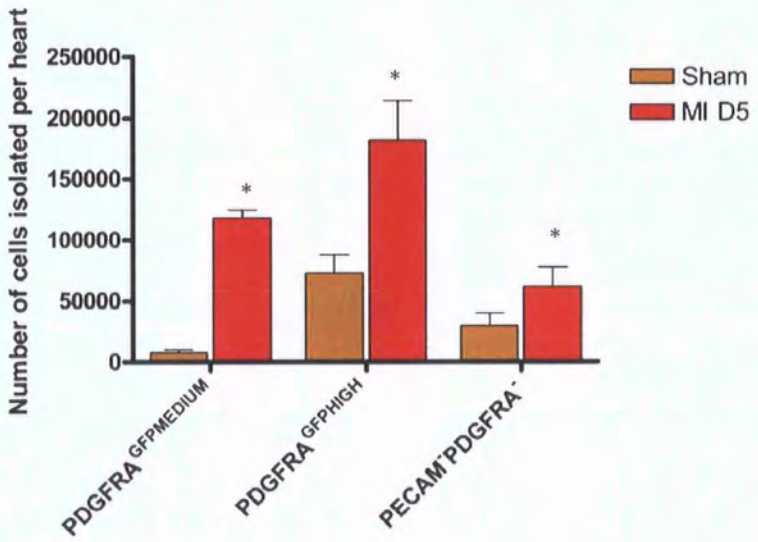

Figure 5.21 Comparison of actual cell numbers isolated by flow cytometry for PDGFRA^{GFPMEDIUM} and PDGFRA^{GFPHIGH} cells in sham hearts and day 5 post MI (D5 MI) – *Pdgfra^{GFP}/mIGF* hearts.

Numbers of PDGFRA^{GFPHIGH} and PDGFRA^{GFPMEDIUM} cells increased significantly post MI ($p<0.05$). Also shown is the increase in PECAM$^-$/PDGFRAGFP$^-$ fraction (labelled as D in figure 5.19). The increase in this fraction could be represented by an influx of inflammatory cells post infarct as explained in section 5.5. * indicates $p<0.05$. N=6 per group.

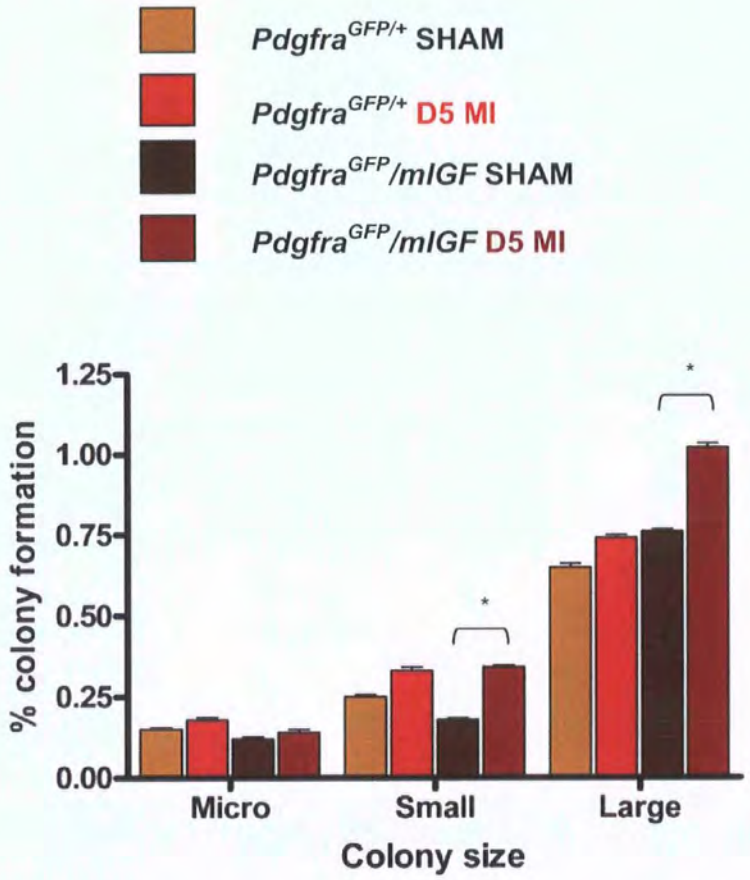

Figure 5.22 Primary colony formation from the PDGFRA^{GFPHIGH} populations in *Pdgfra*$^{GFP/+}$ and *Pdgfra*^{GFP}*/mIGF* mice in sham operated controls and 5 days post MI (D5 MI).

Although there was an increase in colony forming ability post infarct for *Pdgfra*^{GFP}*/mIGF* mice as previously described for *Pdgfra*$^{GFP/+}$ mice , the increase was only significant for small colonies (increasing from 0.18% $\pm$ 0.004 to 0.34% $\pm$ 0.005, $p<0.05$) and large colonies (increasing from 0.76% $\pm$ 0.007 to 1.02% $\pm$ 0.010, $p<0.05$). The increase in colony forming activity from large colonies post MI in the *Pdgfra*^{GFP}*/mIGF* was particularly pronounced. *denotes $p<0.05$. 8 hearts used in this analysis for each Sham and MI group and 5 plates counted per population per heart.

Figure 5.23 Comparison of primary colony formation for the PDGFRA^{GFPMEDIUM} population in *Pdgfra*$^{GFP/+}$ and *Pdfgra*^{GFP}*/mIGF hearts* 5 days post MI.

PDGFRA^{GFPMEDIUM} cells formed primarily micro colonies, with only a few small and large. However the percentage colony formation in *Pdgfra*^{GFP}*/mIGF* hearts was significantly higher for small and large colonies ($p<0.05$). * denotes $p<0.05$. 8 mice were used for each transgenic group and 5 plates counted per population per heart.

5.10 Secondary and tertiary colony formation from *Pdgfra^{GFP}/mIGF* hearts post MI

Comparison of secondary colony formation from the PDGFRA^{GFPMEDIUM} and PDGFRA^{GFPHIGH} populations in sham and MI hearts is shown in figure 5.24a. In contrast to the PDGFRA^{GFPMEDIUM} population isolated from the *Pdgfra$^{GFP/+}$* mice, the same population of cells in the *Pdgfra^{GFP}/mIGF* mice were capable of forming secondary colonies, although these tended to be the micro and small colony types. The *Pdgfra^{GFP}/mIGF* hearts gave an increased number of micro, small and large secondary colonies from small primary colonies compared to *Pdgfra$^{GFP/+}$* hearts, however this difference was not statistically significant. Notably, large primary colonies from *Pdgfra$^{GFP/+}$* hearts and also those from *Pdgfra^{GFP}/mIGF* hearts gave rise to predominantly large colonies, but there was a particularly notable increase in large colonies from *Pdgfra^{GFP}/mIGF* hearts subject to myocardial infarction ($p<0.05$) (figure 5.24b).. On analysis of tertiary colonies it can be noted in figures 5.25 (a) and (b) that PDGFRA^{GFPMEDIUM} cells from *Pdgfra$^{GFP/+}$* hearts did not give rise to tertiary colonies however those from *Pdgfra^{GFP}/mIGF hearts* did form predominantly micro and small colonies. In addition large secondary colonies gave rise to predominantly large tertiary colonies, with a marked increase in Pdgfra^{GFP}/mIGF hearts post MI ($p<0.05$).

These data suggested that the heart contained a Sca1^{+}/PECAM1^{-}/PDGFRA^{GFPHIGH} population which possessed within it cells capable of self renewal and proliferation, and also a Sca1^{+}/PECAM1^{-}/PDGFRA^{GFPMEDIUM} population which had a restricted self renewal and proliferation potential. The numbers and phenotypic profile of these cells changed in response to myocardial infarction and particularly in hearts which over expressed mIGF-1, in a manner which suggested an increase in the regenerative capacity of the heart. Candidate stem cells that show such quantitative and qualitative changes may be expected to also change their anatomical distribution (Urbanek et al., 2005) . In order to investigate whether PDGFRA^{GFP+} cells showed such changes, their distribution in the normal and infarcted heart were assessed by fluorescence microscopy.

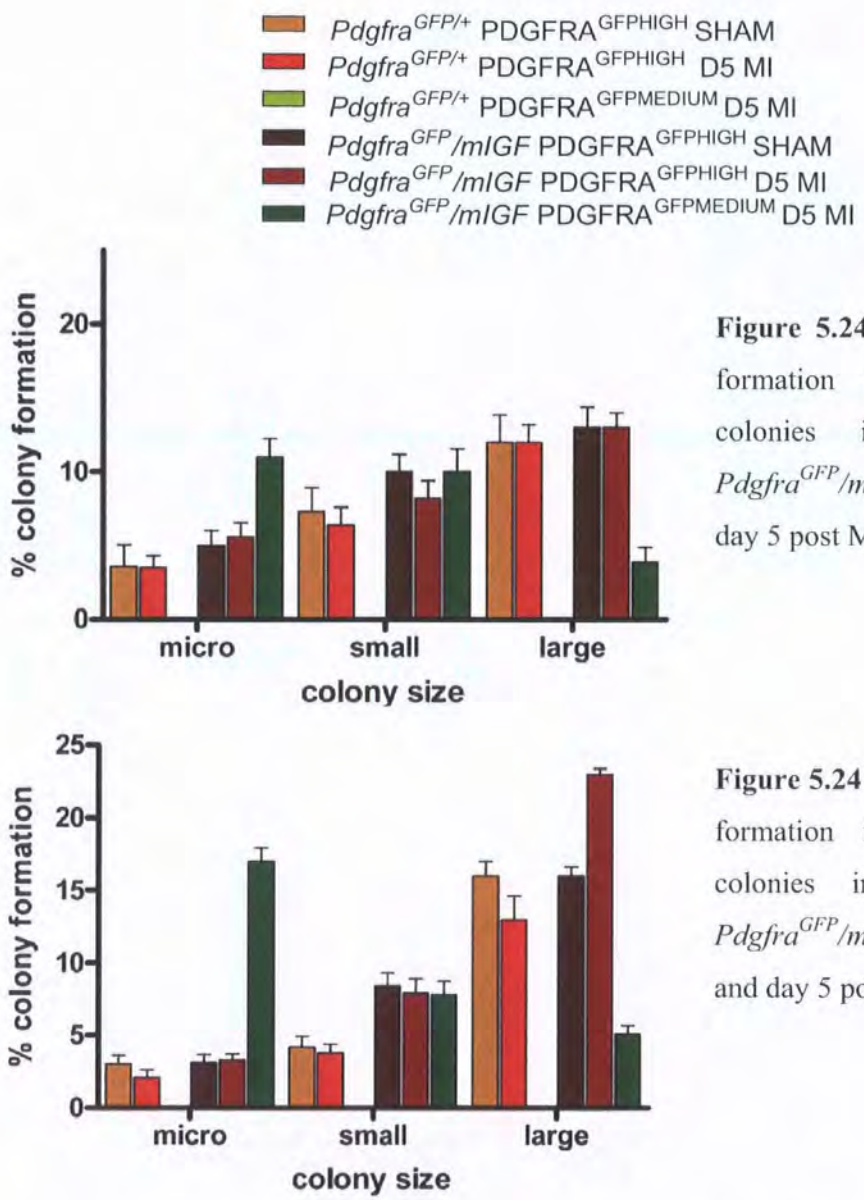

Figure 5.24 (a) Secondary colony formation from small primary colonies in *Pdgfra*$^{GFP/+}$ and *Pdgfra*^{GFP}*/mIGF* mice in sham and day 5 post MI (D5 MI).

Figure 5.24 (b) Secondary colony formation from large primary colonies in *Pdgfra*$^{GFP/+}$ and *Pdgfra*^{GFP}*/mIGF* mice in sham and day 5 post MI (D5 MI).

Figure 5.24 In *Pdgfra*^{GFP}*/mIGF* hearts the PDGFRA^{GFPMEDIUM} population was capable of forming secondary colonies, although these tended to be the micro and small colony types. The *Pdgfra*^{GFP}*/mIGF* hearts gave an increased number of micro, small and large secondary colonies from small primary colonies compared to *Pdgfra*$^{GFP/+}$ hearts, however this difference was not statistically significant. There was a particularly noticeable increase in large colonies from *Pdgfra*^{GFP}*/mIGF* hearts subject to myocardial infarction ($p<0.05$), indicated by *. This is summarised again in section 5.13. 3 mice were used for each type of heart and 30 colonies were counted for each colony type per heart.

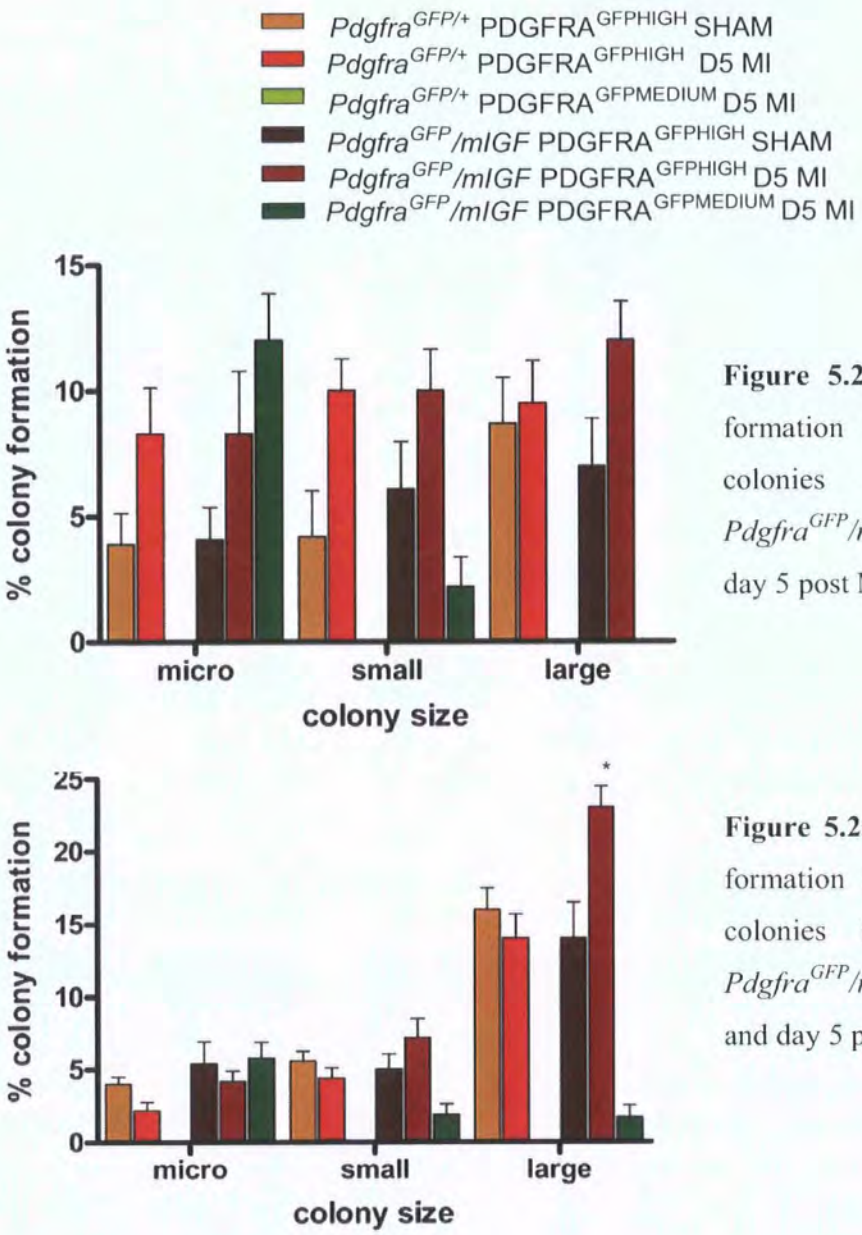

Figure 5.25 (a) Tertiary colony formation from small secondary colonies in *Pdgfra*$^{GFP/+}$ and *Pdgfra*^{GFP}*/mIGF* mice in sham and day 5 post MI (D5 MI).

Figure 5.25 (b) Tertiary colony formation from large secondary colonies in *Pdgfra*$^{GFP/+}$ and *Pdgfra*^{GFP}*/mIGF* mice in sham and day 5 post MI (D5 MI).

Figure 5.25 PDGFRA^{GFPMEDIUM} cells from *Pdgfra*$^{GFP/+}$ hearts did not give rise to tertiary colonies however those from *Pdgfra*^{GFP}*/mIGF hearts* did form predominantly micro and small colonies. In addition large secondary colonies gave rise to predominantly large tertiary colonies, with a marked increase in Pdgfra^{GFP}/mIGF hearts post MI ($p<0.05$) indicated by *. This is summarized again in section 5.13. 3 mice were used for each type of heart and 30 colonies were counted for each colony type.

5.11 Anatomic location of PDGFRA^{GFP+} cells

Normal adult hearts from *Pdgfra*$^{GFP/+}$ mice were assessed for GFP expression by fluorescence microscopy. As can be seen in figures 5.26a-d, PDGFRA^{GFP+} cells were found distributed throughout the adult heart, including the atria and ventricles, the atrio-ventricular valves and peri-aortic adventitia. This pattern is similar to that reported for the embryonic heart, where, although the PDGFRA^{GFP+} cells are found primarily in the proepicardium at E9.0 and also on the epicardial surface of the heart from late E9.0 to E10.5, from E12.5 they are prevalent throughout the interstitium of the myocardium (personal communication Dr Owen Prall, Victor Chang Cardiac Research Institute, Australia). In order to address whether the quantitative changes observed by flow cytometry following MI were reflected by changes in tissue distribution, the infarcted heart was investigated also by fluorescence microscopy. As can be seen in figure 5.27, compared with ventricle wall remote from the infarct site, the peri-infarct area surrounding the site of ischaemic injury was rich in PDGFRA^{GFP+} cells. Quantitative assessment was carried out by counting PDGFRA^{GFP+} cells per high power field (x 40) in sequential sections taken from the left ventricular (LV) free wall (below level of coronary artery ligation in those mice subject to MI), an area remote from the LV free wall (remote LV), in the peri-infarct area (or equivalent anatomical location of the peri-infarct area for the sham and non-operated hearts). Sham operated and non-operated hearts showed no differences in cell counts. At day 5 post MI, there was a significantly increased number of PDGFRA^{GFP+} cells in the peri-infarct area ($p<0.05$), with no significant changes in other regions. At day 12 post MI, although the number of PDGFRA^{GFP+} cells counted per high power field was significantly increased in the peri-infarct area compared to sham, normal and day 5 post infarct, there was actually a greater number of PDGFRA^{GFP+} cells in the infarct area itself (figure 5.28) ($p<0.05$). The previous results from flow cytometry showed that although there was an increase in PDGFRA^{GFPMEDIUM} and PDGFRA^{GFPHIGH} cells post infarct, the predominant population post infarct was PDGFRA^{GFPHIGH}. These quantitative changes as assessed by fluorescence microscopy were consistent with the observations for PDGFRA^{GFP+} cells by flow cytometry (section 5.4).

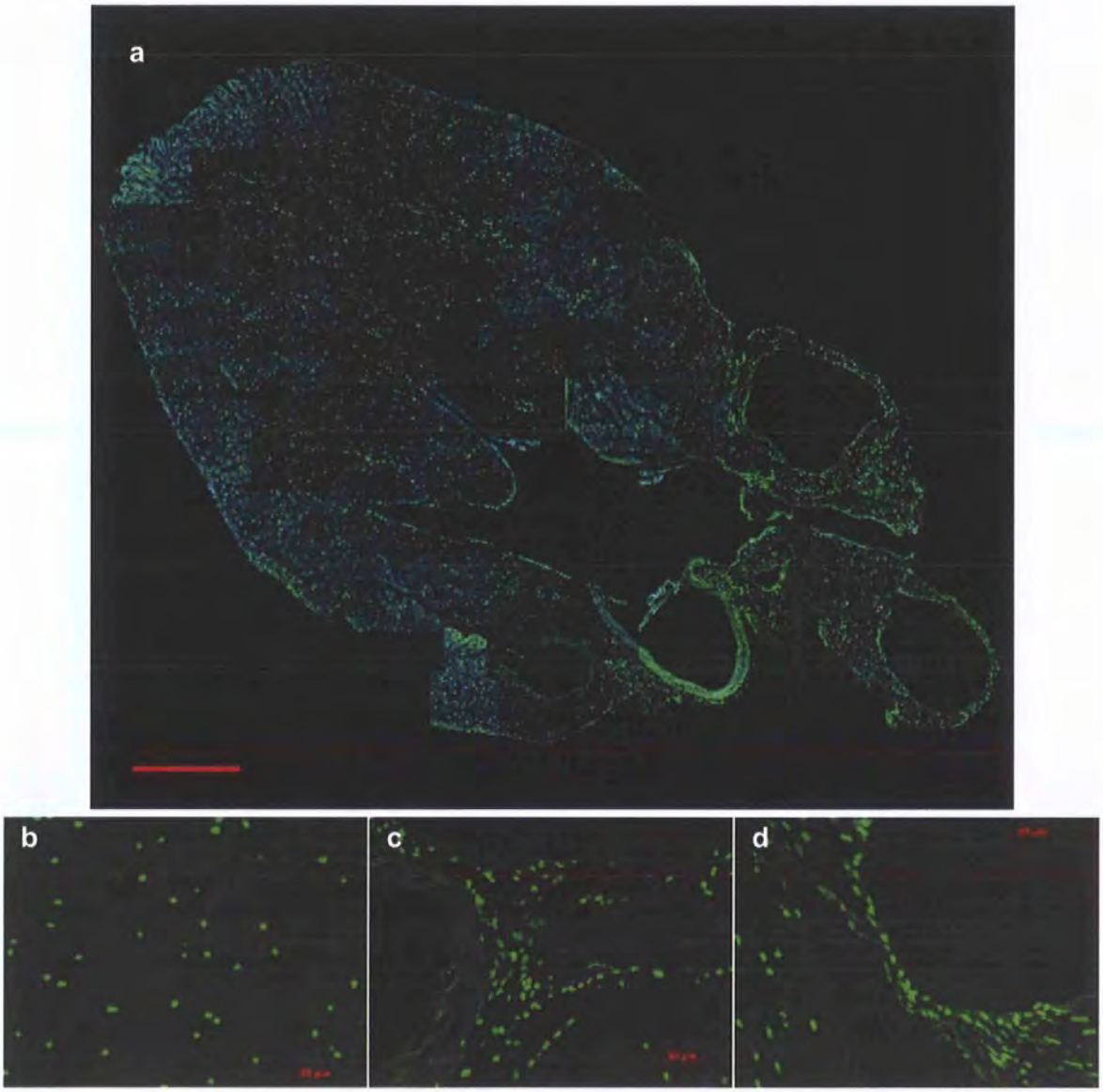

Figure 5.26 Sections through *Pdgfra*$^{GFP/+}$ heart examined by fluorescence microscopy.

(a) Reconstructed longitudinal section demonstrates the widespread distribution throughout the atria and ventricles of PDGFRA^{GFP+} cells and also their perivascular position around the aorta. Scale bar = 1mm.

Magnified images shown in panels b-d further illustrate the PDGFRA^{GFP+} cells distributed throughout the heart including within the valves and peri- aortic adventitia. A-V = Atrioventricular. LV = Left ventricular. GFP = green. Hoechst nuclei staining = blue. Scale bar = 50μm. Reconstruction by Dr M Xaymardan, Victor Chang Cardiac Reseach Institute, Australia.

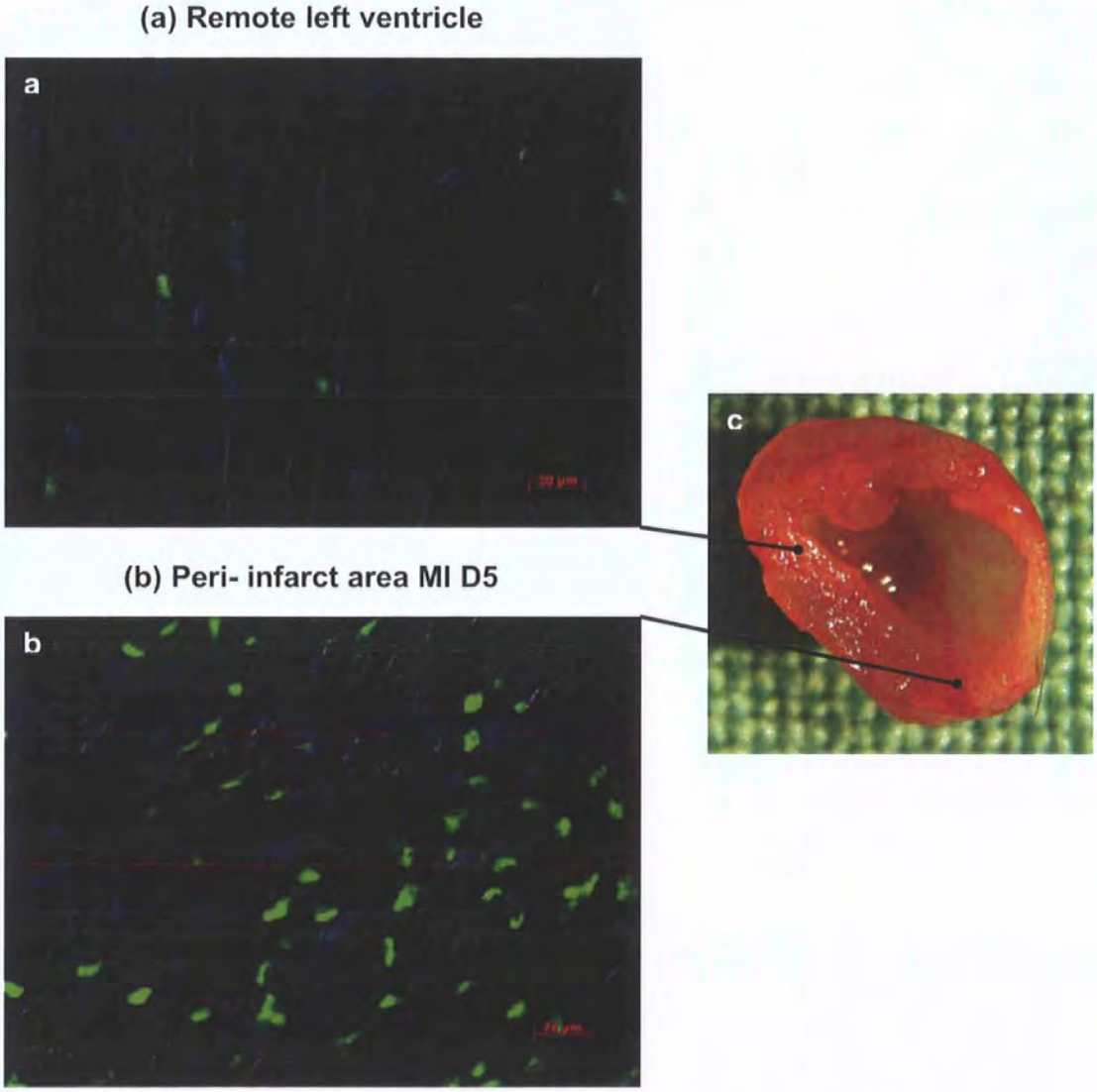

Figure 5.27 Fluorecence microscopy of *Pdfgra*$^{GFP/+}$ heart 5 days post MI.

The PDGFRA^{GFP+} cells were primarily located in the peri-infarct area at day 5 post infarct. (a) remote left ventricle (b) Peri-infarct area 5 days post infarct (MI D5) . Green = GFP. Hoechst nuclei stain = blue. *Pdgfra*$^{GFP/+}$ *heart.* Scale bar = 20μm.
(c) Photograph showing cross section of ventricle demonstrating region from which sections taken. Thinning of the free wall and loss of normal muscle architecture can be noted in this photograph at 5 days post MI.

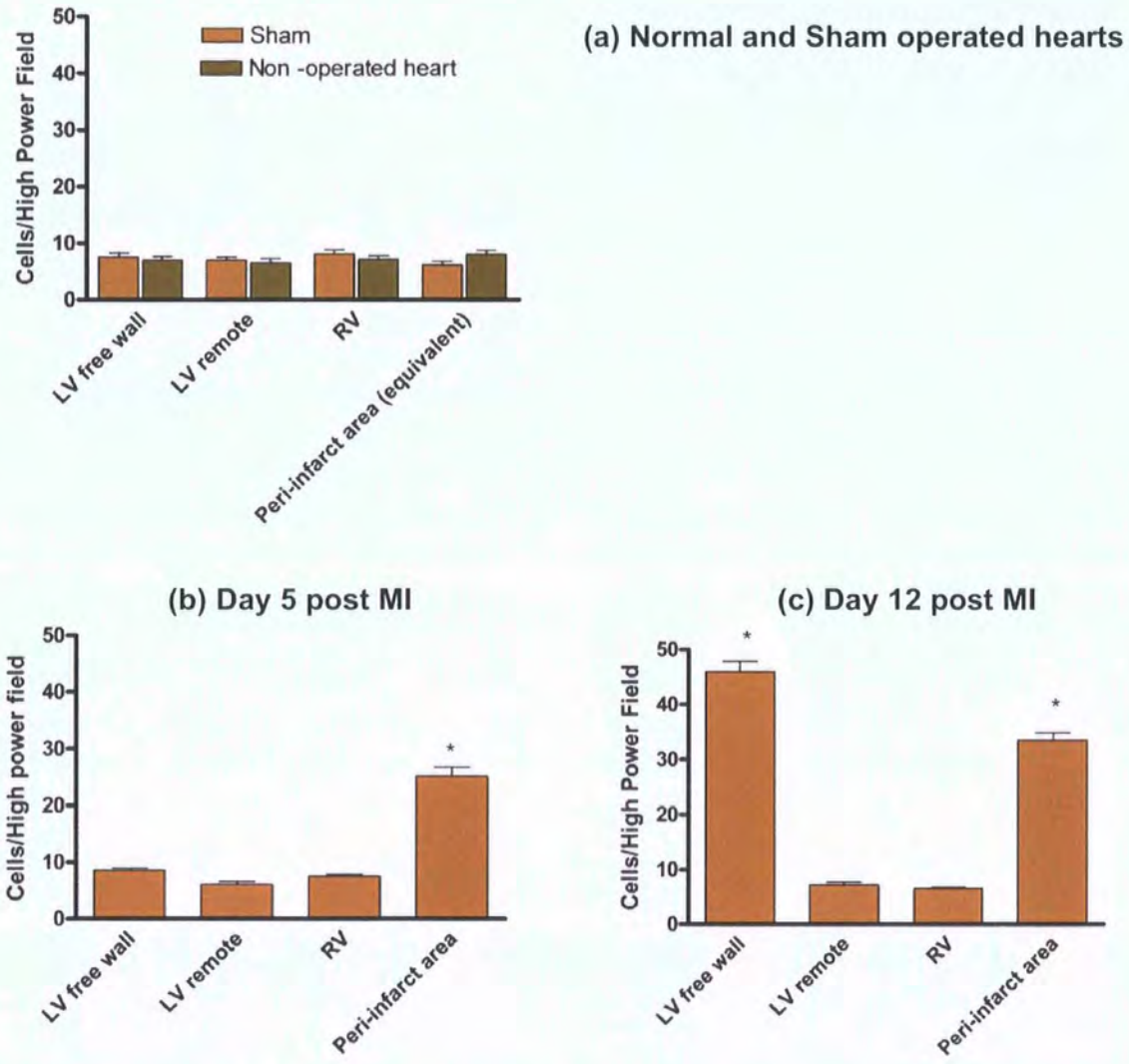

Figure 5.28 PDGFRA^{GFP+} cell counts per high power field (x 40) in *Pdgfra*$^{GFP/+}$ hearts.

(a) Sham operated and non-operated hearts showed no difference in cell counts. At day 5 post MI (b), there were significantly increased numbers of PDGFRA^{GFP+} cells in the peri-infarct area, with no significant changes in other regions. At day 12 post MI although the number of PDGFRA^{GFP+} cells counted per high power field was significantly increased in the peri-infarct area compared to sham, normal and day 5 post infarct, there was actually a greater number of PDGFRA^{GFP+} cells in the infarct area itself ($p<0.05$). * denotes $p<0.05$.

5.12 Differentiation assays in vitro

Cells which formed primary colonies from the $PDGFRA^{GFPHIGH}$ and $PDGFRA^{GFPMEDIUM}$ fractions were subject to cardiogenic, smooth muscle, endothelial, adipogenic and osteogenic differentiation assays as described in chapter 2. $PDGFRA^{GFPHIGH}$ cells showed an ability after exposure to the differentiation conditions described in chapter 2 to differentiate into cells expressing appropriate markers of all these cell types, whereas $PDGFRA^{GFPMEDIUM}$ cells had much more limited ability and showed ability to differentiate only into cells with adipocyte markers (figures 5.29-5.33). No spontaneous contraction was observed however in the cells expressing the biochemical marker of α-sarcomeric actinin.

5.13 Discussion

A CFU-F assay has been used to delineate a population of cells which demonstrate self-renewal and proliferation *in vitro*. In this assay, after plating of cells, each colony formed was generally assumed to arise from a single cell, therefore plating cells to form primary, secondary and tertiary colonies gave an indication of their potential for proliferation and self renewal. At each passage colonies contained both self renewing cells and more differentiated cells. Together with differentiation assays, this enabled a distinction to be made between those cells which may be putative stem cells and those which could be progenitors by their ability to self renew. This assay has been applied in the examination of hearts in a normal state, post infarct and a proregenerative model.

As identified in Chapter 1, there have been a number of different markers used in attempts to try to identify cardiac stem cells which may be resident in the heart, however there does not appear to be any specific marker or group of markers to encompass this population. Hence, although cell specific markers may be useful, this thesis has used markers in conjunction with a CFU-F assay, which enabled enrichment of the initial population by assessment of self renewal and proliferation potential. Brent Reynolds' group have performed similar assessments on putative neural stem cells (Louis et al.,

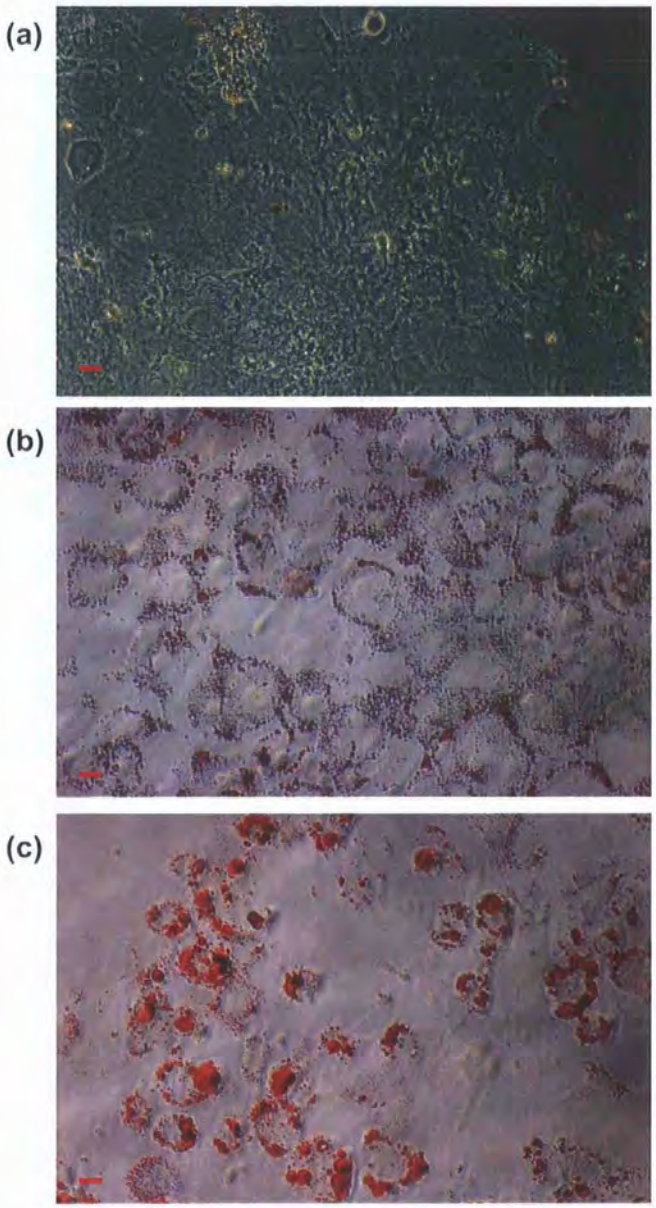

Figure 5.29 Adipocyte differentiation assay

(a) Negative control cells not exposed to differentiation media. (b) PDGFRA^{GFPHIGH} cells. (c) PDGFRA^{GFPMEDIUM} cells. Lipid droplets within both PDGFRA^{GFPHIGH} and PDGFRA^{GFPMEDIUM} cells can be seen stained red with Oil red O. The PDGFRA^{GFPHIGH} cells proliferated at a faster rate and associated with this, the large lipid droplets dispersed much quicker in this population in comparison to PDGFRA^{GFPMEDIUM} cells. Scale bar = 10μm.

Cultures grown and photographed by Dr V Chandrakanthan, Victor Chang Cardiac Research Institute, Sydney. Cells isolated from *Pdgfra*$^{GFP/+}$ heart.

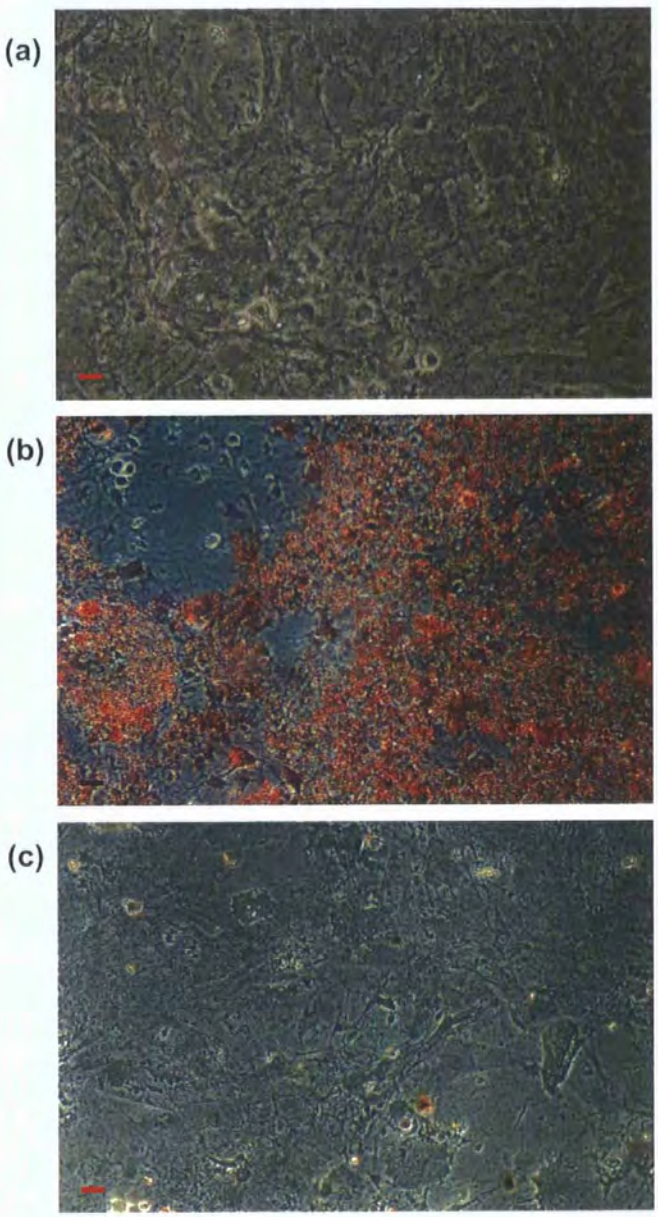

Figure 5.30 Osteogenic differentiation assay .

(a) Negative control-cells not exposed to differentiation media. (b) PDGFRA^{GFPHIGH} cells. (c) PDGFRA^{GFPMEDIUM} cells. Calcium deposits in the differentiated cells complexed with alizarin red were seen visible as orange/red stain in the PDGFRA^{GFPHIGH} cells only. Scale bar = 10µm.

Cultures grown and photographed by Dr V Chandrakanthan, Victor Chang Cardiac Research Institute, Sydney. Cells isolated from *Pdgfra*$^{GFP/+}$ heart.

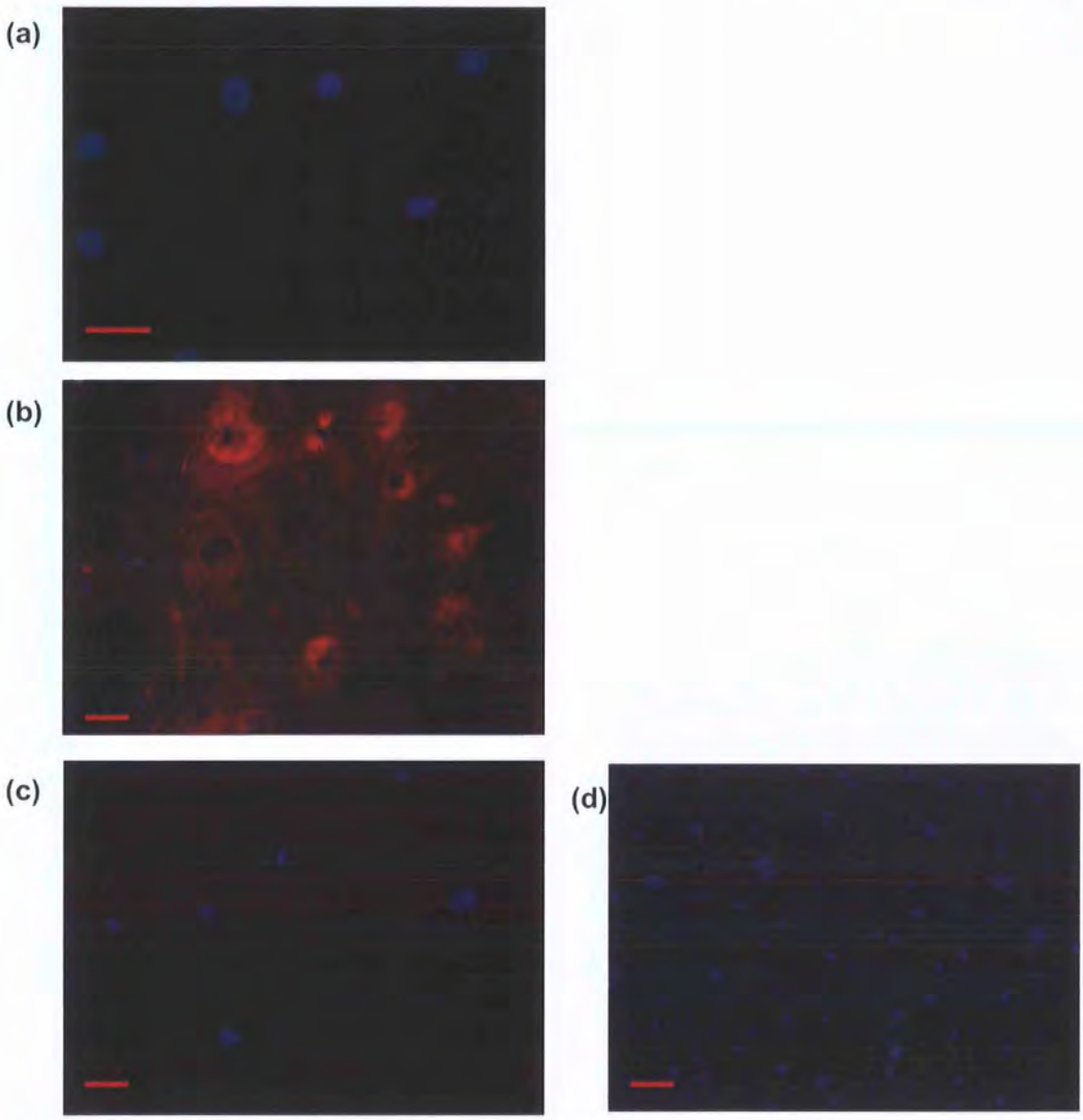

Figure 5.31 Endothelial differentiation assay .

(a) Negative control-cells not exposed to differentiation media. (b) PDGFRA^{GFPHIGH} cells (c) PDGFRA^{GFPMEDIUM} cells (d) Ab Control-PDGFRA^{GFPHIGH} cells exposed to endothelial differentiation medium, secondary antibody only. Positive staining for PECAM1 was observed in the PDGFRA^{GFPHIGH} population only. PECAM staining shown in red. Hoechst nuclei staining shown in blue. Scale bar = 10μm.
Cultures grown and photographed by Dr V Chandrakanthan, Victor Chang Cardiac Research Institute, Sydney. Cells isolated from *Pdgfra*$^{GFP/+}$ heart.

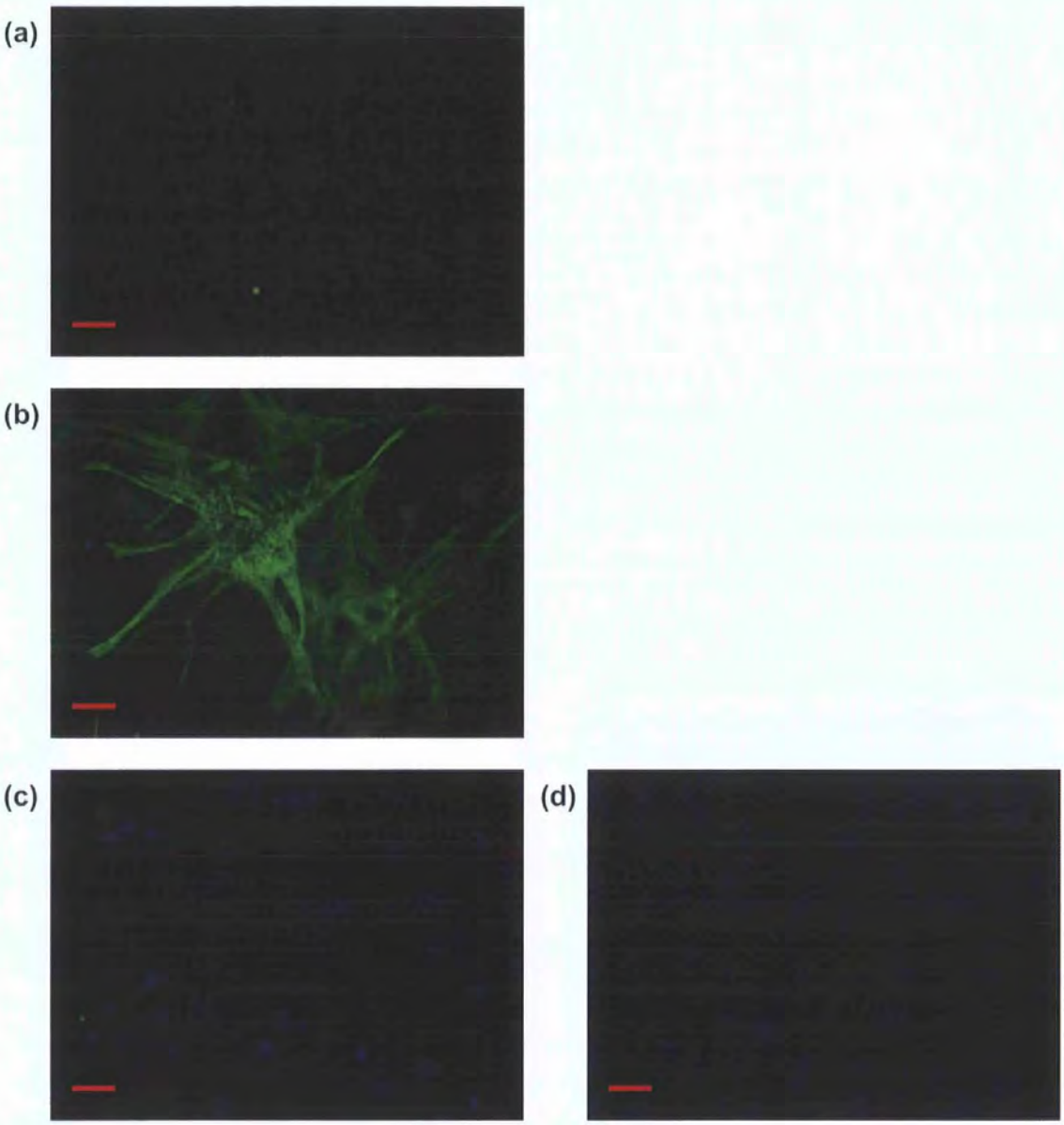

Figure 5.32 Smooth muscle differentiation assay.

(a) Negative control-cells not exposed to differentiation media. b) PDGFRA^{GFPHIGH} cells. (c) PDGFRA^{GFPMEDIUM} cells. (d) Ab Control. PDGFRA^{GFPHIGH} cells exposed to differentiation medium, secondary antibody only. Positive staining for smooth muscle myosin heavy chain seen in PDGFRA^{GFPHIGH} cells only. Smooth muscle myosin heavy chain staining shown in green. Hoechst nuclei staining shown in blue. Scale bar = 10μm. Cultures grown and photographed by Dr V Chandrakanthan, Victor Chang Cardiac Research Institute, Sydney. Cells isolated from *Pdgfra*$^{GFP/+}$ heart.

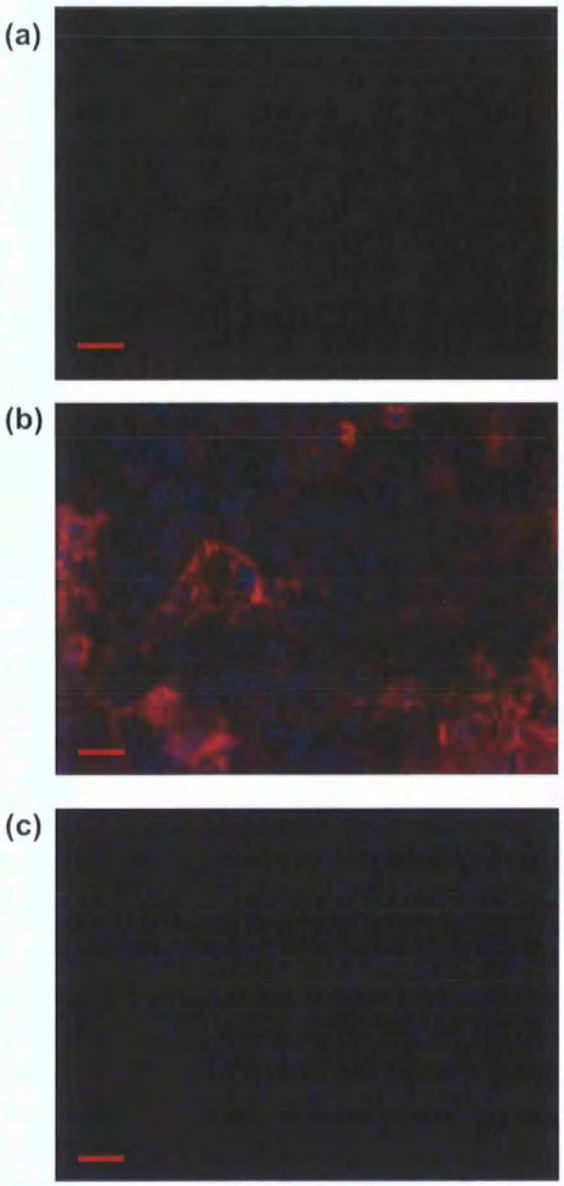

Figure 5.33 Cardiomyocyte differentiation assay.

(a) Negative control-cells not exposed to differentiation media. (b) $PDGFRA^{GFPHIGH}$ cells. (c) Ab Control. $PDGFRA^{GFPHIGH}$ cells exposed to differentiation medium, secondary antibody only. Positive staining for α-sarcomeric actinin shown in red. Hoechst staining shown in blue (nuclei). Scale bar=10μm.

Cultures grown and photographed by Dr V Chandrakanthan, Victor Chang Cardiac Research Institute, Sydney. Cells isolated from *Pdgfra*$^{GFP/+}$ heart.

2008). Louis et al used a colony forming assay and divided colonies according to size (ie their proliferative ability) as in the present study, to try to discriminate between putative progenitor cells and putative stem cells in the brain, which, like the heart, was once thought to be a terminally differentiated organ with very limited regenerative potential. Louis et al showed that as well as having different self renewal and proliferative potential, the different size colonies also had differences in their differentiation capacity, with colonies <2mm being unipotent and colonies >2mm being multipotent. Altogether, they concluded the size of colonies enabled them to make a distinction between stem cells and progenitors. Similarly, in the present study, different colony sizes also reflected differences in self renewal and proliferation. $PDGFRA^{GFPHIGH}$ and $PDGFRA^{GFPMEDIUM}$ populations had different rates of proliferation and abilities to self renew, and in addition the $PDGFRA^{GFPHIGH}$ cells which primarily formed large colonies had a broader differentiation capacity *in vitro* in comparison to the $PDGFRA^{GFPMEDIUM}$ population which primarily formed the smaller colonies. Although previous studies have suggested that demonstration of secondary or tertiary self renewal may be adequate to satisfy the stem cell requirement of self renewal, in this experiment a more rigorous approach was taken and colonies were passaged over 15 times if possible to assess self renewal ability. Large $PDGFRA^{GFPHIGH}$ colonies showed prolonged self renewal by being able to be passaged over 15 times, however small colonies from this fraction only passaged to P4 with microcolonies not even forming secondary colonies. $PDGFRA^{MEDIUM}$ cells in $Pdgfra^{GFP/+}$ hearts did not form secondary colonies, however in the $Pdgfra^{GFP}$/mIGF proregenerative model, secondary and tertiary colonies did form from this population suggesting an increased 'stemness' of this population in the proregenerative model.

In an effort to enrich the CFU-F population isolated from the whole heart, it was fractionated into a $Sca\text{-}1^{+}/PECAM1^{-}/PDGFRA^{GFPHIGH}$ sub population. Sca-1 was selected as previous work has identified a $Sca\text{-}1^{+}$ cardiac resident population which were CD45 negative (as were the cells isolated in the present study) which showed *in vitro* evidence of being able to express α-sarcomeric actin and cardiac Troponin I. Further work by the same group showed that these $Sca\text{-}1^{+}$ cells could home to the infarct area after systemic injection and show some degree of contributing to new cardiomyocyte formation (Oh et

al., 2003). Furthermore, consistent with the present findings, Wang et al have demonstrated a Sca1^{+}/PECAM1^{-} population in the adult mouse heart which are reported to increase in number in the infarct and peri- infarct area post MI. In addition they were able to demonstrate differentiation in vitro into cells expressing cardiomyocyte and endothelial markers in agreement with present data (Wang et al., 2006). An interesting observation by Wang et al which was not tested in this thesis was that flow cytometry analysis of Sca-1^{+}/PECAM1^{-} cells from bone marrow and circulating blood did not change post infarct providing weight to their hypothesis that the Sca-1^{+}/PECAM1^{-} cells are cardiac resident and do not migrate in from extracardiac tissue such as bone marrow. Notably in the present study no PDGFRA^{GFP+} cells were found in the bone marrow of *Pdgfra*$^{GFP/+}$ mice (data not shown). In addition to previous work using Sca-1^{+}/PECAM1^{-} cell populations isolated from the adult mouse heart, the present study has also taken a smaller subpopulation of PDFGRA^{GFP+} cells from the Sca-1^{+}/PECAM1^{-} population to assess changes post infarct in this population as well as assess the colony forming ability as described above. Note that colony forming ability was only found in the PDFGRA^{GFP+} subfraction indicating a potential of these cells to have stem cell characteristics. Although other literature has not quantitated the colony forming ability of Sca-1^{+} cells as in the present study, interestingly, recent work by Tateishi and co-workers also examined a functional phenotype of a putative stem cell population in the heart (Tateishi et al., 2007). They reasoned that a putative stem cell population in the heart would express telomerase reverse transcriptase (TERT), and by using a transgenic mouse that expresses GFP under the control of the TERT promoter, the TERT^{GFP+} fractions of clonal cells from the heart were found to be enriched for Sca-1^{+} cells. The cells isolated were negative for PECAM1, CD34 and CD45, however they did express CD90, an antigen commonly found on mesenchymal stem cells as did the colony forming fraction in the present study (data not shown). As previously documented in Chapter 1, a specific progenitor population has been identified known as the side population (SP), characterized by their intrinsic capacity to efflux Hoescht dye. Pfister and colleagues examined this population and found that Sca-1 was widely expressed, but it was largely negative for CD45 and CD34, and negative for c-kit. Similar to the present study they found an enrichment for colony forming activity in the Sca-1^{+} fraction compared to the whole population and in

addition only the PECAM1$^-$ fraction of Sca-1$^+$ cells exhibited *in vitro* cardiomyogenic potential. Due to the overlapping behaviour of the populations discussed, it is likely that an overlapping population of Sca-1$^+$ cells is being examined by these investigators and also in the present study.

In comparison to the cardiac c-kit$^+$ population which has been extensively studied by Anversa and colleagues, the PDGFRA^{GFP+} population studied here were distributed throughout the myocardium, whereas Anversa and colleagues reported that the majority of ckit$^+$ cells they found were located at the apex of the heart and in the atria (Urbanek et al., 2005). Although a proportion of c-kit $^+$ cells do express Sca-1, in the present study very few c-kit cells could be isolated from the adult mouse heart. It must be noted however that as well as the work in the present study other investigators have also found difficulty locating c-kit $^+$ cells in the adult heart (Li et al., 2008; Pfister et al., 2005) which may be attributable to enzymatic cleavage of the c-kit receptor from the cell surface during the digestion process (Pfister et al., 2005), or due to the fact that c-kit$^+$ cells only migrate into the heart after ischaemic injury as reported by Fazel et al (Fazel et al., 2006).In addition when c-kit $^+$ cells have been localized to the myocardium up to 30% have been found to be CD45 positive (Fazel et al., 2006) . Hence it appears less likely that the population being studied in this study correlate with the c-kit $^+$ population described by others.

In an effort to enrich the colony forming fraction further, and also to attempt to isolate a putative cardiac resident population, the PDGFRA^{GFP+} population was taken from the Sca-1$^+$/PECAM1$^-$ fraction. PDGFRA^{GFP+} cells in the adult may be derived from the same population that appear in the embryonic cardiac interstitium at E12.5. The anatomic location of the PDGFRA^{GFP+} cells in the heart of the embryonic and adult *Pdgfra*$^{GFP/+}$ mice together with the phenotypic changes of death by E10.5 with multiple cardiac defects in *Pdgfra*$^{-/-}$ mice, suggest an important developmental role for these cells in the developing heart and potentially a continuing stem cell role in the adult, particularly as all of the colony forming activity was isolated to the PDGFRA^{GFP+} cells in the heart. Post MI there was a shift in colony forming potential, which could also be interpreted as an

increase in the heart's 'stemness' or regenerative potential. The PDGFRA^{GFPHIGH} cells showed the cardinal features of stem cells - proliferation, long term self renewal and multipotency, with the PDGFRA^{GFPMEDIUM} cells having a phenotype consistent with a more restricted downstream progenitor type cell with its limited proliferation, self renewal and differentiation capacity. In a similar manner to other studies this putative stem/progenitor population increased in number post infarct and appeared to localize in the peri-infarct and infarct area (Fazel et al., 2006; Wang et al., 2006).

The importance of platelet derived growth factor signaling post MI has been outlined earlier from work by Zymeck and colleagues (Zymek et al., 2006). They found that platelet derived growth factor receptor alpha and beta were both involved in post infarct repair, primarily in modulating fibrosis and angiogenesis. It is known that cardiac over expression of the PDGFRA ligand PDGF-C induces fibrosis (Ponten et al., 2003) and that inhibition of PDGFRA significantly decreases collagen deposition in the infarcted myocardium. Hence it appears that PDGFRA and its ligands are crucial not only in cardiac development but also in the well orchestrated response post injury which regulates fibrous tissue deposition and facilitates scar formation. Work by Santini et al has shown that in a *αMHC/mIGF-1* transgenic mouse there appeared to be a modulation of the inflammatory response which enabled restoration of cardiac function and reduced scar formation, however although they found an increase in the number of proliferating cells at 4 weeks post infarct it is not yet clear whether these cells contributed to tissue reconstruction after myocardial injury (Santini et al., 2007). Of note from the present study was that in the *Pdgfra^{GFP}/mIGF* hearts, there was an increase in number of PDGFRA^{GFPMEDIUM} cells and colony forming potential of both PDGFRA^{GFPHIGH} and PDGFRA^{GFPMEDIUM} cells compared to *Pdgfra$^{GFP/+}$* hearts. IGF-1 has previously been implicated in the ischaemic heart as being cardioprotective and reducing apoptosis in surviving myocytes (Li et al., 1997), however with the results of the present study in combination with the data gathered by Santini et al ((Santini et al., 2007), there is a possibility that as well as reducing death in local myocytes and activating prosurvival signaling, mIGF overexpression may also be implicated in increasing the regenerative and repairative ability of the heart post MI. The effect of IGF-1 overexpression is

strengthened by work by Anversa and colleagues who showed that IGF-1, together with Hepatocyte growth factor (HGF) stimulated migration, proliferation and differentiation of endogenous cardiac stem cells. Specifically IGF-1 intramyocardial injection at the time of MI showed anti-apoptotic and proliferative effects on cardiac stem cells in the heart resulting in cardiac regeneration and improved survival and function (Urbanek et al., 2005).

In humans no cardiac phenotype related to PDGFRA mutation has been described however it is noted that mutations in PDFRA are found in patients with gastrointestinal stromal tumours (Heinrich et al., 2003) and also expression of PDGFRA has been found to be associated with tumour progression in renal cell carcinoma(Sulzbacher et al., 2003). In this respect the tyrosine kinase inhibitor sunitinib has been used in treatment of patients with metastatic renal carcinoma (Motzer et al., 2006) and gastrointestinal stromal tumours (Demetri et al., 2006), however there has been an accumulation of evidence of sunitinib associated heart failure (Khakoo et al., 2008). It must be noted that sunitinib would also act on the tyrosine kinase receptor c-kit also and may affect cardiac function in a tyrosine kinase independent manner. At present the mechanism of Sunitinib associated heart failure has not been elucidated, however without any described cardiac phenotype in humans for mutations in PDGFRA this remains an interesting observation.

In contrast to the $PDGFRA^{GFP+}$ population described in the present study, $Isl1^{+}$ cells, although being shown to be an important cell in development, primarily contributing to the right ventricle and outflow tract (Cai et al., 2003) very few $Isl1^{+}$ cells are found in the postnatal heart (Laugwitz et al., 2008). In addition, $Isl1^{+}$ cells are found in the second heart field and not in the proepicardium of the embryonic heart as are $PDGFRA^{GFP+}$ cells (Cai et al., 2008).

Hence it appears that the $PDGFRA^{GFP+}$ population examined in the present study overlaps with other work which has investigated $Sca1^{+}$ cells and side population cells in the heart and isolates a population which is largely separate from the $Isl1^{+}$ and $c\text{-}kit^{+}$ population described in previous studies. The $PDGFRA^{GFP+}$ population has been shown

to have stem/progenitor cell characteristics which further underlines the possibility that the heart remains capable of adaptation to stress and ischaemic injury through adult life via a stem cell mechanism.

Chapter 6

Final discussion

6.1 Discussion

It is common knowledge that the regenerative capacity of human myocardium is inadequate to compensate for the significant loss of heart muscle that occurs in acute myocardial infarction (Murry et al., 2006). Other tissues which are known to have stem cells such as the gut also respond poorly to ischaemic injury, therefore failure to regenerate after such an injury does not necessarily mean that the growth reserve of the myocardium is insufficient for reconstitution. Many scientists have now demonstrated that the adult myocardium may have within it putative cardiac stem and progenitor cells as outlined in Chapter 1. The fact that regenerative mechanisms have been shown to exist in the adult heart points to the problem of the barriers that may be preventing regeneration and exacerbating the injury such as ischaemia, inflammation and fibrosis. This hostile microenvironment may prevent the activation and function of cardiac stem cells described in the literature as well as adding to the injury burden. Interestingly Santini et al studied the ability of locally acting IGF-1 on the restoration of heart function after injury (Santini et al., 2007). They concluded that the apparent improved function of the transgenic mice at 2 months post injury was facilitated by modulation of the inflammatory response and increased anti-apoptotic signaling, however no evidence was shown of new regenerating myocytes in this study, simply that the hearts appeared to recover better than in the WT. Note that as well as the inflammatory response having deleterious components, it also has a useful role post infarct, with granulation tissue formation being a critical step in infarct repair. After coronary occlusion macrophages phagocytose necrotic myocytes and myofibroblasts and endothelial cells migrate into the infarct zone. This granulation tissue provides a matrix rich in proteoglycans and matrix proteins which is eventually replaced by a deposition of collagen by myofibroblasts (Virag and Murry, 2003). The amount of granulation tissue peaks at 7 days after which it is replaced by scar tissue. As well as modulating deleterious components of post infarct inflammation, modulation of this inflammatory granulation tissue formation could also improve remodeling and post infarct mechanics. Fazel and colleagues postulated that the $ckit^{+}$ cells they isolated post infarct influenced cardiac function after ischaemic injury by

contributing to angiogenesis and therefore granulation tissue mediated infarct stabilization (Fazel et al., 2006).

In light of these findings an initial investigation was made into the efficacy of an antibody against the human C5aR (7F3 mAb) which had been previously shown to dramatically reduce the inflammation in a mouse model of rheumatoid arthritis (Lee et al., 2006). At the time of myocardial infarction the intense inflammatory reaction that results actually causes neutrophil mediated damage to the tissue at the site of the infarct (Frangogiannis et al., 2002). A potent anaphylotoxin for neutrophil infiltration is C5 hence the C5/C5aR axis was an interesting target to aim to reduce inflammation and therefore reduce myocardial damage and infarct size, possibly by modulation of a stem cell or granulation tissue response. The complement system has been used as a target previously (as documented in Chapter 1) however, results have been mixed in animal and human studies using small molecules and antibodies against C3, C5 and C5a. It was hoped that such a specific target of the C5aR would have similar positive outcomes to those shown by Lee et al in their rheumatoid arthritis model (Lee et al., 2006), and also would not have the potential immunodeficiency outcomes of inhibitors which act at C3. This was the first time a monoclonal antibody was being used against the C5aR in the setting of myocardial ischaemia. As shown in chapter 4, inflammatory influx of neutrophils was significantly reduced, however this did not influence infarct size measured at 3 days post surgery. Hence although inflammation is a major contributor to myocardial injury, it was shown that inhibition of this process using 7F3 mAb was not enough to reduce ischaemic damage or trigger regenerative events at the time points examined, and other mechanisms must be studied to evaluate ways post ischaemic damage or repair could be influenced.

Hence a putative stem cell population within the heart was investigated. The myriad of cardiac resident cell types that have been put forward as potentially being candidate putative stem cells for the heart point to the as yet unsolved question of which cell type is the most appropriate and how their ability may be harnessed (Segers and Lee, 2008). It was therefore important to examine the myocardium in the context of work by others to

search for cells which may have the potential to repair and regenerate the heart after ischaemic insult, to quantitate any changes in number and examine changes in phenotype after myocardial infarction. Although there are a number of cells which have been isolated from the heart as stem cell candidates, the majority of investigators have used surface markers to isolate them before assessing any phenotype *in vitro* or *in vivo*. In the present study a colony forming assay was used in a manner similar to which Louis et al had successfully demonstrated self renewal and proliferation in a population of neural stem cells. They showed that differences in colony size reflected self renewal and differentiation ability, enabling the distinction between putative progenitor and stem cells to be made (Louis et al., 2008). Recent work has demonstrated the importance of the epicardium as a source of cells which may be able to contribute to cardiac regeneration (Cai et al., 2003; Lepilina et al., 2006; Zhou et al., 2008) and in this regard cells have been found in the proepicardial organ, epicardium and interstitium of the developing heart which express PDGFRA (personal communication, unpublished data, Dr O Prall Victor Chang Cardiac Research Institute). Due to the similar anatomic location of these cells in particular stages of the embryo and adult hearts and also the fact that the *Pdgfra*$^{-/-}$ phenotype was found to be lethal with cardiac defects including aortic malformations and septal defects, it could be suggested that as well as being important at a developmental level these cells may have a role in regeneration of the adult heart. In addition PDGFRA and associated ligands have been found to be involved in modulation of fibrosis and scar formation in post infarct repair (Zymek et al., 2006), which as pointed out by Virag and Murry is a critical step in the repair mechanism after myocardial infarction (Virag and Murry, 2003). It is useful to note that the c-kit^{+} putative stem cell population isolated by Fazel and colleagues was reported to improve post infarct function by primarily contributing to the angiogenesis aspect of granulation tissue repair (Fazel et al., 2006).

The phenotype of the population of cells isolated by flow cytometry in this thesis from *Pdgfra*$^{GFP/+}$ hearts was Sca-1^{+}/PECAM^{-}/PDGFRA^{GFP+}. As annotated in Chapter 5 this population did have characteristics which overlapped with other Sca-1^{+} populations isolated by previous investigators and less phenotypic similarities to the c-kit^{+} or Isl1^{+} populations (Fazel et al., 2006; Laugwitz et al., 2008; Pfister et al., 2005; Tateishi et al.,

2007; Urbanek et al., 2005; Wang et al., 2006). In a similar way to how Louis et al (Louis et al., 2008) made assessment of their putative stem and progenitor cells, PDGFRA^{GFPHIGH} and PDGFRA^{GFPMEDIUM} cell populations were shown to have markedly different abilities to form large colonies, which had greater self renewing potential than smaller ones, indicating that of these two populations the PDGFRA^{GFPHIGH} population had characteristics more associated with putative stem cells , particularly with its broader in vitro differentiation potential in comparison to PDGFRA^{GFPMEDIUM} cells which although formed colonies had limited ability to self renew and limited differentiation capacity in the assays which were used in the present study, suggesting PDGFRA^{GFPMEDIUM} may be a progenitor type population.

6.2 Conclusions

This thesis set out to examine the effect of an anti-inflammatory C5aR antibody in the setting of acute MI and also to examine the adult heart for cells which may be putative stem cells or progenitor cells. Initially a model of murine myocardial infarction was shown to be successfully established with a relatively low mortality and reproducible infarct size which could be used in future experiments. The intense inflammatory response post MI was targeted with a C5aR antibody and although this was shown to reduce the neutrophil infiltration, a significant change in infarct size was not shown at the 3 day time point analysed. It was apparent that other factors needed to be targeted to improve heart function and influence recovery from myocardial injury. To assess the presence of a stem cell population in the adult heart a simple yet reproducible and robust assay (CFU-F) was used in conjunction with markers of Sca-1, PECAM1 and PDGFRA to isolate a population which may remain from the developing heart. A *Pdgfra*$^{GFP/+}$ mouse was used to enable localization of the cells expressing PDGFRA. Two populations were found which formed colonies, the PDGFRA^{GFPHIGH} population which had 'stem cell' like properties in terms of proliferation, prolonged self renewal and multipotent *in vitro* differentiation, and the PDGFRA^{GFPMEDIUM} population which had 'progenitor cell' properties in that although it had proliferative ability, the potential of this population to continue to self renew and differentiate into multiple lineages was restricted. Hence in a

similar way to the *in vitro* work from Louis et al (Louis et al., 2008), this suggested the $PDGFR^{GFPHIGH}$ population could be a putative stem cell population isolated from the heart and the $PDFGR^{GFPMEDIUM}$ population may be a putative progenitor population. Interestingly the number of cells from both these populations increased significantly post MI and the colony forming ability of the $PDGFRA^{GFPHIGH}$ population was significantly enhanced. Furthermore in a model which has been associated with a proregenerative status by its overexpression of IGF-1 and enhanced recovery post MI, the numbers isolated from both these populations was significantly increased after myocardial infarction, particularly of the $PDGFRA^{GFPMEDIUM}$ population, with an associated increase in colony forming ability of both populations and self renewal ability of the $PDGFRA^{GFPMEDIUM}$ population.

These results suggest that although reducing the inflammatory response by inhibiting C5aR reduces infarct associated neutrophil infiltration , this was inadequate to reduce myocardial injury at the time point of 3 days post infarct. However, a population of putative stem and progenitor cells, whose stem cell-like phenotype appears to change in a manner which increases the heart's 'stemness' post MI , particularly in the prescence of IGF-1 expression, can be found in the myocardium, which may be able to enhance repair and regeneration after ischaemic injury. Further studies would help to evaluate in detail their role, particularly in an *in vivo* environment.

6.3 Future directions

Many possibilities for future study have arisen as a result of this research and it would be opportune to use this as a platform from which to investigate further the mechanics involved in post infarct repair and regeneration.

In relation to the work using the C5aR mAb (7F3 mAb), despite the outstanding results demonstrated by Lee et al in using 7F3 mAb in a rheumatoid arthritis model (Lee et al., 2006), the outcome of the present study showed no change in size of MI at 3 days despite a significant reduction in neutrophil infiltration. It would be useful to examine long term

outcomes of infarct size and mortality after using 7F3 mAb, particularly in the light of findings from the COMMA trial showing that despite no difference in myocardial injury, there was a difference in 90 day mortality between treated and untreated groups (Granger et al., 2003). In addition it would be interesting to examine changes in phenotype of the PDGFRA population in mice which were treated with 7F3 mAb and if the antibody was to be considered for clinical use it would be important to show efficacy when administered after an ischaemic event and also in the setting of ischaemia reperfusion.

In regard to analyzing the $PDGFRA^{GFP+}$ population, although *in vitro* differentiation data is useful, in terms of interpreting a cell's phenotypic potential, it is important to realise that growing cells in tissue culture can result in cell states that are unlike those seen *in vivo* (Jaenisch and Young, 2008), and represent a proxy for the *in vivo* situation. Hence it would be useful for the $PDGFRA^{GFP+}$ cells to be transplanted into heart in an in vivo environment and assess their ability to differentiate into cells which contribute to the cardiac architecture such as endothelium, cardiac myocytes, smooth muscle and fibroblasts, as well as how well they integrate with native tissue and demonstrate functional phenotypes for example synchronous contractility and demonstration of calcium transients. This would then add strong evidence to the hypothesis that these may be putative cardiac stem cells. Although some investigators have had promising results using cell transplantation of putative cardiac stem cells (Dawn et al., 2005), many others have shown that unfortunately cells transplanted have simply fused to native cells without changing their phenotype or functionally integrating (Oh et al., 2003). Despite many studies where putative cardiac stem cells have been transplanted into an infarcted heart, the majority show that regardless of cell type, approximately 90% of cells successfully delivered to the heart die within the first week (Laflamme and Murry, 2005). In specific relation to $Sca\text{-}1^{+}$ cells Wang and colleagues found that in the first 2 weeks following transplantation, only 2% of cells were found in the heart and after 3 weeks the number of identifiable engrafted cells decreased to less than 1% (Wang et al., 2006). Despite this, Wang et al, showed cell transplantation was associated with improved LV function and a significant increase in myocardial neovascularisation and modest cardiomyocyte regeneration suggesting effects seen may have had a paracrine mechanism. In support of

such a mechanism, work by Gnecchi et al found that just the conditioned media from cultured mesenchymal stem cells could reduce the infarct size when injected into the myocardium 30 minutes after MI (Gnecchi et al., 2005). Hence with this and other evidence demonstrating the effects of IGF-1 in the heart post infarct (Santini et al., 2007; Urbanek et al., 2005), particularly in the light of the changes in the $PDGFRA^{GFP+}$ populations post infarct and in the prescence of IGF-1, it would seem appropriate to analyse in further detail the effect of PDGF ligands and mIGF-1 on the phenotype of $PDGFRA^{GFP+}$ cells in vitro and in vivo in healthy and diseased hearts to see if restorative changes can be brought about by influencing the cells within the heart itself, rather than relying on the integration of transplanted cells. This would be particularly useful as it would avoid technical issues of cell delivery and problems with cell rejection, and more conveniently it would harness the heart's endogenous mechanisms to initiate repair.

.

Although the most appropriate intervention at the time of acute ischaemia is restoration of blood flow by revascularisation, it is still possible that cells within the heart may be able to influence cardiac remodelling at this crucial time and influence outcomes by modulating the granulation tissue response, hence influencing repair as well as instigating regeneration. This has been shown by Fazel and colleagues in relation to $c\text{-}kit^{+}$ cells (Fazel et al., 2006). Taking into account the fact that PDGF is an important hub in stimulation of fibroblast migration, proliferation and activation and also vascular maturation, the $PDGFRA^{GFP+}$ cells investigated in this thesis would be well placed to take part in such a response also (Zymek et al., 2006). Translating this to a clinical level it may mean that influencing such a cell type using PDGFR ligands or IGF-1 could also be a means of regulating the granulation tissue response especially as an increase in their number and self renewal ability is seen post MI.

Finally, despite the fact that the adult heart has been shown to contain cell populations of putative stem cells, the exact lineage relationships between these adult cardiac progenitor cell populations and embryonic cardiac stem and progenitor cells is unknown. Sophisticated genetic approaches in mice are now available and provide a unique opportunity to determine embryonic and lineage origins, as well as the fate of cardiac

stem and progenitor cells, which could bring the science of mammalian cardiac regeneration a step closer to clinical reality.

Chapter 7

Bibliography

Abdullah, I., Lepore, J.J., Epstein, J.A., Parmacek, M.S., and Gruber, P.J. (2005). MRL mice fail to heal the heart in response to ischemia-reperfusion injury. Wound Repair Regen *13*, 205-208.

Adams, D.H., and Shaw, S. (1994). Leucocyte-endothelial interactions and regulation of leucocyte migration. Lancet *343*, 831-836.

Aikawa, E., Nahrendorf, M., Sosnovik, D., Lok, V.M., Jaffer, F.A., Aikawa, M., and Weissleder, R. (2007). Multimodality molecular imaging identifies proteolytic and osteogenic activities in early aortic valve disease. Circulation *115*, 377-386.

Amsterdam, E.A., Pan, H.L., Rendig, S.V., Symons, J.D., Fletcher, M.P., and Longhurst, J.C. (1993). Limitation of myocardial infarct size in pigs with a dual lipoxygenase-cyclooxygenase blocking agent by inhibition of neutrophil activity without reduction of neutrophil migration. J Am Coll Cardiol *22*, 1738-1744.

Amsterdam, E.A., Stahl, G.L., Pan, H.L., Rendig, S.V., Fletcher, M.P., and Longhurst, J.C. (1995). Limitation of reperfusion injury by a monoclonal antibody to C5a during myocardial infarction in pigs. Am J Physiol *268*, H448-457.

Anversa, P., and Kajstura, J. (1998). Ventricular myocytes are not terminally differentiated in the adult mammalian heart. Circ Res *83*, 1-14.

Anversa, P., Palackal, T., Sonnenblick, E.H., Olivetti, G., Meggs, L.G., and Capasso, J.M. (1990). Myocyte cell loss and myocyte cellular hyperplasia in the hypertrophied aging rat heart. Circ Res *67*, 871-885.

Aoyama, T., Matsui, T., Novikov, M., Park, J., Hemmings, B., and Rosenzweig, A. (2005). Serum and glucocorticoid-responsive kinase-1 regulates cardiomyocyte survival and hypertrophic response. Circulation *111*, 1652-1659.

Armstrong, P.W., Granger, C.B., Adams, P.X., Hamm, C., Holmes, D., Jr., O'Neill, W.W., Todaro, T.G., Vahanian, A., and Van de Werf, F. (2007). Pexelizumab for acute ST-elevation myocardial infarction in patients undergoing primary percutaneous coronary intervention: a randomized controlled trial. Jama *297*, 43-51.

Arsenijevic, Y., Weiss, S., Schneider, B., and Aebischer, P. (2001). Insulin-like growth factor-I is necessary for neural stem cell proliferation and demonstrates distinct actions of epidermal growth factor and fibroblast growth factor-2. J Neurosci *21*, 7194-7202.

Arumugam, T.V., Shiels, I.A., Strachan, A.J., Abbenante, G., Fairlie, D.P., and Taylor, S.M. (2003). A small molecule C5a receptor antagonist protects kidneys from ischemia/reperfusion injury in rats. Kidney Int *63*, 134-142.

Arumugam, T.V., Shiels, I.A., Woodruff, T.M., Reid, R.C., Fairlie, D.P., and Taylor, S.M. (2002). Protective effect of a new C5a receptor antagonist against ischemia-reperfusion injury in the rat small intestine. J Surg Res *103*, 260-267.

Arumugam, T.V., Woodruff, T.M., Stocks, S.Z., Proctor, L.M., Pollitt, S., Shiels, I.A., Reid, R.C., Fairlie, D.P., and Taylor, S.M. (2004). Protective effect of a human C5a receptor antagonist against hepatic ischaemia-reperfusion injury in rats. J Hepatol *40*, 934-941.

Askari, A.T., Brennan, M.L., Zhou, X., Drinko, J., Morehead, A., Thomas, J.D., Topol, E.J., Hazen, S.L., and Penn, M.S. (2003). Myeloperoxidase and plasminogen activator inhibitor 1 play a central role in ventricular remodeling after myocardial infarction. J Exp Med *197*, 615-624.

Barbee, R.W., Perry, B.D., Re, R.N., and Murgo, J.P. (1992). Microsphere and dilution techniques for the determination of blood flows and volumes in conscious mice. Am J Physiol *263*, R728-733.

Bayes de Luna, A. (1999). International cooperation in world cardiology: the role of the World Heart Federation. Circulation *99*, 986-989.

Beltrami, A.P., Barlucchi, L., Torella, D., Baker, M., Limana, F., Chimenti, S., Kasahara, H., Rota, M., Musso, E., Urbanek, K., *et al.* (2003). Adult cardiac stem cells are multipotent and support myocardial regeneration. Cell *114*, 763-776.

Beltrami, A.P., Urbanek, K., Kajstura, J., Yan, S.M., Finato, N., Bussani, R., Nadal-Ginard, B., Silvestri, F., Leri, A., Beltrami, C.A., *et al.* (2001). Evidence that human cardiac myocytes divide after myocardial infarction. N Engl J Med *344*, 1750-1757.

Bergamaschini, L., Gobbo, G., Gatti, S., Caccamo, L., Prato, P., Maggioni, M., Braidotti, P., Di Stefano, R., and Fassati, L.R. (2001). Endothelial targeting with C1-inhibitor reduces complement activation in vitro and during ex vivo reperfusion of pig liver. Clinical and experimental immunology *126*, 412-420.

Biben, C., Weber, R., Kesteven, S., Stanley, E., McDonald, L., Elliott, D.A., Barnett, L., Koentgen, F., Robb, L., Feneley, M., *et al.* (2000). Cardiac septal and valvular dysmorphogenesis in mice heterozygous for mutations in the homeobox gene Nkx2-5. Circ Res *87*, 888-895.

Bonow, R.O., Smaha, L.A., Smith, S.C., Jr., Mensah, G.A., and Lenfant, C. (2002). World Heart Day 2002: the international burden of cardiovascular disease: responding to the emerging global epidemic. Circulation *106*, 1602-1605.

Bradley, P.P., Christensen, R.D., and Rothstein, G. (1982). Cellular and extracellular myeloperoxidase in pyogenic inflammation. Blood *60*, 618-622.

Braunwald, E. (2001). Acute Myocardial Infarction Chapter 35. In Heart Disease A textbook of Cardiovascular Medicine, pp. 1114-1229.

Braunwald, E., and Bristow, M.R. (2000). Congestive heart failure: fifty years of progress. Circulation *102*, IV14-23.
Bristow, M.R., Saxon, L.A., Boehmer, J., Krueger, S., Kass, D.A., De Marco, T., Carson, P., DiCarlo, L., DeMets, D., White, B.G., *et al.* (2004). Cardiac-resynchronization therapy with or without an implantable defibrillator in advanced chronic heart failure. N Engl J Med *350*, 2140-2150.

Brockes, J.P., and Kumar, A. (2002). Plasticity and reprogramming of differentiated cells in amphibian regeneration. Nat Rev Mol Cell Biol *3*, 566-574.

Brown, C.O., 3rd, Chi, X., Garcia-Gras, E., Shirai, M., Feng, X.H., and Schwartz, R.J. (2004). The cardiac determination factor, Nkx2-5, is activated by mutual cofactors GATA-4 and Smad1/4 via a novel upstream enhancer. J Biol Chem *279*, 10659-10669.

Buckingham, M., Meilhac, S., and Zaffran, S. (2005). Building the mammalian heart from two sources of myocardial cells. Nature reviews *6*, 826-835.

Cai, C.L., Liang, X., Shi, Y., Chu, P.H., Pfaff, S.L., Chen, J., and Evans, S. (2003). Isl1 identifies a cardiac progenitor population that proliferates prior to differentiation and contributes a majority of cells to the heart. Dev Cell *5*, 877-889.

Cai, C.L., Martin, J.C., Sun, Y., Cui, L., Wang, L., Ouyang, K., Yang, L., Bu, L., Liang, X., Zhang, X., *et al.* (2008). A myocardial lineage derives from Tbx18 epicardial cells. Nature *454*, 104-108.

Chao, W., Matsui, T., Novikov, M.S., Tao, J., Li, L., Liu, H., Ahn, Y., and Rosenzweig, A. (2003). Strategic advantages of insulin-like growth factor-I expression for cardioprotection. The journal of gene medicine *5*, 277-286.

Clark, L.D., Clark, R.K., and Heber-Katz, E. (1998). A new murine model for mammalian wound repair and regeneration. Clinical immunology and immunopathology *88*, 35-45.

Cleland, J.G., Daubert, J.C., Erdmann, E., Freemantle, N., Gras, D., Kappenberger, L., and Tavazzi, L. (2005). The effect of cardiac resynchronization on morbidity and mortality in heart failure. N Engl J Med *352*, 1539-1549.

Dalla-Favera, R., Gallo, R.C., Giallongo, A., and Croce, C.M. (1982). Chromosomal localization of the human homolog (c-sis) of the simian sarcoma virus onc gene. Science *218*, 686-688.

Dawn, B., Stein, A.B., Urbanek, K., Rota, M., Whang, B., Rastaldo, R., Torella, D., Tang, X.L., Rezazadeh, A., Kajstura, J., *et al.* (2005). Cardiac stem cells delivered

intravascularly traverse the vessel barrier, regenerate infarcted myocardium, and improve cardiac function. Proc Natl Acad Sci U S A *102*, 3766-3771.

De Caterina, R., Libby, P., Peng, H.B., Thannickal, V.J., Rajavashisth, T.B., Gimbrone, M.A., Jr., Shin, W.S., and Liao, J.K. (1995). Nitric oxide decreases cytokine-induced endothelial activation. Nitric oxide selectively reduces endothelial expression of adhesion molecules and proinflammatory cytokines. J Clin Invest *96*, 60-68.

De Simoni, M.G., Storini, C., Barba, M., Catapano, L., Arabia, A.M., Rossi, E., and Bergamaschini, L. (2003). Neuroprotection by complement (C1) inhibitor in mouse transient brain ischemia. J Cereb Blood Flow Metab *23*, 232-239.

de Vries, B., Kohl, J., Leclercq, W.K., Wolfs, T.G., van Bijnen, A.A., Heeringa, P., and Buurman, W.A. (2003). Complement factor C5a mediates renal ischemia-reperfusion injury independent from neutrophils. J Immunol *170*, 3883-3889.

de Zwaan, C., Kleine, A.H., Diris, J.H., Glatz, J.F., Wellens, H.J., Strengers, P.F., Tissing, M., Hack, C.E., van Dieijen-Visser, M.P., and Hermens, W.T. (2002). Continuous 48-h C1-inhibitor treatment, following reperfusion therapy, in patients with acute myocardial infarction. Eur Heart J *23*, 1670-1677.

Demetri, G.D., van Oosterom, A.T., Garrett, C.R., Blackstein, M.E., Shah, M.H., Verweij, J., McArthur, G., Judson, I.R., Heinrich, M.C., Morgan, J.A., *et al.* (2006). Efficacy and safety of sunitinib in patients with advanced gastrointestinal stromal tumour after failure of imatinib: a randomised controlled trial. Lancet *368*, 1329-1338.

Demeule, M., Labelle, M., Regina, A., Berthelet, F., and Beliveau, R. (2001). Isolation of endothelial cells from brain, lung, and kidney: expression of the multidrug resistance P-glycoprotein isoforms. Biochem Biophys Res Commun *281*, 827-834.

Digirolamo, C.M., Stokes, D., Colter, D., Phinney, D.G., Class, R., and Prockop, D.J. (1999). Propagation and senescence of human marrow stromal cells in culture: a simple colony-forming assay identifies samples with the greatest potential to propagate and differentiate. Br J Haematol *107*, 275-281.

Ding, H., Wu, X., Bostrom, H., Kim, I., Wong, N., Tsoi, B., O'Rourke, M., Koh, G.Y., Soriano, P., Betsholtz, C., *et al.* (2004). A specific requirement for PDGF-C in palate formation and PDGFR-alpha signaling. Nat Genet *36*, 1111-1116.

Engler, R.L., Dahlgren, M.D., Morris, D.D., Peterson, M.A., and Schmid-Schonbein, G.W. (1986). Role of leukocytes in response to acute myocardial ischemia and reflow in dogs. Am J Physiol *251*, H314-323.

Fantl, W.J., Johnson, D.E., and Williams, L.T. (1993). Signalling by receptor tyrosine kinases. Annual review of biochemistry *62*, 453-481.

Fazel, S., Cimini, M., Chen, L., Li, S., Angoulvant, D., Fedak, P., Verma, S., Weisel, R.D., Keating, A., and Li, R.K. (2006). Cardioprotective c-kit+ cells are from the bone marrow and regulate the myocardial balance of angiogenic cytokines. J Clin Invest *116*, 1865-1877.

Fishbein, M.C., Maclean, D., and Maroko, P.R. (1978). The histopathologic evolution of myocardial infarction. Chest *73*, 843-849.

Fitch, J.C., Rollins, S., Matis, L., Alford, B., Aranki, S., Collard, C.D., Dewar, M., Elefteriades, J., Hines, R., Kopf, G., *et al.* (1999). Pharmacology and biological efficacy of a recombinant, humanized, single-chain antibody C5 complement inhibitor in patients undergoing coronary artery bypass graft surgery with cardiopulmonary bypass. Circulation *100*, 2499-2506.

Foreman, K.E., Glovsky, M.M., Warner, R.L., Horvath, S.J., and Ward, P.A. (1996). Comparative effect of C3a and C5a on adhesion molecule expression on neutrophils and endothelial cells. Inflammation *20*, 1-9.

Foreman, K.E., Vaporciyan, A.A., Bonish, B.K., Jones, M.L., Johnson, K.J., Glovsky, M.M., Eddy, S.M., and Ward, P.A. (1994). C5a-induced expression of P-selectin in endothelial cells. J Clin Invest *94*, 1147-1155.

Frangogiannis, N.G., Smith, C.W., and Entman, M.L. (2002). The inflammatory response in myocardial infarction. Cardiovasc Res *53*, 31-47.

Friedenstein, A.J., Chailakhjan, R.K., and Lalykina, K.S. (1970). The development of fibroblast colonies in monolayer cultures of guinea-pig bone marrow and spleen cells. Cell Tissue Kinetics *3*, 393-403.

Gan, L.M., Wikstrom, J., Bergstrom, G., and Wandt, B. (2004). Non-invasive imaging of coronary arteries in living mice using high-resolution echocardiography. Scand Cardiovasc J *38*, 121-126.

Gao, X.M., Wang, B.H., Woodcock, E., and Du, X.J. (2000). Expression of active alpha(1B)-adrenergic receptors in the heart does not alleviate ischemic reperfusion injury. J Mol Cell Cardiol *32*, 1679-1686.

Gao, X.M., Xu, Q., Kiriazis, H., Dart, A.M., and Du, X.J. (2005). Mouse model of post-infarct ventricular rupture: time course, strain- and gender-dependency, tensile strength, and histopathology. Cardiovasc Res *65*, 469-477.

Gerard, C., and Gerard, N.P. (1994). C5A anaphylatoxin and its seven transmembrane-segment receptor. Annu Rev Immunol *12*, 775-808

Gerard, N.P., Lu, B., Liu, P., Craig, S., Fujiwara, Y., Okinaga, S., and Gerard, C. (2005). An anti-inflammatory function for the complement anaphylatoxin C5a-binding protein, C5L2. J Biol Chem *280*, 39677-39680

Gnecchi, M., He, H., Liang, O.D., Melo, L.G., Morello, F., Mu, H., Noiseux, N., Zhang, L., Pratt, R.E., Ingwall, J.S., *et al.* (2005). Paracrine action accounts for marked protection of ischemic heart by Akt-modified mesenchymal stem cells. Nat Med *11*, 367-368.

Goldspink, G. (2002). Gene expression in skeletal muscle. Biochemical Society transactions *30*, 285-290.

Goodell, M.A., Brose, K., Paradis, G., Conner, A.S., and Mulligan, R.C. (1996). Isolation and functional properties of murine hematopoietic stem cells that are replicating in vivo. J Exp Med *183*, 1797-1806.

Granger, C.B., Mahaffey, K.W., Weaver, W.D., Theroux, P., Hochman, J.S., Filloon, T.G., Rollins, S., Todaro, T.G., Nicolau, J.C., Ruzyllo, W., *et al.* (2003). Pexelizumab, an anti-C5 complement antibody, as adjunctive therapy to primary percutaneous coronary intervention in acute myocardial infarction: the COMplement inhibition in Myocardial infarction treated with Angioplasty (COMMA) trial. Circulation *108*, 1184-1190.

Gu, X.H., Kompa, A.R., and Summers, R.J. (1998). Regulation of beta-adrenoceptors in a rat model of cardiac failure: effect of perindopril. J Cardiovasc Pharmacol *32*, 66-74.

Guo, R.F., and Ward, P.A. (2005). Role of C5a in inflammatory responses. Annu Rev Immunol *23*, 821-852.

Hall, R.I., Smith, M.S., and Rocker, G. (1997). The systemic inflammatory response to cardiopulmonary bypass: pathophysiological, therapeutic, and pharmacological considerations. Anesthesia and analgesia *85*, 766-782.

Hamilton, T.G., Klinghoffer, R.A., Corrin, P.D., and Soriano, P. (2003). Evolutionary divergence of platelet-derived growth factor alpha receptor signaling mechanisms. Molecular and cellular biology *23*, 4013-4025.

Hammerman, H., Kloner, R.A., Hale, S., Schoen, F.J., and Braunwald, E. (1983a). Dose-dependent effects of short-term methylprednisolone on myocardial infarct extent, scar formation, and ventricular function. Circulation *68*, 446-452.

Hammerman, H., Kloner, R.A., Schoen, F.J., Brown, E.J., Jr., Hale, S., and Braunwald, E. (1983b). Indomethacin-induced scar thinning after experimental myocardial infarction. Circulation *67*, 1290-1295.

Hasenfuss, G. (1998). Animal models of human cardiovascular disease, heart failure and hypertrophy. Cardiovasc Res *39*, 60-76.

Heinrich, M.C., Corless, C.L., Duensing, A., McGreevey, L., Chen, C.J., Joseph, N., Singer, S., Griffith, D.J., Haley, A., Town, A., *et al.* (2003). PDGFRA activating mutations in gastrointestinal stromal tumors. Science *299*, 708-710.

Heldin, C.H. (1996). Role of platelet-derived growth factor in vivo. The Molecular and Cellular biology of Wound Repair, 249-273.

Heldin, C.H., and Westermark, B. (1999). Mechanism of action and in vivo role of platelet-derived growth factor. Physiol Rev *79*, 1283-1316.

Hellermann, J.P., Jacobsen, S.J., Gersh, B.J., Rodeheffer, R.J., Reeder, G.S., and Roger, V.L. (2002). Heart failure after myocardial infarction: a review. Am J Med *113*, 324-330.

Hellstrom, M., Kalen, M., Lindahl, P., Abramsson, A., and Betsholtz, C. (1999). Role of PDGF-B and PDGFR-beta in recruitment of vascular smooth muscle cells and pericytes during embryonic blood vessel formation in the mouse. Development *126*, 3047-3055.

Hill, J.H., and Ward, P.A. (1971). The phlogistic role of C3 leukotactic fragments in myocardial infarcts of rats. J Exp Med *133*, 885-900.

Hirschi, K.K., Rohovsky, S.A., Beck, L.H., Smith, S.R., and D'Amore, P.A. (1999). Endothelial cells modulate the proliferation of mural cell precursors via platelet-derived growth factor-BB and heterotypic cell contact. Circ Res *84*, 298-305.

Hoerter, J., Gonzalez-Barroso, M.D., Couplan, E., Mateo, P., Gelly, C., Cassard-Doulcier, A.M., Diolez, P., and Bouillaud, F. (2004). Mitochondrial uncoupling protein 1 expressed in the heart of transgenic mice protects against ischemic-reperfusion damage. Circulation *110*, 528-533.

Horstick, G., Berg, O., Heimann, A., Gotze, O., Loos, M., Hafner, G., Bierbach, B., Petersen, S., Bhakdi, S., Darius, H., *et al.* (2001). Application of C1-esterase inhibitor during reperfusion of ischemic myocardium: dose-related beneficial versus detrimental effects. Circulation *104*, 3125-3131.

Hsieh, P.C., Segers, V.F., Davis, M.E., MacGillivray, C., Gannon, J., Molkentin, J.D., Robbins, J., and Lee, R.T. (2007). Evidence from a genetic fate-mapping study that stem cells refresh adult mammalian cardiomyocytes after injury. Nat Med *13*, 970-974.

Huber-Lang, M., Sarma, J.V., Zetoune, F.S., Rittirsch, D., Neff, T.A., McGuire, S.R., Lambris, J.D., Warner, R.L., Flierl, M.A., Hoesel, L.M., *et al.* (2006). Generation of C5a in the absence of C3: a new complement activation pathway. Nat Med *12*, 682-687.

Hutchins, G.M., and Bulkley, B.H. (1978). Infarct expansion versus extension: two different complications of acute myocardial infarction. Am J Cardiol *41*, 1127-1132.

Ivey, C.L., Williams, F.M., Collins, P.D., Jose, P.J., and Williams, T.J. (1995). Neutrophil chemoattractants generated in two phases during reperfusion of ischemic myocardium in the rabbit. Evidence for a role for C5a and interleukin-8. J Clin Invest *95*, 2720-2728.

Jackson, K.A., Majka, S.M., Wang, H., Pocius, J., Hartley, C.J., Majesky, M.W., Entman, M.L., Michael, L.H., Hirschi, K.K., and Goodell, M.A. (2001). Regeneration of ischemic cardiac muscle and vascular endothelium by adult stem cells. J Clin Invest *107*, 1395-1402.

Jaenisch, R., and Young, R. (2008). Stem cells, the molecular circuitry of pluripotency and nuclear reprogramming. Cell *132*, 567-582.

James, J.F., Hewett, T.E., and Robbins, J. (1998). Cardiac physiology in transgenic mice. Circ Res *82*, 407-415.

Jiang, X., Gurel, O., Mendiaz, E.A., Stearns, G.W., Clogston, C.L., Lu, H.S., Osslund, T.D., Syed, R.S., Langley, K.E., and Hendrickson, W.A. (2000a). Structure of the active core of human stem cell factor and analysis of binding to its receptor kit. Embo J *19*, 3192-3203.

Jiang, X., Rowitch, D.H., Soriano, P., McMahon, A.P., and Sucov, H.M. (2000b). Fate of the mammalian cardiac neural crest. Development *127*, 1607-1616.

Jordan, J.E., Zhao, Z.Q., and Vinten-Johansen, J. (1999). The role of neutrophils in myocardial ischemia-reperfusion injury. Cardiovasc Res *43*, 860-878.

Kajstura, J., Cheng, W., Sarangarajan, R., Li, P., Li, B., Nitahara, J.A., Chapnick, S., Reiss, K., Olivetti, G., and Anversa, P. (1996). Necrotic and apoptotic myocyte cell death in the aging heart of Fischer 344 rats. Am J Physiol *271*, H1215-1228.

Kajstura, J., Leri, A., Finato, N., Di Loreto, C., Beltrami, C.A., and Anversa, P. (1998). Myocyte proliferation in end-stage cardiac failure in humans. Proc Natl Acad Sci U S A *95*, 8801-8805.

Kajstura, J., Rota, M., Whang, B., Cascapera, S., Hosoda, T., Bearzi, C., Nurzynska, D., Kasahara, H., Zias, E., Bonafe, M., *et al.* (2005). Bone marrow cells differentiate in cardiac cell lineages after infarction independently of cell fusion. Circ Res *96*, 127-137.

Khakoo, A.Y., Kassiotis, C.M., Tannir, N., Plana, J.C., Halushka, M., Bickford, C., Trent, J., 2nd, Champion, J.C., Durand, J.B., and Lenihan, D.J. (2008). Heart failure associated with sunitinib malate: a multitargeted receptor tyrosine kinase inhibitor. Cancer *112*, 2500-2508.

Kim, M., Turnquist, H., Jackson, J., Sgagias, M., Yan, Y., Gong, M., Dean, M., Sharp, J.G., and Cowan, K. (2002). The multidrug resistance transporter ABCG2 (breast cancer resistance protein 1) effluxes Hoechst 33342 and is overexpressed in hematopoietic stem cells. Clin Cancer Res *8*, 22-28.

Kohler, N., and Lipton, A. (1974). Platelets as a source of fibroblast growth-promoting activity. Experimental cell research *87*, 297-301.

Kubes, P., Suzuki, M., and Granger, D.N. (1991). Nitric oxide: an endogenous modulator of leukocyte adhesion. Proc Natl Acad Sci U S A *88*, 4651-4655.

Kumar, D., Hacker, T.A., Buck, J., Whitesell, L.F., Kaji, E.H., Douglas, P.S., and Kamp, T.J. (2005). Distinct mouse coronary anatomy and myocardial infarction consequent to ligation. Coron Artery Dis *16*, 41-44.

Laflamme, M.A., and Murry, C.E. (2005). Regenerating the heart. Nat Biotechnol *23*, 845-856.

Laugwitz, K.L., Moretti, A., Caron, L., Nakano, A., and Chien, K.R. (2008). Islet1 cardiovascular progenitors: a single source for heart lineages? Development *135*, 193-205.

Laugwitz, K.L., Moretti, A., Lam, J., Gruber, P., Chen, Y., Woodard, S., Lin, L.Z., Cai, C.L., Lu, M.M., Reth, M., *et al.* (2005). Postnatal isl1+ cardioblasts enter fully differentiated cardiomyocyte lineages. Nature *433*, 647-653.

Lavine, K.J., Yu, K., White, A.C., Zhang, X., Smith, C., Partanen, J., and Ornitz, D.M. (2005). Endocardial and epicardial derived FGF signals regulate myocardial proliferation and differentiation in vivo. Dev Cell *8*, 85-95.

Lee, H., Zahra, D., Vogelzang, A., Newton, R., Thatcher, J., Quan, A., So, T., Zwirner, J., Koentgen, F., Padkjaer, S.B., *et al.* (2006). Human C5aR knock-in mice facilitate the production and assessment of anti-inflammatory monoclonal antibodies. Nat Biotechnol *24*, 1279-1284.

Lee, J.A., Parrett, B.M., Conejero, J.A., Laser, J., Chen, J., Kogon, A.J., Nanda, D., Grant, R.T., and Breitbart, A.S. (2003). Biological alchemy: engineering bone and fat from fat-derived stem cells. Annals of plastic surgery *50*, 610-617.

Leferovich, J.M., Bedelbaeva, K., Samulewicz, S., Zhang, X.M., Zwas, D., Lankford, E.B., and Heber-Katz, E. (2001). Heart regeneration in adult MRL mice. Proc Natl Acad Sci U S A *98*, 9830-9835.

Lepilina, A., Coon, A.N., Kikuchi, K., Holdway, J.E., Roberts, R.W., Burns, C.G., and Poss, K.D. (2006). A dynamic epicardial injury response supports progenitor cell activity during zebrafish heart regeneration. Cell *127*, 607-619.

Leveen, P., Pekny, M., Gebre-Medhin, S., Swolin, B., Larsson, E., and Betsholtz, C. (1994). Mice deficient for PDGF B show renal, cardiovascular, and hematological abnormalities. Genes Dev *8*, 1875-1887.

Li, B., Li, Q., Wang, X., Jana, K.P., Redaelli, G., Kajstura, J., and Anversa, P. (1997a). Coronary constriction impairs cardiac function and induces myocardial damage and ventricular remodeling in mice. Am J Physiol *273*, H2508-2519.
Li, B., Setoguchi, M., Wang, X., Andreoli, A.M., Leri, A., Malhotra, A., Kajstura, J., and Anversa, P. (1999). Insulin-like growth factor-1 attenuates the detrimental impact of nonocclusive coronary artery constriction on the heart. Circ Res *84*, 1007-1019.

Li, M., Naqvi, N., Yahiro, E., Liu, K., Powell, P.C., Bradley, W.E., Martin, D.I., Graham, R.M., Dell'Italia, L.J., and Husain, A. (2008). c-kit is required for cardiomyocyte terminal differentiation. Circ Res *102*, 677-685.

Li, Q., Li, B., Wang, X., Leri, A., Jana, K.P., Liu, Y., Kajstura, J., Baserga, R., and Anversa, P. (1997b). Overexpression of insulin-like growth factor-1 in mice protects from myocyte death after infarction, attenuating ventricular dilation, wall stress, and cardiac hypertrophy. J Clin Invest *100*, 1991-1999.

Li, X., Ponten, A., Aase, K., Karlsson, L., Abramsson, A., Uutela, M., Backstrom, G., Hellstrom, M., Bostrom, H., Li, H., *et al.* (2000). PDGF-C is a new protease-activated ligand for the PDGF alpha-receptor. Nature cell biology *2*, 302-309.

Libby, P., Maroko, P.R., Bloor, C.M., Sobel, B.E., and Braunwald, E. (1973). Reduction of experimental myocardial infarct size by corticosteroid administration. J Clin Invest *52*, 599-607.

Liechty, K.W., Kim, H.B., Adzick, N.S., and Crombleholme, T.M. (2000). Fetal wound repair results in scar formation in interleukin-10-deficient mice in a syngeneic murine model of scarless fetal wound repair. Journal of pediatric surgery *35*, 866-872; discussion 872-863.

Lindahl, P., Johansson, B.R., Leveen, P., and Betsholtz, C. (1997). Pericyte loss and microaneurysm formation in PDGF-B-deficient mice. Science *277*, 242-245.

Linke, A., Muller, P., Nurzynska, D., Casarsa, C., Torella, D., Nascimbene, A., Castaldo, C., Cascapera, S., Bohm, M., Quaini, F., *et al.* (2005). Stem cells in the dog heart are self-renewing, clonogenic, and multipotent and regenerate infarcted myocardium, improving cardiac function. Proc Natl Acad Sci U S A *102*, 8966-8971.

Linzbach, A.J. (1960). Heart failure from the point of view of quantitative anatomy. Am J Cardiol *5*, 370-382.

Liu, Y.H., Yang, X.P., Nass, O., Sabbah, H.N., Peterson, E., and Carretero, O.A. (1997). Chronic heart failure induced by coronary artery ligation in Lewis inbred rats. Am J Physiol *272*, H722-727.

Louis, S.A., Rietze, R.L., Deleyrolle, L., Wagey, R.E., Thomas, T.E., Eaves, A.C., and Reynolds, B.A. (2008). Enumeration of neural stem and progenitor cells in the neural colony-forming cell assay. Stem Cells *26*, 988-996.
Ma, X.L., Weyrich, A.S., Lefer, D.J., Buerke, M., Albertine, K.H., Kishimoto, T.K., and Lefer, A.M. (1993). Monoclonal antibody to L-selectin attenuates neutrophil accumulation and protects ischemic reperfused cat myocardium. Circulation *88*, 649-658.

Mahaffey, K.W., Granger, C.B., Nicolau, J.C., Ruzyllo, W., Weaver, W.D., Theroux, P., Hochman, J.S., Filloon, T.G., Mojcik, C.F., Todaro, T.G., *et al.* (2003). Effect of pexelizumab, an anti-C5 complement antibody, as adjunctive therapy to fibrinolysis in acute myocardial infarction: the COMPlement inhibition in myocardial infarction treated with thromboLYtics (COMPLY) trial. Circulation *108*, 1176-1183.

Makino, S., Fukuda, K., Miyoshi, S., Konishi, F., Kodama, H., Pan, J., Sano, M., Takahashi, T., Hori, S., Abe, H., *et al.* (1999). Cardiomyocytes can be generated from marrow stromal cells in vitro. J Clin Invest *103*, 697-705.

Maroko, P.R., Carpenter, C.B., Chiariello, M., Fishbein, M.C., Radvany, P., Knostman, J.D., and Hale, S.L. (1978). Reduction by cobra venom factor of myocardial necrosis after coronary artery occlusion. J Clin Invest *61*, 661-670.

Martin, C.M., Meeson, A.P., Robertson, S.M., Hawke, T.J., Richardson, J.A., Bates, S., Goetsch, S.C., Gallardo, T.D., and Garry, D.J. (2004). Persistent expression of the ATP-binding cassette transporter, Abcg2, identifies cardiac SP cells in the developing and adult heart. Dev Biol *265*, 262-275.

Matsui, T., Tao, J., del Monte, F., Lee, K.H., Li, L., Picard, M., Force, T.L., Franke, T.F., Hajjar, R.J., and Rosenzweig, A. (2001). Akt activation preserves cardiac function and prevents injury after transient cardiac ischemia in vivo. Circulation *104*, 330-335.

Matsuura, K., Nagai, T., Nishigaki, N., Oyama, T., Nishi, J., Wada, H., Sano, M., Toko, H., Akazawa, H., Sato, T., *et al.* (2004). Adult cardiac Sca-1-positive cells differentiate into beating cardiomyocytes. J Biol Chem *279*, 11384-11391.

McEver, R.P., Moore, K.L., and Cummings, R.D. (1995). Leukocyte trafficking mediated by selectin-carbohydrate interactions. J Biol Chem *270*, 11025-11028.

McMurray, J.J., and Pfeffer, M.A. (2005). Heart failure. Lancet *365*, 1877-1889.

Messina, E., De Angelis, L., Frati, G., Morrone, S., Chimenti, S., Fiordaliso, F., Salio, M., Battaglia, M., Latronico, M.V., Coletta, M., *et al.* (2004). Isolation and expansion of adult cardiac stem cells from human and murine heart. Circ Res *95*, 911-921.

Michael, L.H., Entman, M.L., Hartley, C.J., Youker, K.A., Zhu, J., Hall, S.R., Hawkins, H.K., Berens, K., and Ballantyne, C.M. (1995). Myocardial ischemia and reperfusion: a murine model. Am J Physiol *269*, H2147-2154.

Mikawa, T., and Gourdie, R.G. (1996). Pericardial mesoderm generates a population of coronary smooth muscle cells migrating into the heart along with ingrowth of the epicardial organ. Dev Biol *174*, 221-232.

Molkentin, J.D., Lin, Q., Duncan, S.A., and Olson, E.N. (1997). Requirement of the transcription factor GATA4 for heart tube formation and ventral morphogenesis. Genes Dev *11*, 1061-1072.

Montrucchio, G., Alloatti, G., Mariano, F., Comino, A., Cacace, G., Polloni, R., De Filippi, P.G., Emanuelli, G., and Camussi, G. (1993). Role of platelet-activating factor in polymorphonuclear neutrophil recruitment in reperfused ischemic rabbit heart. Am J Pathol *142*, 471-480.

Moore, A.W., McInnes, L., Kreidberg, J., Hastie, N.D., and Schedl, A. (1999). YAC complementation shows a requirement for Wt1 in the development of epicardium, adrenal gland and throughout nephrogenesis. Development *126*, 1845-1857.

Moretti, A., Caron, L., Nakano, A., Lam, J.T., Bernshausen, A., Chen, Y., Qyang, Y., Bu, L., Sasaki, M., Martin-Puig, S., *et al.* (2006). Multipotent embryonic isl1+ progenitor cells lead to cardiac, smooth muscle, and endothelial cell diversification. Cell *127*, 1151-1165.

Morgan, E.N., Boyle, E.M., Jr., Yun, W., Kovacich, J.C., Canty, T.G., Jr., Chi, E., Pohlman, T.H., and Verrier, E.D. (1999). Platelet-activating factor acetylhydrolase prevents myocardial ischemia-reperfusion injury. Circulation *100*, II365-368.

Morrison, S.J., Wandycz, A.M., Hemmati, H.D., Wright, D.E., and Weissman, I.L. (1997). Identification of a lineage of multipotent hematopoietic progenitors. Development *124*, 1929-1939.

Moss, A.J., Zareba, W., Hall, W.J., Klein, H., Wilber, D.J., Cannom, D.S., Daubert, J.P., Higgins, S.L., Brown, M.W., and Andrews, M.L. (2002). Prophylactic implantation of a defibrillator in patients with myocardial infarction and reduced ejection fraction. N Engl J Med *346*, 877-883.

Motzer, R.J., Rini, B.I., Bukowski, R.M., Curti, B.D., George, D.J., Hudes, G.R., Redman, B.G., Margolin, K.A., Merchan, J.R., Wilding, G., *et al.* (2006). Sunitinib in patients with metastatic renal cell carcinoma. Jama *295*, 2516-2524.

Muders, F., and Elsner, D. (2000). Animal models of chronic heart failure. Pharmacol Res *41*, 605-612.

Mullane, K.M., Read, N., Salmon, J.A., and Moncada, S. (1984). Role of leukocytes in acute myocardial infarction in anesthetized dogs: relationship to myocardial salvage by

anti-inflammatory drugs. The Journal of pharmacology and experimental therapeutics *228*, 510-522.
Murry, C.E., Reinecke, H., and Pabon, L.M. (2006). Regeneration gaps: observations on stem cells and cardiac repair. J Am Coll Cardiol *47*, 1777-1785.

Nadal-Ginard, B., Kajstura, J., Leri, A., and Anversa, P. (2003). Myocyte death, growth, and regeneration in cardiac hypertrophy and failure. Circ Res *92*, 139-150.

Oh, H., Bradfute, S.B., Gallardo, T.D., Nakamura, T., Gaussin, V., Mishina, Y., Pocius, J., Michael, L.H., Behringer, R.R., Garry, D.J., *et al.* (2003). Cardiac progenitor cells from adult myocardium: homing, differentiation, and fusion after infarction. Proc Natl Acad Sci U S A *100*, 12313-12318.

Ohashi, Y., Kawashima, S., Hirata, K., Akita, H., and Yokoyama, M. (1997). Nitric oxide inhibits neutrophil adhesion to cytokine-activated cardiac myocytes. Am J Physiol *272*, H2807-2814.

Okumoto, K., Saito, T., Hattori, E., Ito, J.I., Adachi, T., Takeda, T., Sugahara, K., Watanabe, H., Saito, K., Togashi, H., *et al.* (2003). Differentiation of bone marrow cells into cells that express liver-specific genes in vitro: implication of the Notch signals in differentiation. Biochem Biophys Res Commun *304*, 691-695.

Orlic, D., Kajstura, J., Chimenti, S., Jakoniuk, I., Anderson, S.M., Li, B., Pickel, J., McKay, R., Nadal-Ginard, B., Bodine, D.M., *et al.* (2001). Bone marrow cells regenerate infarcted myocardium. Nature *410*, 701-705.

Orr-Urtreger, A., Bedford, M.T., Do, M.S., Eisenbach, L., and Lonai, P. (1992). Developmental expression of the alpha receptor for platelet-derived growth factor, which is deleted in the embryonic lethal Patch mutation. Development *115*, 289-303.

Parmar, K., Sauk-Schubert, C., Burdick, D., Handley, M., and Mauch, P. (2003). Sca+CD34- murine side population cells are highly enriched for primitive stem cells. Exp Hematol *31*, 244-250.

Perez-Pomares, J.M., Macias, D., Garcia-Garrido, L., and Munoz-Chapuli, R. (1998). The origin of the subepicardial mesenchyme in the avian embryo: an immunohistochemical and quail-chick chimera study. Dev Biol *200*, 57-68.

Pfeffer, M.A., and Braunwald, E. (1990). Ventricular remodeling after myocardial infarction. Experimental observations and clinical implications. Circulation *81*, 1161-1172.

Pfeffer, M.A., Pfeffer, J.M., Fishbein, M.C., Fletcher, P.J., Spadaro, J., Kloner, R.A., and Braunwald, E. (1979). Myocardial infarct size and ventricular function in rats. Circ Res *44*, 503-512.

Pfister, O., Mouquet, F., Jain, M., Summer, R., Helmes, M., Fine, A., Colucci, W.S., and Liao, R. (2005). CD31- but Not CD31+ cardiac side population cells exhibit functional cardiomyogenic differentiation. Circ Res *97*, 52-61.

Pinckard, R.N., O'Rourke, R.A., Crawford, M.H., Grover, F.S., McManus, L.M., Ghidoni, J.J., Storrs, S.B., and Olson, M.S. (1980). Complement localization and mediation of ischemic injury in baboon myocardium. J Clin Invest *66*, 1050-1056.

Poelmann, R.E., Gittenberger-de Groot, A.C., Mentink, M.M., Bokenkamp, R., and Hogers, B. (1993). Development of the cardiac coronary vascular endothelium, studied with antiendothelial antibodies, in chicken-quail chimeras. Circ Res *73*, 559-568.

Ponten, A., Li, X., Thoren, P., Aase, K., Sjoblom, T., Ostman, A., and Eriksson, U. (2003). Transgenic overexpression of platelet-derived growth factor-C in the mouse heart induces cardiac fibrosis, hypertrophy, and dilated cardiomyopathy. Am J Pathol *163*, 673-682.

Poss, K.D., Wilson, L.G., and Keating, M.T. (2002). Heart regeneration in zebrafish. Science *298*, 2188-2190.

Potten, C.S., and Loeffler, M. (1990). Stem cells: attributes, cycles, spirals, pitfalls and uncertainties. Lessons for and from the crypt. Development *110*, 1001-1020.

Powell, E.M., Mars, W.M., and Levitt, P. (2001). Hepatocyte growth factor/scatter factor is a motogen for interneurons migrating from the ventral to dorsal telencephalon. Neuron *30*, 79-89.

Pullen, N., Dennis, P.B., Andjelkovic, M., Dufner, A., Kozma, S.C., Hemmings, B.A., and Thomas, G. (1998). Phosphorylation and activation of p70s6k by PDK1. Science *279*, 707-710.

Quaini, F., Urbanek, K., Beltrami, A.P., Finato, N., Beltrami, C.A., Nadal-Ginard, B., Kajstura, J., Leri, A., and Anversa, P. (2002). Chimerism of the transplanted heart. N Engl J Med *346*, 5-15.

Raghavan, M., and Bjorkman, P.J. (1996). Fc receptors and their interactions with immunoglobulins. Annual review of cell and developmental biology *12*, 181-220.

Raines, E.W. (2004). PDGF and cardiovascular disease. Cytokine & growth factor reviews *15*, 237-254.

Reichert, J.M., Rosensweig, C.J., Faden, L.B., and Dewitz, M.C. (2005). Monoclonal antibody successes in the clinic. Nat Biotechnol *23*, 1073-1078.

Ren, G., Michael, L.H., Entman, M.L., and Frangogiannis, N.G. (2002). Morphological characteristics of the microvasculature in healing myocardial infarcts. J Histochem Cytochem *50*, 71-79.

Reynolds, B.A., and Rietze, R.L. (2005). Neural stem cells and neurospheres--re-evaluating the relationship. Nature methods *2*, 333-336.

Roberts, R., DeMello, V., and Sobel, B.E. (1976). Deleterious effects of methylprednisolone in patients with myocardial infarction. Circulation *53*, I204-206.

Romanov, Y.A., Svintsitskaya, V.A., and Smirnov, V.N. (2003). Searching for alternative sources of postnatal human mesenchymal stem cells: candidate MSC-like cells from umbilical cord. Stem Cells *21*, 105-110.

Rose, E.A., Gelijns, A.C., Moskowitz, A.J., Heitjan, D.F., Stevenson, L.W., Dembitsky, W., Long, J.W., Ascheim, D.D., Tierney, A.R., Levitan, R.G., *et al.* (2001). Long-term mechanical left ventricular assistance for end-stage heart failure. N Engl J Med *345*, 1435-1443.

Ross, R., Glomset, J., Kariya, B., and Harker, L. (1974). A platelet-dependent serum factor that stimulates the proliferation of arterial smooth muscle cells in vitro. Proc Natl Acad Sci U S A *71*, 1207-1210.

Rumyantsev, P. (1964). DNA synthesis and nuclear division in embryonical and postnatal histogenesis of myocardium. Archives of Anatomy *47*, 59-65.

Santini, M.P., Tsao, L., Monassier, L., Theodoropoulos, C., Carter, J., Lara-Pezzi, E., Slonimsky, E., Salimova, E., Delafontaine, P., Song, Y.H., *et al.* (2007). Enhancing repair of the mammalian heart. Circ Res *100*, 1732-1740.

Sato, H., Zhao, Z.Q., and Vinten-Johansen, J. (1996). L-Arginine inhibits neutrophil adherence and coronary artery dysfunction. Cardiovasc Res *31*, 63-72.

Seaberg, R.M., and van der Kooy, D. (2003). Stem and progenitor cells: the premature desertion of rigorous definitions. Trends in neurosciences *26*, 125-131.

Segers, V.F., and Lee, R.T. (2008). Stem-cell therapy for cardiac disease. Nature *451*, 937-942.

Shandelya, S.M., Kuppusamy, P., Herskowitz, A., Weisfeldt, M.L., and Zweier, J.L. (1993a). Soluble complement receptor type 1 inhibits the complement pathway and prevents contractile failure in the postischemic heart. Evidence that complement activation is required for neutrophil-mediated reperfusion injury. Circulation *88*, 2812-2826.

Shandelya, S.M., Kuppusamy, P., Weisfeldt, M.L., and Zweier, J.L. (1993b). Evaluation of the role of polymorphonuclear leukocytes on contractile function in myocardial reperfusion injury. Evidence for plasma-mediated leukocyte activation. Circulation *87*, 536-546.

Simm, A., Nestler, M., and Hoppe, V. (1998). Mitogenic effect of PDGF-AA on cardiac fibroblasts. Basic research in cardiology *93 Suppl 3*, 40-43.

Smith, E.F., 3rd, Egan, J.W., Bugelski, P.J., Hillegass, L.M., Hill, D.E., and Griswold, D.E. (1988). Temporal relation between neutrophil accumulation and myocardial reperfusion injury. Am J Physiol *255*, H1060-1068.

Smith, R.R., Barile, L., Cho, H.C., Leppo, M.K., Hare, J.M., Messina, E., Giacomello, A., Abraham, M.R., and Marban, E. (2007). Regenerative potential of cardiosphere-derived cells expanded from percutaneous endomyocardial biopsy specimens. Circulation *115*, 896-908.

Soriano, P. (1994). Abnormal kidney development and hematological disorders in PDGF beta-receptor mutant mice. Genes Dev *8*, 1888-1896.

Soriano, P. (1997). The PDGF alpha receptor is required for neural crest cell development and for normal patterning of the somites. Development *124*, 2691-2700.

Srivastava, D., and Olson, E.N. (2000). A genetic blueprint for cardiac development. Nature *407*, 221-226.

Sulzbacher, I., Birner, P., Traxler, M., Marberger, M., and Haitel, A. (2003). Expression of platelet-derived growth factor-alpha alpha receptor is associated with tumor progression in clear cell renal cell carcinoma. American journal of clinical pathology *120*, 107-112.

Takakura, N., Yoshida, H., Ogura, Y., Kataoka, H., Nishikawa, S., and Nishikawa, S. (1997). PDGFR alpha expression during mouse embryogenesis: immunolocalization analyzed by whole-mount immunohistostaining using the monoclonal anti-mouse PDGFR alpha antibody APA5. J Histochem Cytochem *45*, 883-893.

Tallquist, M.D., and Soriano, P. (2003). Cell autonomous requirement for PDGFRalpha in populations of cranial and cardiac neural crest cells. Development *130*, 507-518.

Tateishi, K., Ashihara, E., Takehara, N., Nomura, T., Honsho, S., Nakagami, T., Morikawa, S., Takahashi, T., Ueyama, T., Matsubara, H., *et al.* (2007). Clonally amplified cardiac stem cells are regulated by Sca-1 signaling for efficient cardiovascular regeneration. J Cell Sci *120*, 1791-1800.

Thiebaut, F., Tsuruo, T., Hamada, H., Gottesman, M.M., Pastan, I., and Willingham, M.C. (1987). Cellular localization of the multidrug-resistance gene product P-glycoprotein in normal human tissues. Proc Natl Acad Sci U S A *84*, 7735-7738.

Torrente, Y., Tremblay, J.P., Pisati, F., Belicchi, M., Rossi, B., Sironi, M., Fortunato, F., El Fahime, M., D'Angelo, M.G., Caron, N.J., *et al.* (2001). Intraarterial injection of muscle-derived CD34(+)Sca-1(+) stem cells restores dystrophin in mdx mice. J Cell Biol *152*, 335-348.

Urbanek, K., Rota, M., Cascapera, S., Bearzi, C., Nascimbene, A., De Angelis, A., Hosoda, T., Chimenti, S., Baker, M., Limana, F., *et al.* (2005). Cardiac stem cells possess growth factor-receptor systems that after activation regenerate the infarcted myocardium, improving ventricular function and long-term survival. Circ Res *97*, 663-673.

Vakeva, A.P., Agah, A., Rollins, S.A., Matis, L.A., Li, L., and Stahl, G.L. (1998). Myocardial infarction and apoptosis after myocardial ischemia and reperfusion: role of the terminal complement components and inhibition by anti-C5 therapy. Circulation *97*, 2259-2267.

Vanhaesebroeck, B., Leevers, S.J., Panayotou, G., and Waterfield, M.D. (1997). Phosphoinositide 3-kinases: a conserved family of signal transducers. Trends in biochemical sciences *22*, 267-272.

Verrier, E.D., Shernan, S.K., Taylor, K.M., Van de Werf, F., Newman, M.F., Chen, J.C., Carrier, M., Haverich, A., Malloy, K.J., Adams, P.X., *et al.* (2004). Terminal complement blockade with pexelizumab during coronary artery bypass graft surgery requiring cardiopulmonary bypass: a randomized trial. Jama *291*, 2319-2327.

Virag, J.I., and Murry, C.E. (2003). Myofibroblast and endothelial cell proliferation during murine myocardial infarct repair. Am J Pathol *163*, 2433-2440.

Wan, S., LeClerc, J.L., and Vincent, J.L. (1997). Inflammatory response to cardiopulmonary bypass: mechanisms involved and possible therapeutic strategies. Chest *112*, 676-692.

Wang, X., Hu, Q., Nakamura, Y., Lee, J., Zhang, G., From, A.H., and Zhang, J. (2006). The role of the sca-1+/CD31- cardiac progenitor cell population in postinfarction left ventricular remodeling. Stem Cells *24*, 1779-1788.

Wang, Y. (2006). Complementary therapies for inflammation. Nat Biotechnol *24*, 1224-1226.

Weisman, H.F., Bartow, T., Leppo, M.K., Marsh, H.C., Jr., Carson, G.R., Concino, M.F., Boyle, M.P., Roux, K.H., Weisfeldt, M.L., and Fearon, D.T. (1990). Soluble human complement receptor type 1: in vivo inhibitor of complement suppressing post-ischemic myocardial inflammation and necrosis. Science *249*, 146-151.

Wessels, A., and Perez-Pomares, J.M. (2004). The epicardium and epicardially derived cells (EPDCs) as cardiac stem cells. Anat Rec A Discov Mol Cell Evol Biol *276*, 43-57.
Weyrich, A.S., Ma, X.Y., Lefer, D.J., Albertine, K.H., and Lefer, A.M. (1993). In vivo neutralization of P-selectin protects feline heart and endothelium in myocardial ischemia and reperfusion injury. J Clin Invest *91*, 2620-2629.

Wu, M., Hemesath, T.J., Takemoto, C.M., Horstmann, M.A., Wells, A.G., Price, E.R., Fisher, D.Z., and Fisher, D.E. (2000). c-Kit triggers dual phosphorylations, which couple activation and degradation of the essential melanocyte factor Mi. Genes Dev *14*, 301-312.

Yamashita, J., Itoh, H., Hirashima, M., Ogawa, M., Nishikawa, S., Yurugi, T., Naito, M., Nakao, K., and Nishikawa, S. (2000). Flk1-positive cells derived from embryonic stem cells serve as vascular progenitors. Nature *408*, 92-96.

Yoon, Y.S., Wecker, A., Heyd, L., Park, J.S., Tkebuchava, T., Kusano, K., Hanley, A., Scadova, H., Qin, G., Cha, D.H., *et al.* (2005). Clonally expanded novel multipotent stem cells from human bone marrow regenerate myocardium after myocardial infarction. J Clin Invest *115*, 326-338.

Yoshida, H., Takakura, N., Hirashima, M., Kataoka, H., Tsuchida, K., Nishikawa, S., and Nishikawa, S. (1998). Hematopoietic tissues, as a playground of receptor tyrosine kinases of the PDGF-receptor family. Developmental and comparative immunology *22*, 321-332.

Yu, J., Moon, A., and Kim, H.R. (2001). Both platelet-derived growth factor receptor (PDGFR)-alpha and PDGFR-beta promote murine fibroblast cell migration. Biochem Biophys Res Commun *282*, 697-700.

Zacharowski, K., Otto, M., Hafner, G., Marsh, H.C., Jr., and Thiemermann, C. (1999). Reduction of myocardial infarct size with sCR1sLe(x), an alternatively glycosylated form of human soluble complement receptor type 1 (sCR1), possessing sialyl Lewis x. British journal of pharmacology *128*, 945-952.

Zhao, L., Weber, P.A., Smith, J.R., Comerford, M.L., and Elliott, G.T. (1997). Role of inducible nitric oxide synthase in pharmacological "preconditioning" with monophosphoryl lipid A. J Mol Cell Cardiol *29*, 1567-1576.

Zhou, B., Ma, Q., Rajagopal, S., Wu, S.M., Domian, I., Rivera-Feliciano, J., Jiang, D., von Gise, A., Ikeda, S., Chien, K.R., *et al.* (2008). Epicardial progenitors contribute to the cardiomyocyte lineage in the developing heart. Nature *454*, 109-113.

Zymek, P., Bujak, M., Chatila, K., Cieslak, A., Thakker, G., Entman, M.L., and Frangogiannis, N.G. (2006). The role of platelet-derived growth factor signaling in healing myocardial infarcts. J Am Coll Cardiol *48*, 2315-2323.